Vol. 48 • No. 12
December 2005

Microwave Journal

MTT-S RWS Show Issue

San Diego, CA

Symposium and Exhibition Preview

Package Environment Influence on Capacitive RF-MEMS Switches

RF Linear Power Amplifier Gain Stabilization

horizon house®
Founded in 1958

www.mwjournal.com

Microwave Journal

DECEMBER 2005 VOL. 48 • NO. 12

2006 IEEE MTT-S RADIO AND WIRELESS SYMPOSIUM & EXHIBITION

FEATURES

48 Years of Publishing Excellence

Microwave Journal (USPS 396-250) (ISSN 0192-6225) is published monthly by Horizon House Publications Inc., 685 Canton St., Norwood, MA 02062. Periodicals postage paid at Norwood, MA 02062 and additional mailing offices.

POSTMASTER: Send address corrections to *Microwave Journal*, PO Box 3256, Northbrook, IL 60065-3256 or e-mail mwj@omeda.com. Subscription information: (847) 291-5216. This journal is issued without charge upon written request to qualified persons working in that part of the electronics industry, including governmental and university installation, that deal with VHF through light frequencies. Other subscriptions are: domestic, $120.00 per year, two-year subscriptions, $185.00; foreign, $200.00 per year, two-year subscriptions, $370.00; back issues (if available) and single copies, $10.00 domestic and $20.00 foreign. Claims for missing issues must be filed within 90 days of date of issue for complimentary replacement.

Posted under Canadian international publications mail agreement #0738654

Microwave Journal

FEATURES

DEPARTMENTS

Cover photograph courtesy of the San Diego Convention Center; additional photographs courtesy of the San Diego Convention and Visitors Bureau; Show Guide designed by Janet MacDonald

STAFF

Publisher: Carl Sheffres
Associate Publisher: Edward Johnson
Editor: Harlan Howe, Jr.
Managing Editor: Keith W. Moore
Technical Editor: Frank M. Bashore
Associate Technical Editor: Dan Massé
Staff Editor: Jennifer DiMarco
Editorial Assistant: Barbara Walsh
Consulting Editor: Howard I. Ellowitz
Consulting Editor: Theodore S. Saad
Consulting Editor: Peter Staecker
Assistant to the Publisher: Kristen Dednah
Traffic Manager: Edward Kiessling
Traffic Administrator: Ken Hernandez
Director of Production & Distribution: Robert Bass
Design Director: R.A. Pike
DTP Coordinator: Janet A. MacDonald

EUROPE

Deputy Publisher: Michel Zoghob
European Editor: Richard Mumford
Office Manager: Eugenie Hardy

CORPORATE STAFF

Chairman: William Bazzy
President & CEO: Charles A. Ayotte
Executive Vice President: William M. Bazzy
Executive Vice President: Joan B. Egan
Senior Vice President & Group Publisher: David B. Egan

Executive Editorial Office:

685 Canton Street, Norwood, MA 02062
Tel: (781) 769-9750
FAX: (781) 769-5037
e-mail: mwj@mwjournal.com

European Editorial Office:

46 Gillingham Street, London SW1V 1HH, England
Tel: Editorial: +44 207 596 8730 Sales: +44 207 596 8740
FAX: +44 207 596 8749

www.mwjournal.com

Printed in the USA

Northrop Grumman Demonstrates JTRS Power Amplifier for Army

Northrop Grumman Corp. has successfully demonstrated the capabilities of an advanced high power amplifier for the US Army that is capable of enabling critical communications for the network-centric Future Force. Army Future Force concepts include information superiority and improved situational understanding through the integration of data from joint forces. These capabilities require a highly secure wideband network to share large amounts of real-time information among forces on the ground, sea and air. A key enabler of this capability is an efficient power amplifier with enough power to transmit wideband data waveforms such as the Wideband Networking Waveform (WNW) over distances warfighters require. WNW is currently under development by the Joint Tactical Radio System (JTRS) program. Nine months after the program's start, Northrop Grumman demonstrated that its software-defined radio (SDR) power amplifier could provide enough output power to enable WNW communications at the required range and throughput. In addition, Northrop Grumman's high efficiency design met the difficult size, weight and thermal requirements of the JTRS ground platform. All high risk areas were addressed and high efficiency and output power over an extremely wide bandwidth were achieved. Northrop Grumman's SDR power amplifier is being developed under the Army Communications-electronics Research Development & Engineering Center (CERDEC). CERDEC's Radio Enabling Technologies and Nextgen Application Army Technology Objective program develops and transitions technology insertion solutions to the JTRS program. Northrop Grumman's test program for the advanced power amplifier included an unusual stress test to explore the ability to transmit a large amount of data in a short time. The amplifier was subjected to a full-power, 100 percent duty cycle stress test for four minutes. The amplifier operated normally during the entire test and key component temperatures remained within their limits even at the end of the test interval.

Aegis Weapon System Successful in Ballistic Missile Tracking Exercise

The Aegis Ballistic Missile Defense (BMD) Weapon System successfully detected and tracked an unarmed US Air Force Minuteman III intercontinental ballistic missile (ICBM). Aegis detected the missile when it rose above the horizon and immediately began BMD tracking operations. Lockheed Martin develops the Aegis BMD Weapon System for the US Navy and the Missile Defense Agency (MDA) and also serves as the Combat System Engineering Agent. Sailors from USS Russell (DDG 59) also used the Aegis BMD Weapon System to successfully transmit Minuteman III trajectory data via satellite through the Ballistic Missile Defense Communications System to the Ballistic Missile Defense command and control center at the Joint National Integration Center in Colorado Springs, CO. The MDA and the US Navy are jointly developing Aegis BMD as part of the Ballistic Missile Defense System (BMDS). Ultimately, 15 Aegis destroyers and three Aegis cruisers will be outfitted with the capability to conduct Long Range Surveillance and Tracking (LRS&T) and engagement of short and medium range ballistic missile threats using the Aegis BMD Weapon System and its Standard Missile-3 (SM-3). To date, eight Aegis destroyers have been upgraded with the LRS&T capability and two cruisers have been outfitted with the emergency engagement and LRS&T capability. The Aegis Weapon System is the world's premier naval defense system and is the foundation for Aegis BMD, the primary component of the sea-based element of the United States' BMDS.

Harris Corp. Awarded $205 M Contract for US Marine Corps MBMMR Radios

Harris Corp. has been awarded a competitive procurement contract to supply the US Marine Corps' Multiband, Multimission Radio (MBMMR) Standardization Program with its combat-proven Falcon® II AN/117(C) radios. The first delivery orders of $67 M have been awarded as part of a multi-year $205 M blanket purchase agreement. Deliveries of the new MBMMR systems will begin in the company's second fiscal quarter. "We have had the opportunity for the past several years to provide the US Marine Corps with advanced HF and multiband tactical radios and support. The selection of the Falcon II AN/PRC-117F(C) as the MBMMR standard is a strong validation of the operational performance and reliability of our radios," said Dana Mehnert, vice president and general manager of US Government products, Harris RF Communications Division. Under the contract, Harris will supply its AN/PRC-117F(C) manpack and AN/VRC-103(V) vehicular systems. The Harris AN/PRC-117F(C) is an advanced multiband radio covering the entire 30 to 512 MHz frequency spectrum. Its embedded COMSEC has NSA certification, ensuring compliance with secure US Government Type-1 encryption algorithms. In addition, the radio is JITC certified for operations over military standard satellites. The AN/VRC-103(V) vehicular product is a fully integrated, compact communications system that includes the Harris AN/PRC-117(C) tactical radio and the Harris AM-7588 Multiband Power Amplifier. This system also covers the entire 30 to 512 MHz frequency range, offering 50 W PEP transmit power, embedded COMSEC, SATCOM and ECCM capabilities. The radios will be used to upgrade and replace the Marine

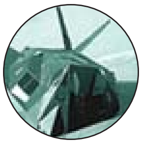

Corps active duty and reserve components legacy's tactical radio systems, and also will be used for other USMC programs such as Target Location, Designation and Hand-off System (TLDHS), Counterintelligence/Human Intelligence (CI/HUMINT) and Assault Breacher Vehicle (ABV).

Raytheon Awarded $52 M Contract to Provide ROTHR Engineering Services

Raytheon Co. has been awarded a $52 M US Navy contract to provide engineering services for the Relocatable Over the Horizon Radar (ROTHR) program. The award is a five-year indefinite delivery, indefinite quantity contract to provide continuing engineering support on the radar systems, including both hardware and software maintenance and upgrades. "This contract reflects the excellent ongoing relationship between the Navy and Raytheon, as well as Raytheon's commitment to satisfying our customer's critical needs for assured technical and program support," said Mary Petryszyn, Raytheon vice president, Joint Battlespace Integration. "We are proud that the Navy continues to look to Raytheon for reliable products and service to ensure our homeland is safe." ROTHR is a high frequency radar system designed, built, operated and maintained by Raytheon to provide long-range surveillance capability to the US Government in support of the US counter drug mission. Demonstrated performance, cost effectiveness and growth potential have led to planning for an expanding role for ROTHR to include surveillance capability for homeland defense. "As an operational and deployed asset with ground-based results, ROTHR is a reliable and cost effective proven solution for improving the security of the US coast line," said Petryszyn. ROTHR has been operational with the US Government for more than 15 years, supporting the counter drug mission in the Caribbean Sea and South America. Each radar system provides in excess of four million square miles of coverage area. The network system of ROTHR radars operates 24/7/365 and tracks 4.5 million aircraft per year. It is currently the US Government's primary surveillance system for the counter drug mission. Raytheon has provided full life cycle mission support for the radars since the initial installations to improve performance and reliability as part of Raytheon's integrated approach to predicting customer needs, sensing problems and preemptively applying solutions. Mission support enables Raytheon to maintain readiness and deliver operational capability on demand, allowing its customers to focus on their mission. ■

Ericsson to Acquire Key Assets of Marconi's Telecommunications Business

Ericsson has reached an agreement with Marconi Corp. plc to acquire the parts of the company's telecommunications business that are strategically important to Ericsson. Ericsson will acquire assets representing about 75 percent of Marconi's turnover and will pay approximately £1.2 B in cash on completion, subject to certain closing adjustments. The acquisition will add roughly £1 B in sales and is expected to have a neutral effect on Ericsson's EPS in 2006 with positive contribution from 2007.

The businesses to be acquired can be divided into two main business types, Network Equipment and Network Services. The former covers the design and supply of communications systems that transmit and switch voice, data and video traffic, including optical networking, broadband access, data networks, microwave radio and next generation switching. The businesses within Marconi's Network Equipment that will be acquired had a turnover of approximately £0.7 B in the financial year ended March 2005.

Network Services covers a broad range of support services to telecommunications operators and other providers of communication networks, including installation, commissioning and maintenance, and value-added services. The businesses within Marconi's Network Services that will be acquired had a turnover of approximately £0.3 B in the financial year ended March 2005.

The acquisition requires approval from Marconi's shareholders and clearance from the relevant competition and other regulatory authorities, including the European Commission. At the time of going to press the Board of Marconi intends to recommend that Marconi shareholders vote in favour of the transaction at an extraordinary general meeting. Subject to receipt of the necessary approvals, the transaction is expected to be completed at year-end 2005.

IEE and IIE Members Vote to Amalgamate

Two of the UK's leading engineering institutions, the Institution of Electrical Engineers (IEE) and the Institution of Incorporated Engineers (IIE), have announced that their members have voted to create a new institution, to be known as the Institution of Engineering and Technology (IET), which will come into being in early 2006. The IEE has 120,000 members worldwide and the IIE 40,000. The IEE voted 73.5 percent in favour while members of the IIE voted 95.7 percent in favour. Now that the decision has been taken, both organizations will begin the process to create the IET, which will require approval by the Privy Council.

Once formed, the IET will have the largest number of professionally registered engineers and engineering technicians in the UK, working in a wide range of sectors including ICT, robotics, manufacturing, power engineering, transport, contracting and building services, defence and the armed services.

Professor John O'Reilly, president of the IEE, said: "This is a historic step for both institutions. Members have shown themselves ready to embrace the future and ensure that institutions that have served decades of engineers remain relevant in the 21st century." He continued, "Engineering is becoming increasingly interdisciplinary and global and it is important that institutions reflect the way in which their members operate."

Likewise, Lord Trefgarne, president of the IIE, commented: "The engineering profession has for far too long been fragmented and undervalued. By bringing together all key members of the technical team, whatever their professional status, IET holds out the hope of creating a more coherent and representative organization for our profession." He added: "The new institution will be better attuned to meet the needs of its members, of employers who need well qualified staff, and of wider society which benefits from the products and services underpinned by our collective efforts."

East European Wireless Profitability Continues to Slide

In its *Wireless Operator Benchmarking Report Q2 2005*, Strategy Analytics reports that average margins per user (AMPU) in Central and Eastern Europe fell almost 30 percent in 2Q 2005. Operators are losing ground with AMPU levels 50 percent below the global average in the current quarter.

"On face value, the rapid fall in the value of new subscribers in Russia and the Ukraine is a cause for concern, although underlying profitability remains strong," explained Sara Harris, senior industry analyst at Strategy Analytics and the report's author. "Exceptional subscriber growth in those countries is driving strong EBITDA growth, ranging from 19 percent at MTS to 55 percent at Vimpelcom. This is still a lucrative region for global operators."

David Kerr, vice president of the Global Wireless Practice, added, "By contrast, EBITDA growth was 10 percent in North America and a meager 2 percent in Western Europe. Following more than three years of growth, AMPUs have posted annual declines for the last three quarters in Western Europe and there is no return to growth in sight. Regulatory pressure on interconnect rates, sluggish data AMPUs, and an increasingly competitive market driven by limited subscriber growth, MVNO activity and 3G launches, are all taking their toll on financial stability in the region."

Northrop Grumman Wins German Navy Radar Contract

Northrop Grumman's UK-based Sperry Marine has been awarded a $4.3 M contract to retrofit new-generation navigation radars on more than 100 German Navy warships from ET Marine Systeme GmbH, prime contractor for the navigation-systems modernisation programme.

Under the four-year contract, the ships' existing navigation radars will be replaced by Sperry Marine's BridgeMaster E 340 radar systems, including commercial, navalized and tactical variants, in X-band, S-band and dual-band configurations. The contract includes training, spares, installation, engineering and project-management support. ET Marine Systeme will integrate the radars with the ships' electronic chart display and information systems and automatic identification systems.

The first installations are scheduled to take place in the first quarter of 2006. In the meantime, Sperry Marine is supplying BridgeMaster E systems for the German Navy training school and test sets.

Harris Gives Nigerian Network More Backbone

MTN Nigeria has selected Harris Corp. to provide microwave radios that will increase the capacity of the existing Y'hello Bahn high capacity GSM network backbone by 75 percent. Orders of $4.1 M have been received for MegaStar 155 PX microwave radios that will augment what is already the largest wireless network backbone in Nigeria, spanning more than 4,500 km and traversing more than 120 towns and villages.

A key requirement of the new agreement is to counteract the difficult propagation conditions in various regions of Nigeria, such as wide variability related to temperature, humidity, geography and vegetation. The MegaStar 155 PX high capacity synchronous digital microwave radio for OC-3 or STM-1 transport meets these requirements. It operates in the 5, 6, 7, 8 and 11 GHz bands, interoperating with standard SONET/SDH multiplexers and ATM switches, and features a wide selection of antenna coupling unit arrangements that accommodate both standard and non-standard channelization plans. ■

Industry/Academic Partnership Brings Electronics Skills to Chicago Students

Members of the Great Lakes Chapter of Surface Mount Technology Association (SMTA) and the Chicago Public Schools-Education to Careers (CPS-ETC) Program reaffirmed their success and commitment to a program that has brought hands-on knowledge of electronic manufacturing into the classrooms of Chicago students eager for real-world experience and education. SMTA and CPS-ETC leaders held a press conference and spoke of the ongoing success of a program well into its third year that prepares students for their lives beyond the classroom, by combining a rigorous academic program with career and technical education, hands-on training and exposure to the career world. The Great Lakes Chapter of SMTA has worked for the last two and a half years with the CPS-ETC program and the local high tech manufacturing community to align ETC's electronics manufacturing curriculum with industry standards. Program leaders engaged Institute of Printed Circuits (IPC), the recognized industry standards authority, and made a substantial financial contribution that allowed ETC electronics instructors to become IPC-certified in August 2005. Working in conjunction with Chicago schools, the Great Lakes Chapter developed the Electronic Manufacturing Education Model program. This program is unique at the high school level and is an example of the collaboration that can make schools and business communities more successful. Richard Wierzbicki, the local teacher who worked with the SMTA to implement the program, said, "Our students have responded with enthusiasm to this program and have shown considerable interest in all aspects of the electronics manufacturing industry and skills, from circuit design and software to actual manufacturing processes such as soldering and tests. The practical, real-world experience that this program provides is something they really want." For more information about the CPS-ETC Electronics Manufacturing Program, visit www.etcchicago.com.

EPC Data Sharing Highlights RFID Collaboration

In early supply chain RFID deployments, the information flowing back to suppliers has been fragmented and limited. But the recent joint announcement by Target and Wal-Mart that they will share EPC data gathered from their RFID systems with 13 manufacturers who supply them with consumer packaged goods (CPG) marks a significant development. According to Erik Michielsen, ABI Research director of RFID and ubiquitous networks, the data-sharing pilot reinforces the notion that there is a need to consolidate data across fewer platforms to ensure its reliability and interoperability in retail environments. The fact that 13 major CPG players will be working together with Target and Wal-Mart also reinforces a second trend in the RFID supply chain. To date, the retailers have driven RFID momentum with mandate announcements and, in the case of Wal-Mart, continued rollout roadmap communication. Michielsen notes, "As analytical tools develop and as CPG cooperate more with one another, the CPG-retailer relationship will evolve from a retail 'push' market to a more balanced retail/CPG 'push-pull' market." The University of Arkansas' out-of-stock RFID findings illustrate that CPGs can benefit from RFID. Tag costs are decreasing, data sharing and analysis tools are improving, and the RFID opportunity is becoming clearer and more compelling. As both industry RFID motivations move toward equilibrium, RFID investments will likewise become more substantive and convincing. Retail and consumer goods RFID deployments involve cooperation, partnership, planning and integration. The latest release of ABI Research's "RFID Research Service" details network infrastructure management opportunities and profiles the stakeholders.

Challenges Loom for Delivery of Wireless Mesh Network Promises

Seemingly, not a day goes by and another governmental organization is announcing plans to build a wireless mesh network. The value of these networks is clear — communities can cost effectively provide high speed wireless voice and data communication services to their employees, residents and visitors. The challenges associated with realizing the benefits of these wireless networks are significant. With ten years of experience in wireless network development and implementation, Wireless Valley's team of wireless industry experts have seen the benefits and pitfalls of these deployments and are helping customers address the challenges. The implementation of a wireless mesh network can be deceivingly simple. Install the access point (AP), plug it into an electrical source and turn it on. The APs automatically identify and connect to other APs in line of sight. In reality, this is rarely, if ever, the case with wireless deployments. Wireless Valley chief product officer, Dr. Roger Skidmore, points out, "If you do not consider and plan for all of the operational and environmental factors which impact each installation, the network will not have the necessary coverage and capacity to provide the quality of service expected by users. In many cases, this renders the network useless for many of the intended applications. This is especially detrimental if public safety or emergency medical teams hope to communicate using the network." In order to properly set up a municipal wireless mesh network, planners need to consider the following three issues:

• *Environment* – Many factors impact the performance of wireless signals. The construction and location of buildings, foliage and other natural and manmade obstructions can degrade or block wireless signals.

• *Use of the network* – The number of users accessing the network and the type of applications they will employ are important to consider. For example, significantly more users will access the network in a government office than in a parking lot. Also, applications such as public safety communications require high bandwidth and secure, uninterrupted service.

• *Coverage and connection* – One of the benefits of a mesh network is that all the APs can potentially share information with each other and transport traffic. However, if the traffic has to travel through too many APs in the mesh before it gets to a backhaul connection, the user will experience unacceptable delays. At the same time, it is important to make sure that there are enough connections available to each AP to ensure redundancy. If one or several APs are not operational, the network should still be able to function efficiently if it has been designed properly. Obviously, this 'balancing act' between coverage and connections can be quite difficult to determine.

The traditional way to plan and design wireless networks is through a site survey. This process involves powering up an AP in a part of the area to be covered, taking measurements of signal strength and coverage and then repeating the exercise until you have covered the entire region. This highly manual and time-consuming process is not practical for most municipal mesh projects, which are usually quite large in scope. Plus this method only enables planning for wireless coverage; it does not consider how the network will be used and what applications will be operating. The preferred alternative is a combination of computer-based design with a limited site survey used to optimize the design. This method enables a repeatable and scalable process in which users place APs and select which ones will have wired connections to the network, run simulations of the proposed network's operation and adjust the design to address any identified coverage holes and capacity problems. Perhaps most important, this method understands and accounts for two items not considered in a site survey: the environmental and interference factors, which impact the wireless signal and the capacity and bandwidth needs of the network. Once the design is complete and the network implemented, the user can conduct a limited site survey to determine any adjustments that might be necessary. Properly planning a wireless mesh network will bring many benefits including more complete coverage, faster speed, strong reliability, ease of deployment, and lower implementation and operational costs. ■

INDUSTRY NEWS

■ **Pendulum Instruments AB**, Stockholm, Sweden, and **XL Microwave Inc.**, Oakland, CA, announced they have reached an agreement for Pendulum to acquire the assets and operations of XL Microwave. XL Microwave develops and produces microwave counters and antenna alignment products and has existing sales partner relationships in the US. Through the acquisition, Pendulum will establish a daughter company called Pendulum Instrument Inc. in the current premises of XL Microwave.

■ **EMS Technologies Inc.** announced the signing of a definitive agreement for the sale of the assets and operating liabilities of its Space and Technology/Montreal division to **MacDonald, Dettwiler and Associates Ltd.**, Vancouver, BC, Canada. The parties are seeking to close the transaction during 2005, subject to the satisfaction of normal closing conditions and clearance by Canadian antitrust authorities. The terms of the transaction were not disclosed.

■ **EPCOS**, a manufacturer of passive electronic components, has decided to sell its Tantalum Capacitors Business Unit. Negotiations with a US manufacturer of capacitors, **Kemet**, are already in an advanced stage. The decision to sell the business unit is part of a repositioning of the product portfolio.

■ **Richardson Electronics Ltd.**, a global provider of engineered solutions for the RF, wireless and power conversion markets, announced it has reached an exclusive agreement with **Mimix Broadband Inc.**, a supplier of gallium arsenide (GaAs) semiconductors. Under the terms of the agreement, Richardson Electronics has secured exclusive global distribution rights to Mimix's diversified line of GaAs semiconductor products that span the spectrum from DC to 50 GHz.

■ **Agilent Technologies Inc.** announced several plans for its product lines following its recent acquisition of the business of Eagleware-Elanix. Expected changes include price decreases, a new customer investment protection program, Advanced Design System translators and a trade-in offer to users of non-Agilent software. The price decrease is for non-US Eagleware-Elanix customers only and is made possible through the efficiency gains Agilent expects to make in its global infrastructure.

■ **Sage Laboratories Inc.** celebrated the opening of its new state-of-the-art manufacturing facility in Hudson, NH. The 55,000 square foot facility was completely renovated to accommodate the RF/microwave production flow of the company's products. From standard catalog components to highly sophisticated integrated subsystem and multi-function assemblies, products follow an efficient manufacturing path from incoming inspection through assembly, test and to the shipping dock. Previously, Sage Laboratories had occupied facilities in Merrimack, NH and Natick, MA. Combining the two groups enhances the capabilities of the company by blending past practice design engineering and manufacturing technologies from each into the facility in Hudson.

■ **Sigma Systems Corp.** announced that it has moved to a 10,000 square foot facility in El Cajon, CA. It is still in the greater San Diego area, and only about 10 minutes from the company's original location of almost 50 years. The new address is: 1817 John Towers Avenue, El Cajon, CA 92020 (619) 258-3700 or fax: (619) 258-3712.

■ **AR Worldwide RF/Microwave Instrumentation** has completed construction of a microelectronic laboratory that meets requirements for Class 100K and Class 10K environment conditions. The new lab is being used to produce hybrid circuits based on thin and thick film substrates. The new microelectronic capabilities enable the company to extend its product frequency range performance from 10 to 25 GHz and eventually beyond.

■ **Microfabrica**, a manufacturer of micro-device and micro-system fabrication, announced it has moved its factory and corporate headquarters from Burbank to a new facility in Van Nuys, CA, spurred by the company's growth. The new site is 39,300 square feet, nearly twice the size of the previous location. The building, located at 7911 Haskell Avenue, contains a state-of-the-art custom-built clean room.

■ **Applied Wave Research Inc.** (AWR®) and **Flomerics** announced a partnership that will enable RF/microwave engineers analyzing circuit layouts using AWR's Microwave Office® software to study the electromagnetic performance of key components in 3D using the Micro-Stripes software from Flomerics.

■ **Chipcon AS**, a supplier of ZigBee-ready integrated circuits, and **Cirronet Inc.**, which has incorporated Chipcon ICs into a broad line of ZigBee products, have aligned to facilitate the creation of third-party ZigBee wireless solutions. Under the arrangement, Chipcon and Cirronet will partner to provide developers complete module-level solutions for industrial ZigBee applications.

■ **Mathsoft®** announced the integration of its Mathcad software with the **National Instruments** LabVIEW graphical development environment to provide advanced joint calculation and measurement solutions. The integration will create an end-to-end design, measurement, analysis and reporting environment that will help engineers more efficiently, accurately and intelligently execute product development work.

■ **Digital Fountain Inc.**, a supplier of forward error correction technology for reliable communications, announced that its patented DF Raptor™ technology has been standardized by **3GPP**, the 3rd Generation Partnership Project, as a mandatory component of the Multimedia Broadcast/Multicast Service for 3rd generation cellular networks.

■ **Dynaco**, a fabricator of high reliability rigid-flex, flex and rigid printed circuit boards and assemblies for the military/aerospace market, has announced that it has been certified as a Small Disadvantaged Business by the US Small Business Administration.

■ **RLC Electronics Inc.** now offers the capability of 10-day production for certain filter items. This service has actually been in place for several years and the company feels confident to roll this official program out across its worldwide customer base. This 10-day production service charge is a nominal 50 percent premium from the base price.

■ **Times Microwave Systems** has significantly lengthened its warranty and now offers a One Year Replacement Warranty on SilverLine™ TuffGrip™ test cables for wireless RF field testing applications. The new warranty stipulates that for a period of one year from shipment, Times will repair or replace the cable, at its option, if the connector attachment fails.

■ **RF Monolithics Inc.**, a developer, manufacturer and supplier of radio frequency wireless solutions, announced that the US Federal Communication Commission (FCC) has certified the company's DM2100™ module, a mesh-enabled low power module. In related news, the company announced it has obtained ISO/TS 16949:2002 automotive quality certification and ISO 14001 certification.

CONTRACTS

■ **M/A-COM** announced that the company has signed a contract to design, deploy, operate and maintain New York's Statewide Wireless Network with the **New York State Office of Technology.** The contract amount is valued at approximately \$2 B over 20 years, making it the largest statewide public safety communications project to be awarded in the United States.

■ **Symmetricom Inc.**, a designer and manufacturer of precise time and frequency products and services, announced the company was awarded a contract from **Dell Inc.**, a diversified information-technology supplier and partner, worth \$995,000 for Symmetricom's TymServe 2100™ versatile GPS network time servers, a durable, dependable and accurate NTP server.

■ **Modelithics™** has completed the first phase of substrate-scalable models for **Dielectric Laboratories'** (DLI) Opti-cap,® Milli-cap,® Ultra High-Q and other surface-mounted capacitors. Modelithics is now distributing free S-parameters for the components from its Web site to the DLI landing page at www.modelithics.com/mvp/dli/. Modelithics also announced the availability of new Global Models™ that represent entire families of components on all common substrate types and thicknesses. The models will be distributed and supported along with future releases of Modelithics CLR Library™ software.

FINANCIAL NEWS

■ **Andrew Corp.** reports sales of \$517 M for the fourth quarter ended September 30, 2005, compared to \$487.8 M for the same period last year. Net income for the quarter was \$7.2 M (\$0.04/per share), compared to a net income of \$0.6 M (\$0.00/per share) for the fourth quarter of last year.

■ **RF Micro Devices Inc.** (RFMD) reports sales of \$177 M for the second quarter of fiscal 2006 ended September 30, 2005, compared to \$149.1 M for the same period last year. Net income for the quarter was \$5.9 M (\$0.03/per diluted share), compared to a net loss of \$6.7 M (\$0.04/per diluted share) for the second quarter of last year. In related news, RFMD announced that it has entered the market for DC-DC converter power management components. Concurrently, the company announced that it has commenced shipments to a tier-one handset manufacturer for use in CDMA handsets.

■ **Silicon Laboratories Inc.** reports sales of \$103.9 M for the third quarter ended October 1, 2005, compared to \$121 M for the same period last year. Net loss for the quarter was \$745,000 (\$0.01/per diluted share), compared to a net income of \$21 M (\$0.39/per diluted share) for the third quarter of last year.

■ **ANADIGICS Inc.** reports sales of \$29.3 M for the third quarter ended October 1, 2005, compared to \$25.1 for the same period last year. Net loss for the quarter was \$6.8 M (\$0.20/per share), compared to a net loss of \$8.3 M (\$0.25/per share) for the third quarter of last year.

■ **WJ Communications Inc.** reports sales of \$8.1 M for the third quarter ended October 2, 2005, compared to \$8.9 M for the same period last year. Net loss for the quarter was \$3.4 M (\$0.05/per common share), compared to a net income of \$1.2 M (\$0.02/per common share) for the third quarter of last year.

■ **Superconductor Technologies Inc.** reports sales of \$3.9 M for the third quarter ended October 1, 2005, compared to \$7.3 M for the same period last year. Net loss for the quarter was \$3.6 M (\$0.03/per diluted share), compared to a net loss of \$5.2 M (\$0.06/per diluted share) for the third quarter of last year.

■ **RF Industries Ltd.** reports sales of \$3.3 M for the third quarter ended July 31, 2005, compared to \$2.7 M for the same period last year. Net income for the quarter was \$194,000 (\$0.05/per diluted share), compared to a net income of \$266,000 (\$0.07/per diluted share) for the third quarter of last year.

PERSONNEL


▲ Kevin Beber

■ California Eastern Laboratories (CEL) announced that **Kevin Beber** has joined the company as vice president of worldwide sales. With twenty years' experience in the high technology and semiconductor industry, Beber will guide the restructuring of the company's sales organization. He comes to CEL from Lumileds Lighting where he served as vice president of Asia Pacific sales. Prior to Lumileds, Beber spent 15 years with Hewlett-Packard and Agilent, most recently serving as director of marketing for Agilent's Wireless Semiconductor Division.

■ Xpedion Design Systems Inc. announced the additions of **Steve Lloyd**, vice president of engineering for Beceem Communications, **Vladimir Aparin**, senior RF designer for Qualcomm, **Asad Abidi**, professor of electrical engineering at UCLA, and **Tom Lee**, associate professor of electrical engineering at Stanford, to its technical advisory board. These additions will provide the company with expert guidance on product direction to meet the demanding needs of future RFIC design.

■ NEC America Inc. announced that **Bruce Blain**, vice president of NEC's Radio Communications Systems Division, has been elected to the National Spectrum Managers Association (NSMA) board of directors. The NSMA is a voluntary international association of top executives in the microwave and wireless telecommunication industries. Having a strong background in the digital microwave radio industry, Blain will provide NSMA valuable insight on market trends, development issues, as well as manufacturing and industry standards.

■ Aeroflex Inc. announced the appointment of **Fred Jiang Qi** as China country manager for its test and measurement group. In this position, Qi will be responsible for all of the company's test solutions sales activities in China. He will also coordinate product installations, customer training and support. Qi comes to Aeroflex with 15 years experience in the test and measurement industry.

■ Aeroflex-Weinschel Inc. announced that **Dave Hardesty** has accepted the position of vice president of sales and marketing for the company. Most recently, Hardesty held the position of manager of Federal Business Development and Marketing at LTI DataComm, a federal systems integrator. He has over 18 years of network engineering, sales and marketing experience with commercial and government customers. He can be reached at (301) 846-9222 or e-mail: david.hardesty@aeroflex-weinschel.com.

■ Elcoteq Network Corp. announced that **Mitchell Schoch**, former VP sales and account management for Solectron, has been appointed vice president, sales and marketing, Elcoteq Americas. Schoch has a strong background in sales, marketing and strategic development and extensive experience working in the EMS industry and high tech companies.

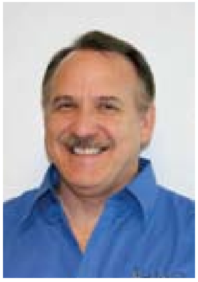

▲ *Bob Bayruns*

■ Jacket Micro Devices Inc. (JMD), a provider of organic RF integrated passive products, announced that **Bob Bayruns** has joined the company as vice president of engineering. Bayruns has over 25 years of experience in the design of RF semiconductor components and systems. Most recently, he served as vice president of engineering and product development at WJ Communications Inc.

■ Renaissance Electronics Corp. announced that **Thomas Daly** has joined the team as a sales and marketing specialist for the Waveguide Division. Daly brings to Renaissance extensive experience in the telecommunication industry along with a proven track record of sales leadership, which will further enhance the company's customer focused expertise.

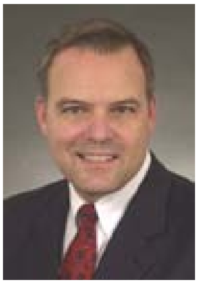

▲ *David Lipari*

■ Rogers Corp. announced that **David Lipari** has been named the new marketing manager of its Advanced Circuit Materials Division, located in Chandler, AZ. In his new assignment, Lipari will be responsible for the management of the business unit's global marketing function, including market development, product management, customer service and technical support. Lipari has served as vice president of marketing/operations at Techloss Consultants and also as international sales and marketing director at Motorola.

REP APPOINTMENTS

■ The founders of **Associated Technical Sales LLC** (ATS) announced the company's debut as manufacturers' representatives in southern California. ATS will provide full-service technical sales representation of technologies for the mixed-signal, RF, microwave and lightwave markets in southern California. For more information, please contact ATS at (877) 287-1737 or visit www.ats1rep.com.

■ **G.T. Microwave Inc.**, Randolph, NJ, announced the appointment of two new representatives to cover foreign territories. **Telecom Associates** has been allotted the task of covering prospective customers in the Asian Rim, Africa and South America. **Telprom S.r.l.** will be responsible for Italy.

■ **Technical Research and Manufacturing**, a designer and manufacturer of RF and microwave passive signal control components, announced several new rep appointments. **RF Microwave Ltd.** will be responsible for all of Canada; **Technical Marketing Associates** will handle northern California; **Con-Tek Marketing** will cover Colorado, Utah and Wyoming; **RF Microwave Inc.** will be responsible for Arizona and New Mexico; and **Ranier Marketing** will handle the Pacific Northwest.

WEB SITE

■ **TestMart** *SellDirect* is a new on-line marketplace that offers free buyer protection, unlimited free seller listings to those buying and selling scientific and technical equipment. The new marketplace eliminates inherent risks, upfront costs and high fees that may be associated with existing pre-owned equipment markets and auction Web sites. More than 3000 equipment listings have been posted at www.selldirect.testmart.com.

RF LINEAR POWER AMPLIFIER GAIN STABILIZATION OVER AMBIENT TEMPERATURE

The temperature stability of the RF output power level has become especially important for different handheld wireless communication systems. For GSM mobile handsets, an analog closed-loop power control, incorporated in the transmitter power amplifier (PA) chain, allows the main parameters of the PA to be stabilized over the ambient temperature range required by industry standards. This can be done due to a fixed level of the input power driving the GSM PA. However, the power level stabilization for the driver stages is still an important issue. This can be done as well, at the expense of some efficiency degradation of the PA. All existing CDMA mobile transmitters (cellular, PCS, UMTS, cdma2000) do not have a direct closed-loop power control of the RF PA, resulting in the need of a careful design, taking into account the temperature stability of the parameters as one of the main features. Gain variations of 3 to 5 dB over the operating temperature range are usual in existing CDMA PA with fixed drive signal levels and fixed bias and control voltages.

For WLAN applications, Intersil (now Conexant) utilizes a closed-loop power control for the 802.11b/g frequency band (2.4 to 2.5 GHz). Here, a power detector samples the transmitter output power and the base band chip adjusts the power with a certain tolerance. This approach works well to compensate for the temperature variations of an entire transmitter chain as well as component production tolerances. However, the component tolerances in the output chain between the power detector and the antenna connector, as well as the accuracy of the detector characteristics using standard components and existing PCB structures from different vendors, are still creating output power variations of at least ±1 dB at temperatures between +25° and +85°C.

ATMEL utilizes an open-loop control circuit approach for its 802.11b WLAN system PA. It uses a thermistor to stabilize the PA parameters.

OLEKSANDR GORBACHOV
STMicroelectronics
Taipei, Taiwan

However, the changes in output power still exceed 2 to 3 dB over the +25° to +85°C temperature range. Not just the transmitter front-end shows variations of output power over temperature because of the output PA used in the circuit. The small-signal RFIC transceiver driving the final PA itself has at least a 1 dB power drop between +25° and +85°C. The test results also depend on the platform used because of the different heat sinking. In the meantime, the PA is the most current consuming device in the transmitter chain and its behaviour plays a crucial role in the output power temperature dependence. An important fact is that the RF PA, used for wireless applications, is a nonlinear device operating under large-signal conditions, resulting in variations of its spectral characteristics over temperature as well (not only gain and power). Because the current need of the industry is low power consumption, the PA vendors are supplying amplifiers with high efficiency. In this case, the spectrum efficiency (ACPR) and digital signal quality (EVM) may be degraded even if one can stabilize the output power by driving the PA input with a closed loop like Intersil. On another side, a large temperature variation requires a larger dynamic range of the transceiver, creating stability problems and increased current consumption (to have a large enough margin to compensate for gain variation). Moreover, the temperature calibration is a time and cost consuming process during mass production. Therefore, one has to stabilize the power output with small variations of the transmitter gain, retaining a reasonable spectrum purity and digital signal quality (such as EVM). This article presents a possible low cost solution that could be used in different wireless communication transmitters using a "linear" PA.

METHODS USED FOR STABILIZATION

The main parameters of RF CDMA power amplifiers, which are influenced by ambient temperature variations, are power gain and linearity expressed in adjacent channel power ratio (ACPR) for adjacent and alternate channels. The gain and ACPR (at the rated output power) variations over temperature are caused by many factors, such as the transistor current gain (β) change with temperature, leading to an alteration of the I-V characteristics, the f_r and f_{max} values change with the particular current setting of the transistor used and the heat dissipation ability from the active cells of the PA to the heat sink, etc.[1] Moreover, all of these variations are dependent on the initial (quiescent) bias conditions of the PA. The situation becomes more complicated with the requirements for a small quiescent current when the idle bias operating point requires class AB or near to class B operation of the PA. The wide range of operating current and self-biasing effects present more challenges with parameter variations.

Consider GaAs HBT power amplifiers that are mostly used today in the wireless industry. The collector current of an HBT, biased by a voltage source through the base resistor R_B, can be expressed as[2]

$$I_C = I_S \exp\left[\frac{q}{kT_0}\left(V_{BE} - I_B R_B + \alpha\left(T - T_0\right)\right)\right] \qquad (1)$$

where

I_S = saturation current
V_{BE} and I_B = base emitter voltage and base current, respectively
T_0 and T = ambient and junction temperature, respectively
α = thermo-electric feedback coefficient ($\alpha \approx$ 1.2 to 1.3 mV/°C for GaAs HBT)

The base current can be represented as

$$I_B = \frac{I_C}{\beta} + I_P = \frac{I_C}{\beta} + CI_C \exp\left(-\frac{\Delta E}{kT}\right) = I_C\left[\frac{1}{\beta} + C \exp\left(-\frac{\Delta E}{kT}\right)\right] \qquad (2)$$

where

I_P = hole current component
C = hole and electron current ratio at the emitter junction at $\Delta E = 0$
ΔE = effective difference in energy barrier seen by electrons and holes

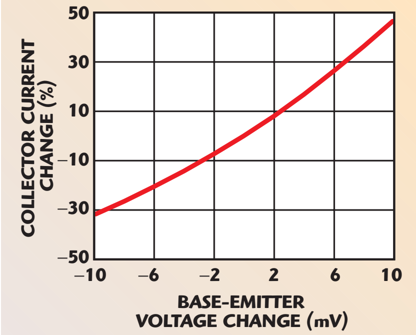

▲ *Fig. 1 Typical collector current variation vs. base voltage for HBT transistors.*

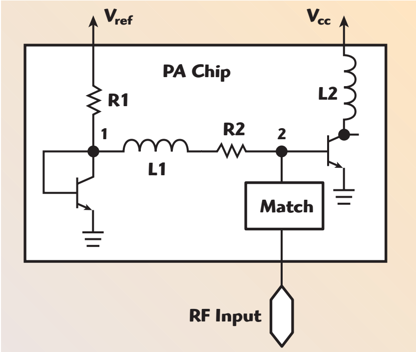

▲ *Fig. 2 Current mirror circuit for biasing PA stages.*

β = current gain

At the collector-emitter voltage V_{CE} applied to the transistor, the junction temperature can be expressed in the form

$$T = T_0 + R_{th} I_C V_{CE} \quad (3)$$

where

R_{th}= thermal resistance of the HBT from the junction to the heat sink

From Equations 1 and 2, one obtains

$$V_{BE}(T) = \frac{kT_0}{q} \ln \frac{I_C(T)}{I_S(T)} + I_C(T) R_B \left[\frac{1}{\beta(T, I_C)} + C(T) \exp\left(-\frac{\Delta E(T)}{kT}\right)\right] - \alpha(T - T_0) \quad (4)$$

For reference, ***Figure 1*** shows the simulation plot (Equation 4) of the collector current change in percent, versus the base voltage change in mV for the reasonably high current levels used in a mobile GaAs HBT-based PA at a fixed temperature (the base ballast resistance has been chosen to be minimum as well). Although the process variations and the absolute temperature may change this plot a little, this curve gives a good starting point to evaluate a PA and tune the circuit.

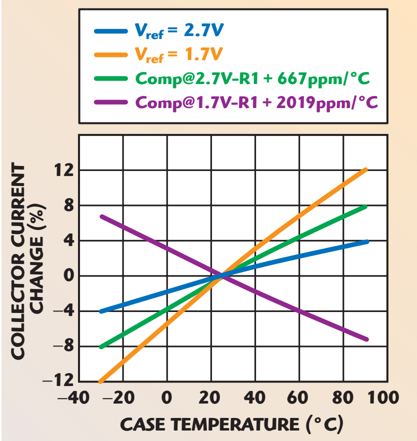

▲ *Fig. 3 Current mirror circuit temperature stability.*

It is known that stabilizing the power gain and collector current over temperature at different power drive levels results in a stable output power and spectrum purity for digitally modulated standards with non-constant power envelope signals such as QPSK, OFDM, etc.[3] From Equation 4, one can see that maintaining a constant base voltage for the transistor results in a very complex temperature dependence of the collector current. Even for a fixed ambient temperature, a positive temperature feedback loop inside the semiconductor hetero-structure results in obvious variations of the I-V characteristics for different base resistances connected for measurements.[2] Connecting a "right" base resistance value can cure this problem for a fixed temperature.[2] This resistance value, however, is dependent on the absolute temperature and this approach cannot be implemented over a wide temperature range. As well, the thermal resistance variations between the transistor and the heat sink play a great role in the compensation. This base ballast resistance is usually chosen as low as possible to prevent the so-called thermal runaway in HBT structures (both GaAs and SiGe devices[4]) and protect them from destruction and, at the same time, to maintain the highest possible power gain value. The β value for the transistors available in industry varies from one vendor to another (within 50 to 300 in most cases) and is dependent on the particular technology process used. Each

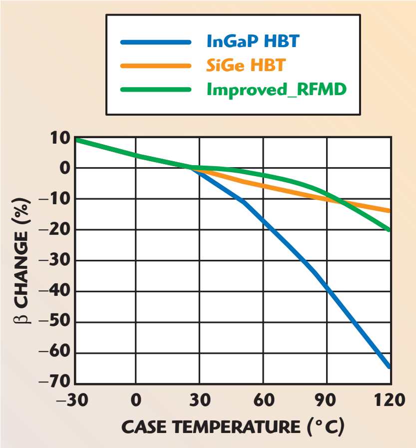

▲ *Fig. 4 Typical current gain change over temperature for different HBTs.*

foundry provides different transistors with different temperature dependence of the current gain.

The common way to stabilize the HBT temperature parameters is the current mirror circuit presented in ***Figure 2***. This circuit allows the collector current to be stabilized over wide temperature variations. R2 is the base ballast resistance. The collector current through L2 is proportional to the current through R1. The simulated collector current change versus temperature for this circuit is shown in ***Figure 3*** for two different reference voltages applied to the V_{ref} pin (2.7 V is often used for high power operation and 1.7 V is often used for low power CDMA PA operation to save current consumption[5]). It shows that the current mirror circuit can maintain the collector current within ±4 percent for large current operation. However, this variation reaches ±12 percent if one wants to implement the low power operation function as well. By choosing

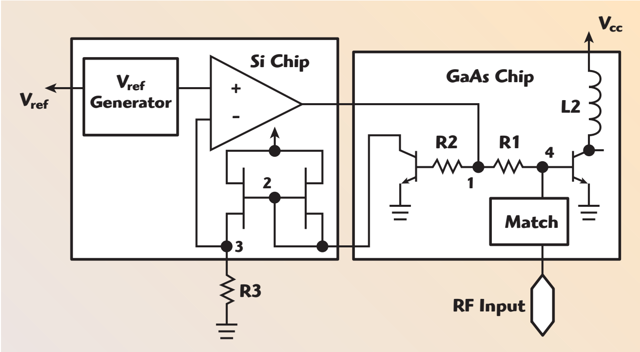

▲ *Fig. 5 RFMD CDMA PA closed-loop current control circuit.*

the resistor R1 as an external one, with a positive temperature coefficient of approximately +667 ppm/°C, one supposedly can stabilize the collector current for large-signal operation. At the same time, the small-signal current stability could also be improved. If one chooses the external resistor R1 with a +2019 ppm/°C temperature coefficient for the final small-signal current stabilization, the large-signal current temperature stability becomes worse. Therefore, some trade-off is needed if one has to use the power saving ability. More complicated current mirror and other biasing circuits are available to minimize the gain variations of bipolar transistors over temperature.[6]

The entire previous discussion above could be true if the β of the transistors used in the circuit is independent of temperature. However, even for the InGaP structures, which claim the "lowest" sensitivity of parameters over temperature (compared to the AlGaAs previously widely used in industry), the β variation over operating temperatures exceeds 40 percent[7] for a fixed collector current and is directly transformed into power gain variations. For reference, ***Figure 4*** shows some typical dependences of β versus temperature for a fixed collector current for InGaP and SiGe HBTs available in the market (the current density has been chosen reasonably high). It is obvious that β is decreasing at elevated temperatures. The SiGe HBT has a much lower temperature dependence than the GaAs device (this depends on the Si and Ge relative contents in the structure). Sometimes β has a maximum value at mid-temperatures that is dependent on the particular structure used and current density chosen. RFMD has developed a special molecular beam epitaxy process (MBE) for InGaP HBTs to keep β almost constant versus temperature. This process is currently used for W-CDMA PAs.[7] Careful design of the SiGe HBT profile avoids variation of β over temperature or even "reverses" its slope.[8] Alvarino, et al.[7] are also using a closed-loop current control circuit shown in ***Figure 5***.

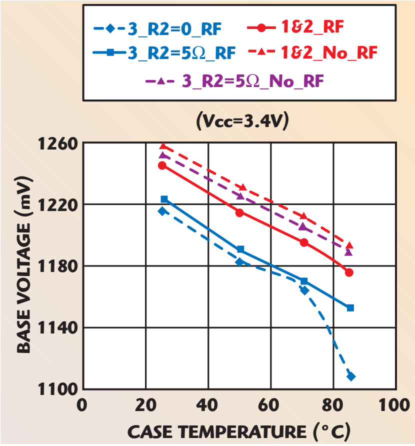

▲ *Fig. 6 Base voltage for constant output power and collector current.*

Each transistor stage on the GaAs chip has a control circuit provided by the silicon chip. Both chips are embedded into the same plastic package. Only the precise reference voltage resistor R3 is placed outside the package. The variation of the quiescent current is within 12 percent of the nominal value at room temperature for a 3.4 V bias supply and standard production tolerances.[7] Although the quiescent current is tightly controlled, the power gain variation versus temperature between –30° and +85°C reaches 5 dB at the frequency extremes for a maximum rated power of 27.5 dBm for WCDMA operation. Therefore, to stabilize the gain at large-signal operation, one has to fix the large-signal current (for reference, the quiescent current for a PA used in mobile communications can be 5 to 10 times lower than the large-signal current).

PROPOSED CIRCUIT AND TEST RESULTS

Usually, all the power amplifiers for wireless communications available in the industry utilize a stable voltage reference provided externally or internally by the low dropout voltage regulator (LDO). This stability requirement is made obvious from the curve of collector current variation as a function of changes in base voltage. Instead of keeping this voltage constant, one has to change it over temperature to keep the gain and output power constant. The question is, what should be this dependence? To evaluate it, the bias mirror circuit (three-stage InGaP HBT PCS-CDMA PA) has been used where the voltage mirrors and each active transistor has been biased directly from the voltage source through the small ballasting resistor R2. All RF matching has been maintained as for standard uplink PCS-CDMA operation with maximum available output power of 28.5 dBm for the particular transistor stage and an ACPR of approximately –50 dBc. Three different size transistor structures (correlated with particular stages) with 250 μm^2, 950 μm^2 and 6750 μm^2 emitter areas have been tested (the current density is approximately 20 kA/cm^2). The reference voltage has been adjusted and the base-emitter voltage has been measured over temperature while keeping the collector current constant. The test results for those transistor stages are shown in ***Figure 6***.

The lower blue dashed line represents directly the base-emitter voltage for the largest transistor (marked as no. 3). The blue solid line is the voltage measured through a 5 Ω resistance inserted in series with the base of the same transistor. It is obvious that the insertion of the 5 Ω resistance is preventing a thermal runaway at temperatures higher than +70°C and it "linearizes" the base voltage curve needed to maintain a constant collector current. The small-size transistors' stages already have series base ballast resistances on-chip greater than 30 Ω and the base voltage versus temperature needed to stabilize the collector current is linear as well. The same behaviour applies for both large-signal operation and idle current. Moreover, it can be seen that all base voltage curves are almost parallel to each other. Therefore, if one can provide a decreasing linear reference voltage dependence over temperature, a stable collector current and output power can be achieved. The same result can be found from Equation 4, using a reasonably large base resistance value. An absolute voltage level is not as important as the temperature slope. Of course, it should not be forgotten to put a large enough value of a ballasting resistance and not to supply the base directly from a voltage source to prevent a thermal runaway. In this case, a simple resistive divider circuit may be used for all stages with biasing from a single voltage reference source.

To verify the proposed principle of output power stabilization over tem-

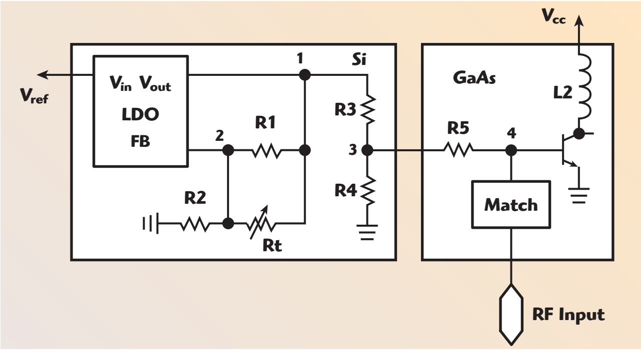

▲ *Fig. 7 Test circuit used for current stabilization over temperature.*

perature, the circuit in ***Figure 7*** has been used. A high precision adjustable LDO, with ±1 percent tolerance, has been used to provide a stable reference voltage to all three transistor stages of the amplifier. In the feedback circuit, a resistive divider with one thermistor has been used to provide a decreasing, "almost" linear voltage at the appropriate level (this approach is similar to the one used by MAXIM to drive LCD displays[9]). The resistors R1, R2 and Rt play the main role; R3, R4 are used just to shift the absolute voltage to the level needed for each particular stage. All three base chains are connected to the point 1 of the circuit through the ballast resistors R5. The LDO used had a 1.235 V nominal reference voltage. The negative temperature coefficient (NTC) thermistor type 0402 has been used as a control element (±5 percent nominal tolerance and B = 3650K ±3 percent). A linear slope of 120 to 130 mV is needed to provide temperature stability of the collector current. This is accomplished by R1 in parallel with Rt and R2. The silicon LDO chip and the GaAs PA chip have been mounted on the same laminate PCB (a modular approach has been used). Rt has been positioned on the same PCB between the silicon and GaAs chips.

The compensation voltages are shown in ***Figure 8***. The red solid line represents the voltage needed at point 3. The three dashed lines below represent the LDO reference voltage data provided by vendor. The upper red dashed line is the theoretical line at point 1 calculated for the reference voltage provided by vendor. The blue solid line is the real measured data at point 1. The brown and green lines present the calculated data for production tolerance margins that may be useful for yield evaluation.

To match the real (blue) line for the point 1 of circuit with the needed (red) line at point 3, the resistive divider R3, R4 is used. It is obvious that the real line can match the needed one with fairly good tolerance (just low temperature and high temperature have some discrepancy). The main intention was to keep the large-signal collector current constant at the 28.5 dBm level for PCS-CDMA operation (up-link mobile) at room temperature. ***Figure 9*** shows the test results of the current changes over

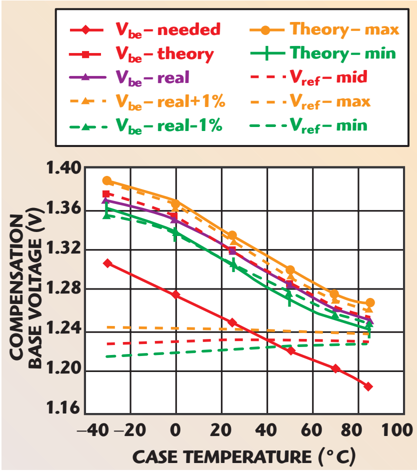

▲ *Fig. 8 Base control voltage test and simulation results.*

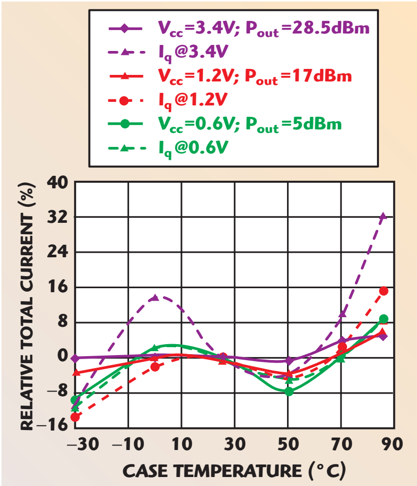

▲ *Fig. 9 Current test results for the proposed circuit.*

temperature for different V_{CC} voltages applied to the PA. It can be seen that the large-signal operation current (for 28.5 dBm at V_{CC} = 3.4 V) has the minimum variations through temperature (+5 to –1 percent), although the quiescent current variations are maximum for this case. Changing the V_{CC} voltage level also results in wider margins of the operating current variations.

The large-signal gain variation is less than 2 dB for V_{CC} = 3.4 V (see ***Figure 10***). Mainly, this gain variation is caused by the discrepancy between the needed and real base voltage curve at low temperatures. For temperatures from +25° to +85°C, the gain varies by less than 0.3 dB. At lower v_{cc} voltages, the gain varies by 2 and 3.5 dB, respectively. However, this is not as important as for V_{CC} = 3.4 V, since the driving circuit has already "enough" gain margin. The large-signal ACPR over temperature, shown in ***Figure 11***, exceeds the standard specification. The room and extreme temperature test results, for gain and ACPR versus output power level (with changing input drive signal level), are shown in ***Figures 12*** and ***13***, respectively. It is obvious that, at low signal levels, the gain variation is larger than for maximum rated power. At the same time, the ACPR margin is well below the standard requirements. The intermediate temperature dependence of the parameters is presented in ***Figures 14*** and ***15***, showing quite well the stability of the parameters.

The low VCC voltage operation gain and ACPR over temperature shown in ***Figures 16*** and ***17*** show the suitability of implementing this thermo-compensating circuit with DC-DC V_{CC} control to substantially increase the efficiency of PA at low and mid power levels.[10]

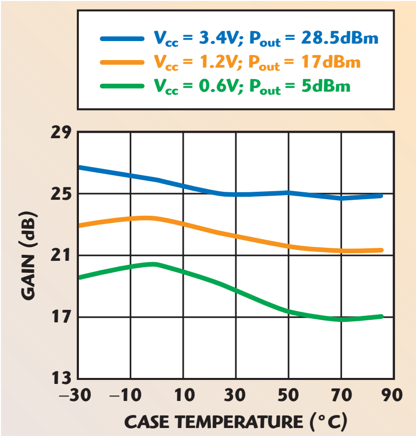

▲ *Fig. 10 Gain test results for the proposed circuit.*

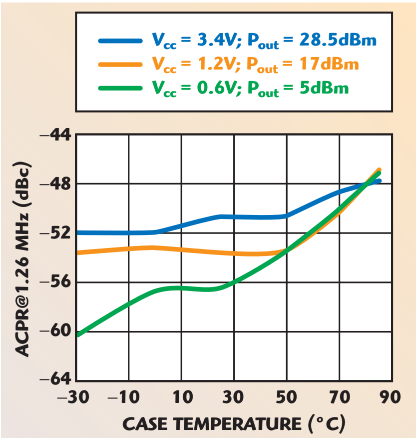

▲ *Fig. 11 ACPR test results for the proposed circuit.*

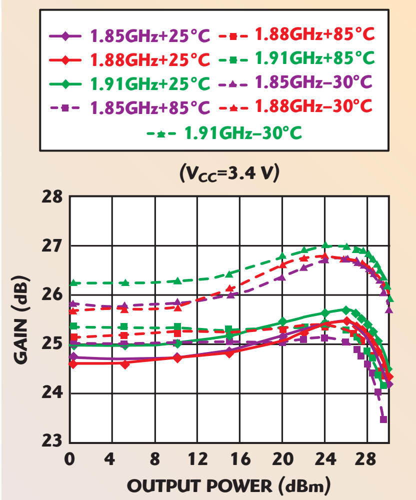

▲ *Fig. 12 Gain test results for the proposed circuit at room and extreme temperatures.*

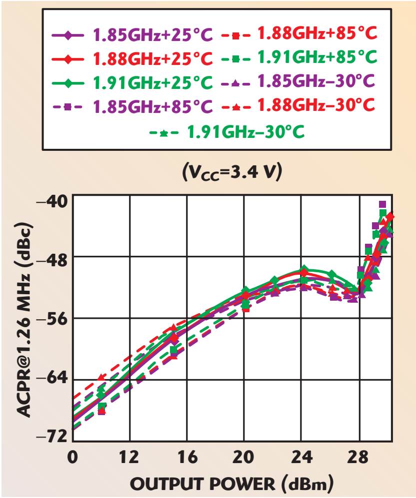

▲ *Fig. 13 ACPR test results for the proposed circuit for room and extreme temperatures.*

CIRCUITS PROPOSED FOR GAIN VERSUS TEMPERATURE STABILIZATION

The proposed power stabilization principle is suitable not only for PA designers but for systems designers as well, with some preliminary knowledge of the PA internal structure.

Consider the circuit in ***Figure 18***. First, one has to evaluate the point 1 voltage dependence required for the current stabilization. A particular LDO should then be chosen with a known temperature dependence of its reference voltage (not only its tolerance) so it results in different final output parameters. It is obvious that different LDO part numbers have a different shape of the reference voltage over temperature even for the same tolerance at room temperature. It should be noted that a smooth shape of the reference voltage versus temperature (increasing or decreasing with temperature such as shown in ***Figure 19***) is preferred to "linearize" the base voltage control curve. Any "bending" or "kneeing" at mid-temperatures has to be avoided. The ATMEL solution, mentioned previously and seen by the author, has this problem with an incorrectly chosen LDO. It is also important to choose the correct tolerance for the other resistors used in a circuit (such as 0.1 to 1.0 percent) and their temperature coefficients as well (±50 ppm/°C is a good choice). In this case, the circuit designed may be suitable for high volume production. By changing the resistor values in the circuit, one can create a different temperature shape of the voltage needed (not only linear). Placing the

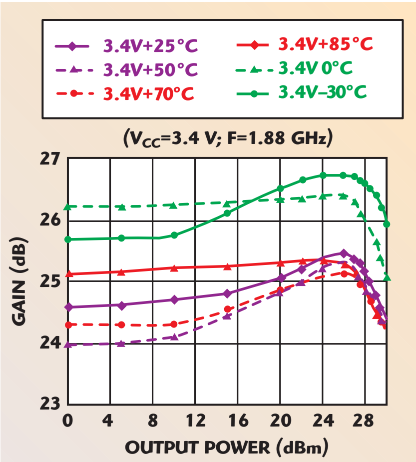

Fig. 14 Gain test results for the proposed circuit for intermediate temperatures.

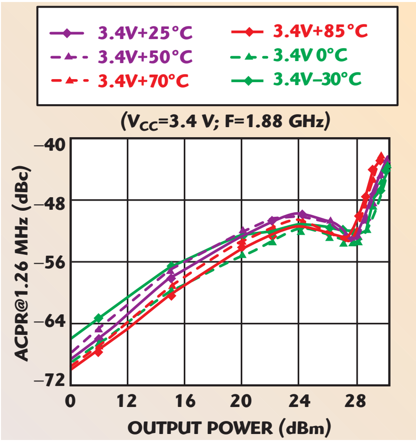

Fig. 15 ACPR test results for the proposed circuit at intermediate temperatures.

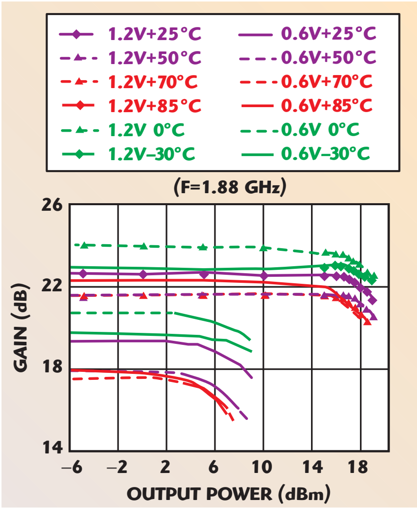

Fig. 16 Low V_{cc} voltage gain test results for the proposed circuit.

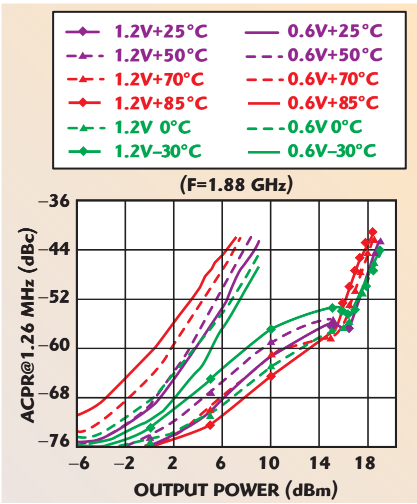

Fig. 17 Low V_{cc} voltage ACPR test results for the proposed circuit.

thermistor, LDO and PA close to each other on a common PCB will allow compensating for the temperature variations of the whole transmitter circuit. It is important to know that one does not need to follow an exact value of temperature. One just needs to shrink the possible range of those variations. Special care should be taken during the assembling process. Thermistors "do not like" overheating during a soldering procedure. The vendors usually provide data sheets with some tolerances that include the soldering procedure margins. Following these assembly procedures is a must.

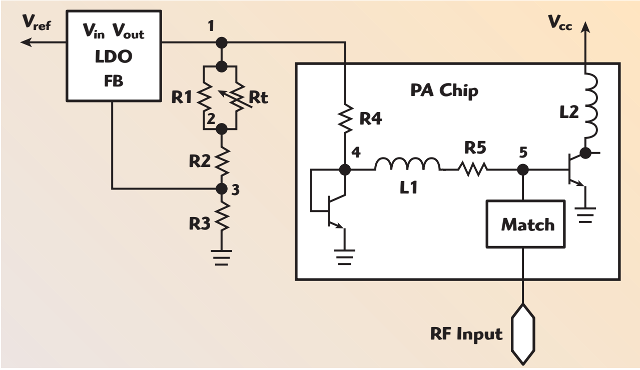

▲ *Fig. 18 Thermo-compensating circuit that may be implemented with any PA.*

An example of the circuit design procedure is described below:

Consider the thermo-compensating circuit shown previously. Let us suppose that the ballast resistance R5 is low and $\beta = 50$. Apply a voltage V1 = 2.8 V to pin1. The voltage at point 4 is approximately +1.25 V at room temperature (for InGaP and AlGaAs HBT). Let the current through resistor R4 be 5 mA. In this case, the resistance R4 value is R4 = (2.8–1.25)/0.005 = 310 Ω. The thermo-electric feedback coefficient is chosen as α = 1.2 mV/°C. By that, one needs the voltages of 2.866 and 2.728 V at point 1 at –30° and +85°C, respectively, to stabilize the collector current. The LDO reference voltage is chosen as V_{ref} = 1.175 V. Let it be stable with temperature. Choosing an NTC type of resistor Rt, with a 1 kΩ nominal value at +25°C and a thermal coefficient B = 3650K, R1 = 750 Ω, R2 = 6.8 kΩ, R3 = 5.227 kΩ results in a voltage variation at point 1 between 2.733 to 2.862 V at –30 to +85°C, which is very close to what one needs. Some fine-tuning is necessary for real devices for which the test data is available.

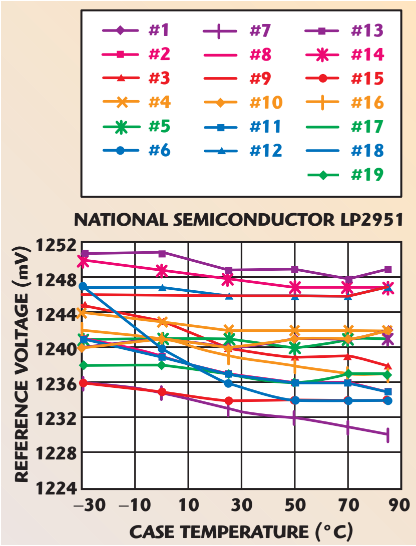

▲ *Fig. 19 Several LDO test results over temperature.*

For very tight control, a high precision LDO may be used, like the MAXIM part with up to ±0.1 percent tolerance (although their price is higher than for less tolerant

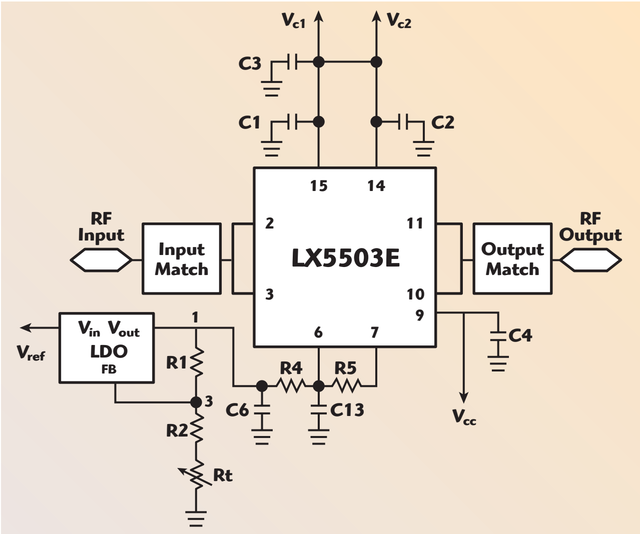

▲ *Fig. 20 Example of a highly linear thermo-compensating circuit.*

ones). For a highly linear voltage control curve, high precision (±0.12 percent) thin film platinum resistance temperature detectors may be used.[11] A 5 GHz WLAN PA with a thermo-compensated circuit is shown in ***Figure 20***. The price of these Pt-RTDs is comparable to the NTC ones. As before, let us consider some real situations. The base current drawn through R4 is 2 mA (as in reality). The voltage at point 1 is 2.9 V at +25°C. The point 1 voltage should be 1.188 and 1.318 V at +85° and –30°C, respectively. Consider only the output transistor stage of the PA with $\beta = 50$. For the same LDO, with a 1.175 V reference voltage, the choice of Rt = 1 kΩ as Pt-RTD, with TCR = 3750 ppm/°C (and ±0.48 percent tolerance), R1 = 7.5 kΩ, R2 = 4 kΩ, results in the perfect match needed.

These examples show that the LDO introduction to the circuit elevates the current consumption of the whole circuit by only 0.2 to 0.3 mA. The circuit proposed allows utilizing easily the power shut-down function and the power control function as well. All the speculations above are valid for different types of RF PA used in wireless communications (GaAs, Si, SiGe, bipolar, HBT, MESFET, CMOS, Bi-CMOS, etc.). Only the absolute voltage levels and their shape over temperature are different. The circuit proposed is very flexible and may be used successfully in different portable wireless systems.

CONCLUSION

The simulation and test data considered in this article, along with the circuits proposed, may be applicable to the existing and future designs for mobile phone and WLAN PAs. Not only the RF PA output power can be stabilized over temperature but the entire transmitter RF chain as well. Certainly, the closed-loop power control approach may be used in addition to the circuits considered (analog-loop or through base band) to eliminate variations of supply voltages and production tolerances as well. By that, one will be aware that the most nonlinear part of the transmitter already has no problems with temperature.

The gain/power stabilization circuit can be implemented as a small size module with one or several adjustable components (resistors) placed externally. The use of this circuit in an entire transmitter chain will replace the LDO currently implemented in many designs (mobile phones, WLAN, etc.) to keep a stable PA control voltage. ■

References

1. M. Hafizi, W.E. Stanchina, R.A. Metzger, P.A. Macdonald and F. Williams, "Temperature Dependence of DC and RF Characteristics of AlInAs/GaInAs HBTs," *IEEE Transactions on Electron Devices*, Vol. 40, No. 9, September 1993, pp. 1583–1587.
2. Y. Zhu, J.K. Twynam, M. Yagura, M. Hasegawa, T. Hasegawa, Y. Eguchi, Y. Amano, E. Suematsu, K. Sakuno, N. Matsumoto, H. Sato and N. Hashizume, "Compensation of Self-heating Effect in DC and Pulse Characteristics of HBTs," *1999 IEEE MTT-S International Microwave Symposium Digest*, pp. 431–434.
3. RF Micro Devices, "A High Gain Power Amplifier with Variable Bias for Multimode WCDMA Applications," *Microwave Journal*, Vol. 45, No. 2, February 2002, pp. 154–167.
4. P.D. Tseng, L.Y. Zhang, G.B. Gao and M.F. Chang, "A 3 V Monolithic SiGe HBT Power Amplifier for Dual-mode (CDMA/AMPS) Cellular Handset Applications," *IEEE Journal of Solid-State Circuits*, Vol. 35, No. 9, September 2000, pp. 1338–1344.
5. J.A. Roche, R.M. Healy, G. Hau and S.A. Caron, "Adaptive DC Power Management for HBT PAs in CDMA Handsets," *RF Design*, February 2002, pp. 42–50.
6. Y. Deval, et al., "1-volt Ratiometric Temperature Stable Current Reference," *1997 IEEE International Symposium on Circuits and Systems Digest*, pp. 1984–1987.
7. K. Alvarino, H. Bui, S. Coryell, S. Egolf, H. Jiang, C. Lazinbat, E.T. Spears, D. Spooner and D.A. Teeter, "Next-generation CDMA2000 1x Power Amplifier Modules," *Applied Microwave & Wireless*, pp. 74–84.
8. T. Johansson and W.X. Ni, "Feasibility Study of 25 V SiGe RF Power Transistors for Cellular Base Station Output Amplifiers," *Material Science & Engineering B89*, Elsevier, 2002, pp. 88–92.
9. "Using Thermistors in Temperature Tracking Power Supplies," *Maxim Integrated Products*, Article A244, September 2001.
10. E.C. Glass, J.H. Huang, J. Staudinger, M. Shields, M.J. Martinez, O.L. Hartin, W. Valentine and E. Lan, "Application of Enhancement Mode FET Technology for Wireless Subscriber Transmit/Receive Circuits," *IEEE Journal of Solid-State Circuits*, Vol. 35, No. 9, Sept. 2000, pp. 1276–1284.
11. Syntec Corp., Taiwan, data sheet, 2003.

Oleksandr Gorbachov *received his PhD degree in electrical engineering from Kiev Polytechnic Institute, Kiev, Ukraine, in 1990. He is currently the RF applications manager at STMicroelectronics, Taipei, Taiwan. His engineering and scientific interests include RF components and modules for wireless communications.*

THE INFLUENCE OF THE PACKAGE ENVIRONMENT ON THE FUNCTIONING AND RELIABILITY OF CAPACITIVE RF-MEMS SWITCHES

This article discusses the influence of the packaging process and environment on the functioning and reliability of capacitive RF-microelectromechanical systems (MEMS). It is shown that the packaging temperature profile can change the mechanical stress in the suspended metal bridge of the MEMS. Decreasing the environmental pressure strongly influences the switching speed of a switch, but if it becomes too low, it causes anomalous vibration effects. When testing at the same pressure, the lifetime of the capacitive switches is shown to be higher in a nitrogen environment than in an ambient air (laboratory) environment. The lifetime is determined by the charging process of the insulator. It is shown that this charge is not stable and that the switch recovers when it is not actuated.

RF-MEMS switches offer a number of advantages for switching in the gigahertz range because of their low insertion loss, high linearity and low power consumption.[1] Several publications have reported on the performance of such switches, but more for non-packaged 'naked' samples. It is clear that the packaging process and the packaging environment can have a large impact, both negative and positive, on the functionality and reliability of these switches. A first possible impact of packaging on a switch is the packaging temperature profile. Often these temperature steps are higher than any step seen by the device before packaging and can, for certain switches, have detrimental effects.[2,3] A second direct problem of packaging is out-gassing of the packaging material. Especially for ohmic switches, this can have a direct impact on the contact resistance.[3] However, the package can also be used to control the pressure inside the cavity, in this way affecting the speed of the switch. The package can also protect the switch against the environment and, as such, solve several switch reliability problems in an indirect way. In this article, the two latter issues are discussed: the effect of pressure on the functionality of the

INGRID DE WOLF, PIOTR CZARNECKI, ANNE JOURDAIN, ROBERT MODLINSKI AND HARRIE A.C. TILMANS
IMEC
Leuven, Belgium
ROBERT PUERS
K.U.
Leuven, Belgium
JOOST T.M. VAN BEEK
Philips Research
Eindhoven, The Netherlands
W. MERLIJN VAN SPENGEN
Leiden University
The Netherlands

switches and the influence of the environment (N_2 versus air) on the reliability of the switches. The results given are for zero-level packaged capacitive RF-MEMS switches.

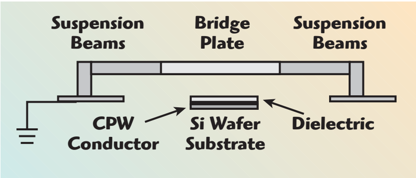

▲ *Fig. 1 Schematic cross-section of a capacitive RF-MEMS device.*

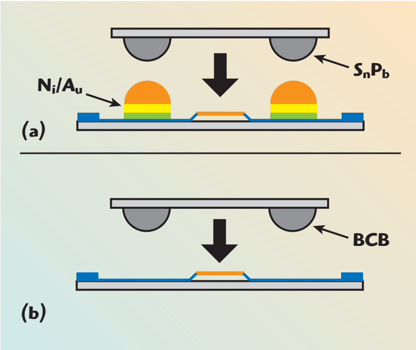

▲ *Fig. 2 Schematic picture of (a) metal/solder sealing and (b) polymer (BCB) sealing of MEMS switches.*

SWITCH AND ZERO-LEVEL PACKAGE

A schematic cross-section of a typical capacitive RF-MEMS switch is shown in ***Figure 1***. The structure is essentially a coplanar waveguide (CPW) with an aluminum "bridge" above it and a dielectric layer located on top of the CPW. A number of etch holes are present in the bridge. When the bridge is up, an RF signal can propagate under the bridge to the other side. Application of an actuation voltage between the bridge and the CPW inner conductor causes an electrostatic attractive force between them, which pulls the bridge down. In the down-state, the capacitance formed by the metal/dielectric/bridge metal stack is large, causing a large mismatch; the RF signal is reflected and the switch is off. A MEMS package has to protect the device against external influences such as pressure, humidity, chemicals and particles. For MEMS processed on a wafer, it is mandatory to encapsulate them at the wafer level, in order to prevent exposure of the free structures to particles and debris produced during the dicing and handling process. For most switches, this process should be done at relatively low temperatures. Two sealing methods, typically used at IMEC, are metal/solder sealing or polymer (BCB) sealing, as shown in ***Figure 2***.[1,4,5] The metal sealing has the advantage to be hermetic, but it requires processing on the MEMS substrate. The BCB sealing requires only processing on the top cavity and at the same time provides electrical isolation but does not provide a hermetic seal. ***Figure 3*** shows an example of RF-MEMS switches packaged on wafer level using a glass cap and BCB seal.[6]

INFLUENCE OF THE PACKAGING TEMPERATURE

The bridge of the RF-MEMS switch is, in general, made of metal, such as Au-, Pt- or Al-alloy. During packaging, the switch will be subjected to different temperature steps. The BCB process, for example, typically requires a curing step at about 250°C.[7] A question that arises is whether the metal of the MEMS bridge can stand this temperature. This was investigated by Modlinski, et al. for several Al-alloys.[2] They measured the bow of a wafer caused by a uniform metal film as a function of temperature, using a laser scanning technique. From the bow, the stress in the metal film can be deduced. ***Figure 4*** shows a typical example measured on an AlCuMgMn alloy. This film was initially under approximately 150 MPa tensile stress at room temperature. When heated up to 200°C and cooled back down, the stress did not change. It can then be expected that a MEMS bridge, made of this material, would not be deformed due to such a temperature

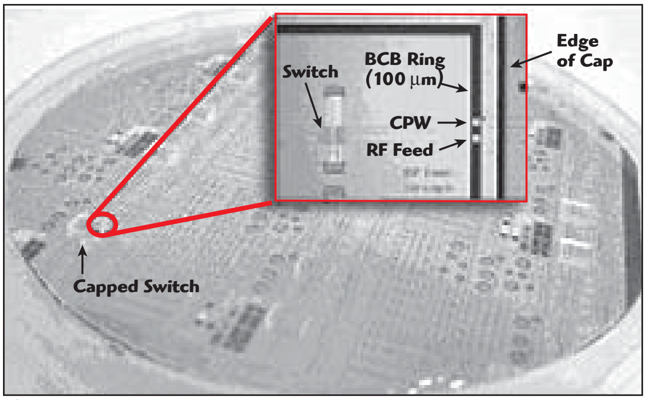

▲ *Fig. 3 Example of zero-level packaged capacitive RF-MEMS switches using a glass cap and BCB sealing.*

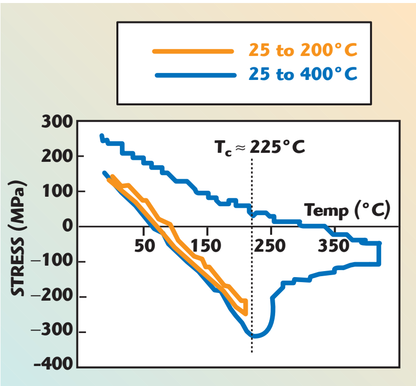

▲ *Fig. 4 Influence of the temperature ramp on the stress in an AlCuMgMm alloy for two temperature ranges.*

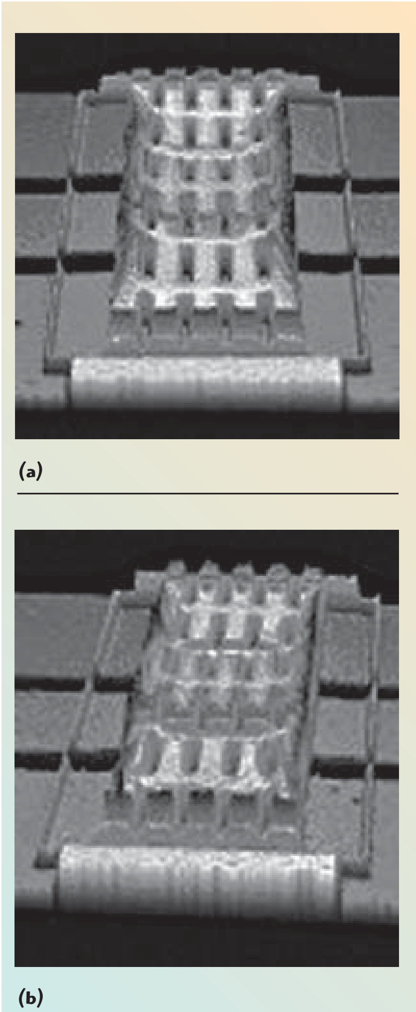

▲ *Fig. 5 Example of a zero-level packaged capacitive RF-MEMS switch; (a) the naked switch and (b) the zero-level packaged switch (glass cap and BCB).*

step. However, when the temperature is increased above 200°C, the stress curve starts deviating from its linear, elastic behavior at a certain critical temperature (T_c = ~225°C) and the stress changes due to plastic deformations in the material. In this experiment, the temperature was increased to 400°C. Cooling down resulted in a higher tensile stress value at room temperature (~300 MPa). Actually, cooling down from any temperature higher than T_c would result in a higher tensile stress. Therefore, if the packaging temperature profile exceeds T_c for a certain material, the stress in the MEMS bridge will change and the bridge might deform. This effect can result in the failure of the switch or an unwanted drift of the switch performance.

The effect of temperature during a packaging step on an RF-MEMS switch is not always destructive. ***Figure 5*** shows an optical profile picture of the metal bridge of a non-packaged metal RF-MEMS switch, taken with a Veeco/Wyko instrument.[8] The bridge is slightly curved downwards. A picture of a similar bridge (on the same chip) was taken after zero-level packaging using BCB and a glass cap. It is clear that in this case the deformation is very small and actually in the "good" direction; the bridge is a little bit less curved downwards. This sample did survive the packaging step. A profile measurement through a glass cap is not possible using conventional profilometry lenses. However, it is possible when a lens with a compensation glass is used. The packaged sample was measured by Veeco Instruments Inc., using a special 10x TTM objective. This objective contains a compensation glass holder in which a glass piece of the same thickness as the glass cap is placed. In this way, fringe contrast images and resulting profile images can be taken even through the glass cap of a zero-level packaged MEMS device.

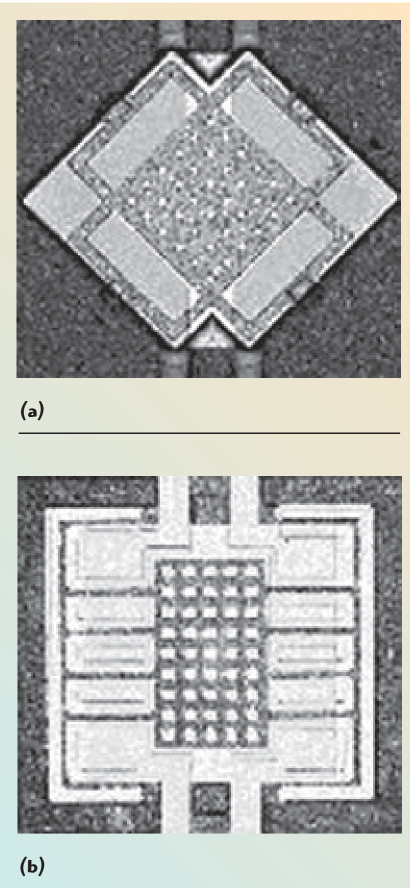

▲ *Fig. 6 Examples of bridge designs; (a) stiff and (b) less stiff.*

INFLUENCE OF THE PRESSURE

The effect of the pressure on the functioning of a switch was studied for two different bridge designs, a mechanically stiff (switch A) with small holes and a less stiff one (switch B) with larger holes, shown in ***Figure 6***. The

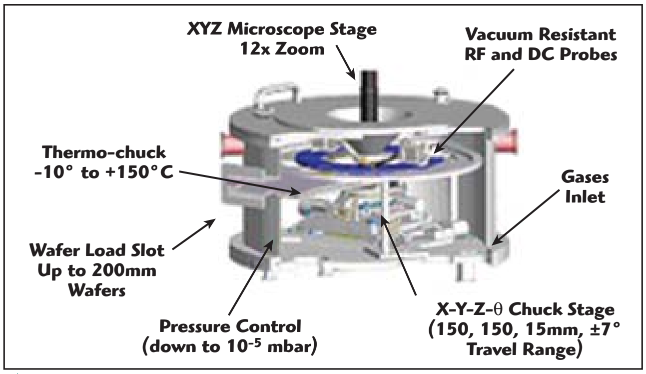

▲ *Fig. 7 Schematic picture of the MEMS test chamber (PAV).*

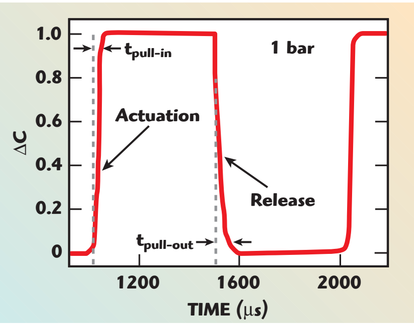

▲ *Fig. 8 Change in capacitance versus time for the switch with a stiff bridge.*

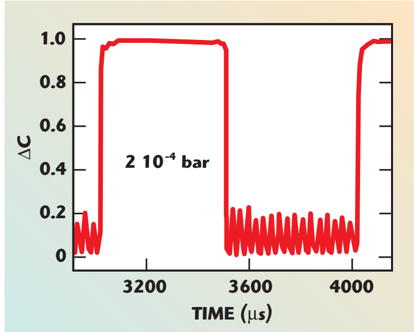

▲ *Fig. 9 Stiff bridge switch operated at low pressure.*

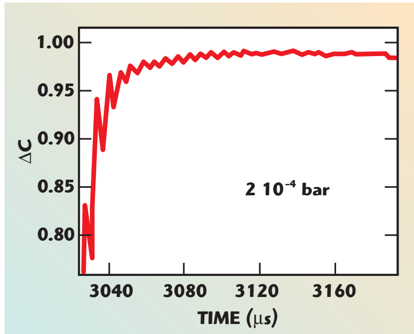

▲ *Fig. 10 Zoom-in of the pull-in time for the stiff bridge switch operated at low pressure.*

switches were realized using the Philips PASSI™ process.[9] The devices are designed to operate at gigahertz signal frequencies, but a dedicated 10.65 MHz "reliability" test set-up, developed at IMEC and called the electrical life test (ELT) system, was used to monitor the capacitance changes of the RF-MEMS switches as a function of time.[10] The devices were actuated at a 1 kHz rate with a 30 V unipolar square wave, and operated in a Suss-MicroTec PAV150 MEMS environmental chamber with a nitrogen atmosphere. A schematic drawing of this chamber is shown in ***Figure 7***. The chamber is dedicated for MEMS testing and allows control of the pressure, temperature and gas composition inside the chamber while electrically testing the MEMS, both with DC and RF probes, and while optically monitoring the MEMS. Changes in capacitance were sampled at a 1 MHz frequency to closely monitor these changes during bridge motion and to study possible bouncing or ringing effects, without inducing errors due to aliasing effects. A typical example of an ELT measurement (at 1 atm N_2) of the capacitance change ΔC during the actuation and release of a capacitive RF-MEMS switch is given in ***Figure 8***. All the changes in capacitance mentioned in this article are plotted in arbitrary units. When the bridge is actuated with a voltage higher than the pull-in voltage of the bridge, the capacitance abruptly increases (the bridge moves down and touches the dielectric). The pull-in time, $t_{pull\text{-}in}$, can be deduced from these curves. Upon release of the switch ($V_{actuation}$ = 0 V), the bridge moves up and the capacitance decreases again. The pull-out time, $t_{pull\text{-}out}$, can also be deduced.

The switching speed is increased drastically if the device is operated at reduced pressure. ***Figure 9*** shows the same device operated at 2×10^{-4} mbar N_2. In this case, the pull-in and

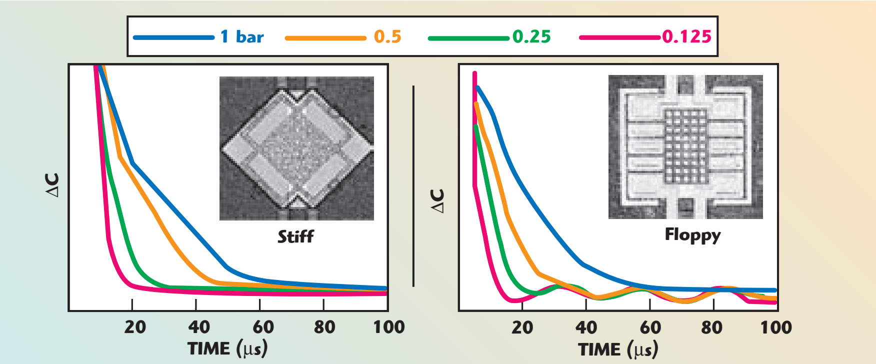

▲ *Fig. 11 Change in capacitance during down-to up-state at different pressures.*

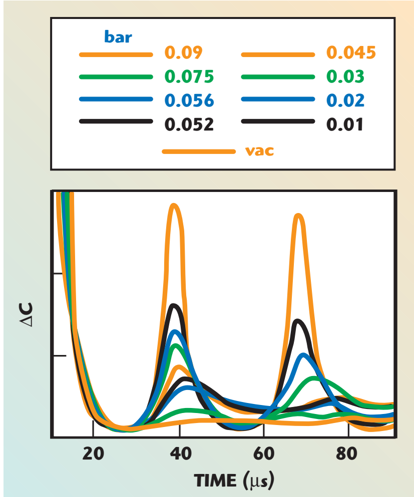

▲ *Fig. 12 Change in capacitance of the stiff switch after the transition from down-to up-state for different pressures.*

pull-out times are much shorter. In addition, however, a large overshoot effect causing a long settling time is observed when the bridge returns to the up-state (low capacitance). Because the device is not damped anymore when not touching the dielectric, it starts vibrating with a large amplitude (overshoot).[11] ***Figure 10*** shows a magnification of part of the signal measured when the bridge reaches the down-position. It is clear that even when going down and touching the dielectric, a vibration effect called bouncing can be observed. This effect has to be avoided and it is clear from the figures that an optimum pressure exists (critical damping), at which the bridge moves very fast, but no overshoot occurs when it moves back up. To experimentally obtain the optimum pressure, a successive approximation method was used. In this method, a pressure interval is determined in which the critical damping is located. This interval is divided in half by performing an experiment at the pressure in the middle of the interval. When overshoot occurs, the critical damping point is located in the higher pressure half of the interval, otherwise in the lower pressure half. The interval in which the critical damping point has been found to be located is cut in half again by performing another measurement, and so on, until the critical damping point has been accurately found. This method is very effective — high speed electronic analog-to-digital (A/D) converters use the same principle to accurately determine the value of a voltage.

Figures 11 and ***12*** show the results for the stiff and for the floppy bridge. Only the pull-out part of the ΔC versus time curve is shown, that is, when the bridge moves from the down position (large C) to the up position (small C). For both designs, there is a clear decrease in pull-out time with decreasing pressure. The stiff bridge does not show overshoot at 0.125 bar. At 0.075 bar, a small overshoot is visible, at 0.09 bar, no overshoot appears, while vacuum (2×10^{-4} mbar) results in a large overshoot. The switch with a less stiff design (switch B) and with a lower surface area shows overshoot already at 0.25 bar, as expected for a less-stiff switch. Not only the pressure inside the package, but also the gases inside the package cavity influence the MEMS. ***Figure 13*** shows lifetime plots of capacitive switches. These measurements were also performed using the ELT system. The plots show the change in capacitance, ΔC (in arbitrary units), between up- and down-state of the switch as a function of the number of cycles. Three switches from different origins and with different insulator material were tested. The first has SiO_2 as the insulator, the second Ta_2O_5 and the last SiN_x. For all switches, ΔC stays rather constant for a certain number of cycles, and then suddenly drops. This 'end-of-life' is caused by the bridge sticking to the insulator; the bridge remains in the down-position. This is a well-known failure mode in capacitive RF-MEMS switches and is caused by a charge that builds up in the insulator when the switch bridge is touching the dielectric.[12–16]

The high voltage required to actuate the switch induces high electrical fields across the insulator, causing charge trapping. The experiments on these switches were performed at different switching frequencies, at different actuation voltages and on different designs, so the lifetime cannot be compared.[16] The three switches were tested in normal (laboratory) air as environment, and, under the same actuation conditions, in nitrogen gas. For all three, the lifetime is clearly a factor of approximately 100 times longer in N_2. These effects are attributed to the humidity of the air and its influence on charge trapping in the insulator.[12]

It is known that humidity enhances the charge trapping, leading to a faster charge build-up and, as is shown here, a shorter lifetime of the capacitive switches. It is interesting to note that for the three different oxides, the increase in lifetime when changing from normal laboratory air to nitrogen gas is very similar, whereas it is well known that these three different insulators have a rather different charge trapping sensitivity. This could indicate that these charging effects occur at the surface of the insulators. Another mechanism that could play a role is the difference in breakdown voltage of the small gap between the bridge and the insulator for the different environments. From these experiments, however, no clear conclusions can be made at this time. It is clear that additional research on these charging mechanisms in different environments is required. The charge typically disappears after some

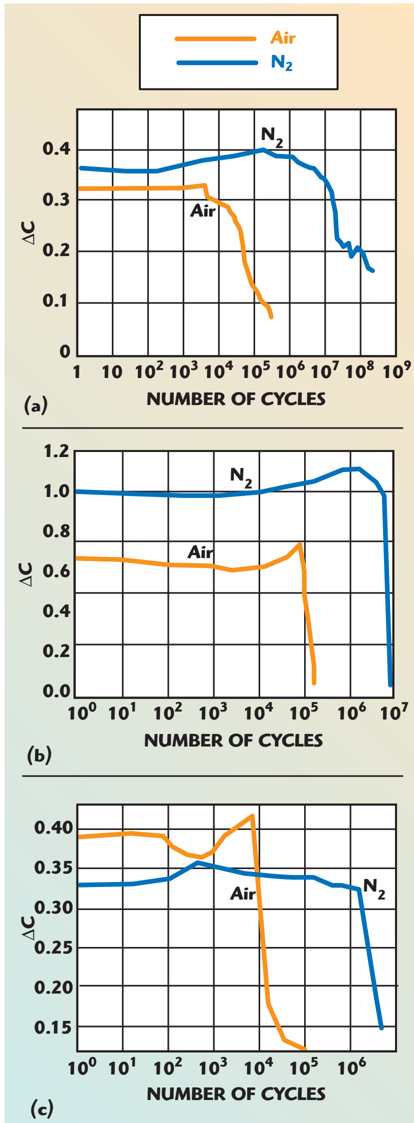

▲ *Fig. 13 Lifetime plots of three different capacitive switches in air and nitrogen environment with (a) S_IO_x, (b) T_IO_5 and (c) S_IN_x insulators.*

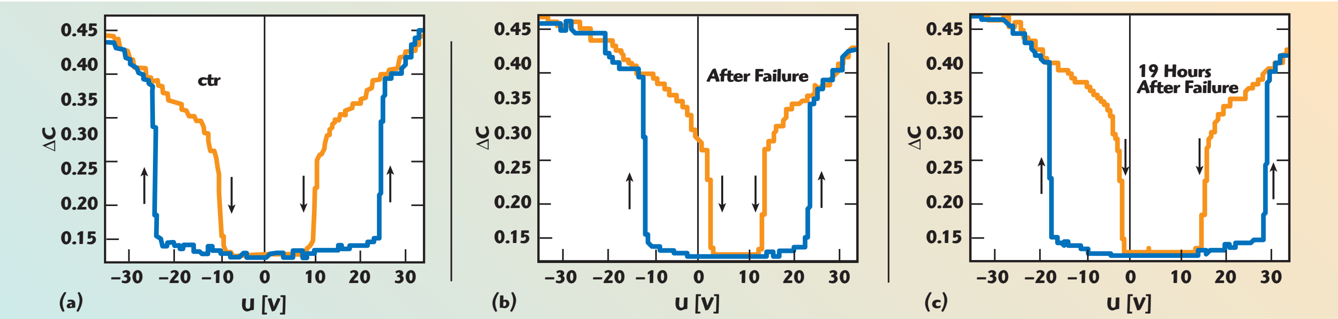

▲ *Fig. 14 Fast C-V measurements of a capacitive switch (a) before test, (b) after test and (c) 19 hours later.*

time. This effect is shown in ***Figure 14***. First, a fast C-V experiment is performed. This is done using the ELT system by applying a triangular waveform to the switch instead of the normal unipolar square waveform to actuate the switch. The fast C-V principle is shown in ***Figure 15***. During application of this triangular pulse, the change in capacitance is measured. The result is plotted in what are called fast C-V curves. The advantage of this measurement method is that it is very fast (~1 ms) compared to conventional C-V measurements (~1 min), so that only limited charge trapping takes place, which is, in general, not the case in conventional C-V measurements.

The results of a fast C-V measurement on a fresh switch are shown first. It is a symmetrical CV curve, showing clear pull-in (approximately ±22 V) and pull-out (approximately ±10 V). Next, a lifetime test is performed at a voltage (35 V) that is higher than the actuation voltage, until the failure of the switch. The results of a fast CV-curve, measured immediately after failure of this switch, are shown. The curve is clearly shifted to the right and is also narrower. The first observation is well known and modeled.[13,14] It is caused by charging of the insulator, causing an increase in the pull-in voltage. The second effect is less well known but often observed in capacitive switches. It is caused by a non-uniform distribution of this charging.[15] During this fast CV measurement, the switch is functioning and pulling in and out during the voltage ramp. In the ELT test, however, the switch is declared 'failed' because when switching fast from 35 V to 0 V, it will stay pulled-in.[14] The results of a fast C-V measurement, performed on the same switch 19 hours later, are then shown. During that time, the switch was kept in a nitrogen environment. One clearly sees a partial recovering of the switch: the C-V curve is shifted back to the left and broadened again. This confirms that the charges decay in time and that this typical failure of capacitive RF-MEMS is not a permanent one. However, even after 19 hours, the charge did not disappear completely, indicating that these traps, whether they are surface or bulk, or holes or electrons, have a rather long decay time.

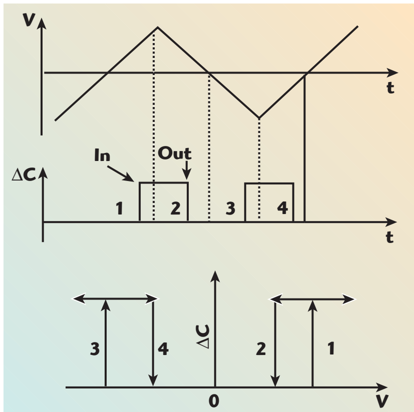

▲ *Fig. 15 Principle of the fast C-V measurement.*

CONCLUSION

This article discussed some influences of the zero-level package on the performance of capacitive RF-MEMS switches. The influences of temperature, pressure and gases were discussed. The packaging process requires a certain temperature profile, which can affect the mechanical stress of the metal MEMS bridge. It is clear that when designing and processing an RF-MEMS, this effect has to be studied and taken into account to avoid that a good functioning RF-MEMS device will fail or change its functionality after being packaged. One of the main disadvantages of MEMS switches compared to, for instance, RF transistors and PIN-diodes, is their low switching speed.[17] For many applications, a high switching speed is mandatory. In this article, it is shown that choosing a suitably low pressure, in combination with a well-selected device stiffness, can be used to optimize the switching speed of RF-MEMS switches. On the other hand, it is shown that a pressure that is too low can result in an anomalous vibration behavior for some MEMS. It is clear that for optimal performance, the devices have to be used in a zero-level package with an internal optimal pressure, or the design has to be adapted, depending on the desired speed for a certain application and on the environmental conditions (space versus earth applications). The first solution requires a constant, well-controlled pressure of the package; the second solution requires adapted MEMS designs taking into account application dependent functioning and reliability issues.

It is also shown that capacitive MEMS switches with SiO_x, SiN_x or Ta_2O_5 insulators exhibit a higher reliability when operated in N_2 than in air. This is most likely related to enhanced charging of the insulator in the presence of humidity. Again these results influence the demands for the zero-level packaging of such switches. A fully hermetic package is likely to be required, and this hermeticity should be kept constant during the lifetime of the device. ■

ACKNOWLEDGMENTS

Much of the material in this article was first presented at the 2005 IEEE International Reliability Physics Symposium and appeared in the Proceedings as "The Influence of the Package Environment on the Functioning and Reliability of RF-MEMS Switches" by W.M. van Spengen, et al., pp. 337–341. This work is supported by the European Union in the framework of the FP5 IST-28231 project MEMS2TUNE, the IST-28276 project MIPA and the FP6 NoE PATENT-DfMM.

References

1. H.A.C. Tilmans, W. De Raedt and E. Beyne, "MEMS for Wireless Communications: From MEMS Components to RF-MEMS-SIP," *Journal of Micromechanics and Microengineering*, Vol. 13, No. 4, July 2003, pp. S139–S163.
2. R. Modlinski, A. Witvrouw, P. Ratchev, A. Jourdain, V. Simons, H.A.C. Tilmans, J. den Toonder, B. Puers and I. De Wolf, "Creep as a Reliability Problem in MEMS," *Microelectronics Reliability*, Vol. 44: (9–11), 2004, pp. 1733–1738.
3. Y. Oya, A. Okubora, M. Van Spengen, P. Soussan, S. Stoukatch, X. Rottenberg, P. Ratchev, H.A.C. Tilmans, W. De Raedt, E. Beyne, P. De Moor, I. De Wolf and K. Baert, "A Reliable and Compact Polymer-based Package for Capacitive RF-MEMS Switches," *Proceedings of the International Electron Device Meeting*, 2004, pp. 31–34.
4. A. Jourdain, P. De Moor, S. Pamidighantam and H.A.C. Tilmans, "Investigation of the Hermeticity of BCB-sealed Cavities for Housing (RF)-MEMS Devices," *Proceedings of MEMS2002*, Las Vegas, NV, pp. 677–680.
5. P. De Moor, "The Minipackage: A Flexible Wafer-level Packaging Solution for MEMS," *Proceedings of the International Microelectronics and Packaging Society 6th Workshop on Packaging of MEMS*, November 2004, Long Beach, CA.
6. H.A.C. Tilmans, H. Ziad, H. Jansen, O. Di Monaco, A. Jourdain, W. De Raedt, X. Rottenberg, E. De Backer, A. De Caussemaeker and K. Baert, "Wafer-level Packaged RF-MEMS Switches Fabricated in a CMOS Fabrication," *Proceedings of the International Electron Device Meeting 2001*, Washington, DC, pp. 921–924.
7. A. Jourdain, H. Ziad, P. De Moor and H.A.C. Tilmans, "Wafer-scale 0-level Packaging of (RF)-MEMS Devices Using BCB," *Proceedings of DTIP 2003*, 5–7 May, Cannes, France, pp. 239–244.
8. Veeco Instruments Inc., 100 Sunnyside Boulevard, Suite B, Woodbury, NY.
9. J.T.M. van Beek, M.H.W.M. van Delden, A. van Dijken, P. van Eerd, A.B.M. Jansman, A.L.A.M. Kemmeren, Th. G.S.M. Rijks, P.G. Steeneken, J. den Toonder, M.J.E. Ulenaers, A. den Dekker, P. Lok, N. Pulsford, F. van Straten, L. van Teeffelen, J. de Coster and R. Puers, "High-Q Integrated RF Passives and RF-MEMS on Silicon," *Material Research Society Symposium Proceedings*, 2003, Vol. 783, pp. B3.1.1–B3.1.12.
10. W.M. van Spengen, R. Puers, R. Mertens and I. De Wolf, "A Low Frequency Electrical Test Set-up for the Reliability Assessment of Capacitive RF-MEMS Switches," *Journal of Micromechanics and Microengineering*, Vol. 13, 2003, p. 604.
11. P.G. Steeneken, Th. G.S.M. Rijks, J.T.M. van Beek, M.J.E. Ulenaers, J. De Coster and R. Puers, "Dynamics and Squeeze Film Gas Damping of a Capacitive RF-MEMS Switch," *Journal of Micromechanics and Microengineering*, Vol. 15, 2005, p. 176.
12. J. Wibbeler, G. Pfeifer and M. Hietschold, "Parasitic Charging of Dielectric Surfaces in Capacitive Microelectromechanical Systems (MEMS)," *Sensors and Actuators A*, Vol. 71, 1998, pp. 74–80.
13. W.M. van Spengen, R. Puers, R.P. Mertens and I. De Wolf, "A Comprehensive Model to Predict the Charging and Reliability of Capacitive RF-MEMS Switches," *Journal of Micromechanics and Microengineering*, Vol. 14, 2004, pp. 514–521.
14. J.R. Reid, "Simulation and Measurement of Dielectric Charging in Electrostatically Actuated Capacitive Microwave Switches," *Technical Proceedings of the 2002 International Conference on Modeling and Simulation of Microsystems, Chapter 5: MEMS Applications and Characterization*, 2002, pp. 250–253.
15. X. Rottenberg, B. Nauwelaers, W. De Raedt and H.A.C. Tilmans, "Distributed Dielectric Charging and its Impact on RF-MEMS Devices," *Proceedings of the 34th European Microwave Conference*, 2004, pp. 77–80.
16. W.M. van Spengen, R. Puers, R. Mertens and I. De Wolf, *Proceedings of the International Electron Devices Meeting*, 2002, pp. 901–904.
17. J.J. Yao, "RF MEMS From a Device Perspective," *Journal of Micromechanics and Microengineering*, Vol. 10, 2000, R9.

TRANSISTOR LC OSCILLATORS FOR WIRELESS APPLICATIONS: THEORY AND DESIGN ASPECTS, PART III

In Part I of this tutorial article,[1] a detailed discussion and analysis of the start-up and steady-state oscillation conditions for transistor LC oscillators was given, with emphasis on CMOS devices. Part II[2] presented both linear and nonlinear phase noise models for parallel feedback and negative resistance oscillators. Part III describes a new impulse response model for phase noise, which became popular recently. It specifies the contribution of the noise components located near integer multiples of the oscillation frequency in terms of waveform properties and circuit parameters.[3,4] By using this nonlinear approach, it is impossible to derive an explicit relationship between the oscillator stability conditions, amplitude-to-phase conversion and phase noise power density, unlike using the Kurokawa approach. However, such an approach, based on the inherent time-varying nature of the oscillator, provides an important design insight by identifying and quantifying the major sources of phase noise degradation. The derivation of the expression for excess phase was based on postulating the unit impulse response as a function of the oscillator waveform. The relationship between excess phase and the circuit parameters, however, can be explicitly derived using a well-known phase plane approach.[5]

The impulse response model for the oscillator phase noise, which has become popular recently, is explained based on a well-known phase plane approach.

IMPULSE RESPONSE NOISE MODEL

Phase Plane Approach

The behavior of autonomous, second-order, weakly nonlinear oscillation systems with low damping factor close to linear conservation systems and small time-varying external force f(t) can be described by

$$\frac{d^2x}{d\tau^2} + x = n(t) \qquad (1)$$

ANDREI GREBENNIKOV
M/A-COM Eurotec Operations
Cork, Ireland

where

x = time-dependent variable, voltage or current

$\tau = \omega_0 t$ = time normalized by the angular resonant frequency ω_0

The phase plane method[6] is one of the theoretical approaches that allows one to analyze qualitatively and quantitatively the dynamics of the oscillation systems described by the second-order differential equations such as Equation 1. By setting the small external force equal to zero, the solution of the linear second-order differential equation takes the form of

$$x = A\cos(\tau + \phi) = A\cos\psi \tag{2}$$

$$\frac{dx}{d\tau} = -A\sin(\tau + \phi) = -A\sin\psi \tag{3}$$

where

A = amplitude of the oscillation
ϕ = phase of the oscillation

The phase portrait shown in ***Figure 1*** represents the family of circular trajectories enclosing each other with radii r = A depending on the energy stored in the system. Such an isolated closed trajectory is called a limit cycle.

Let us define the variations of the amplitude A(t) and phase $\phi(t)$ under effect of the external force applied to the oscillation system.[6] Assuming that the effect of the external force is small and these variations are slow, the amplitude and phase can be considered constant during a natural period of the oscillation. Equation 1 can then be rewritten in the form of two first-order equations as

$$\frac{dx}{d\tau} = y \tag{4}$$

$$\frac{dy}{d\tau} = -x + n(t) \tag{5}$$

From Equations 4 and 5, it follows that the instantaneous change of the ordinate y by a value of $d_n y = n d\tau$ will occur, due to the small external force injected into the oscillation system. This corresponds to a step change of the representative point M_0 from the position K to the position L, resulting in the amplitude and phase changes, as shown. These changes can be determined from the consideration of a triangle KLN by

$$dA = -d_n y \sin\psi = -n \sin\psi d\tau \tag{6}$$

$$d\phi = -\frac{d_n y}{A}\cos\psi = -\frac{n}{A}\cos\psi d\tau \tag{7}$$

Thus, the separate first-order differential equations for the time-varying amplitude and phase can be obtained from Equations 6 and 7 as

$$\frac{dA}{d\tau} = -n\sin\psi \tag{8}$$

$$\frac{d\theta}{d\tau} = -\frac{n}{A}\cos\psi \tag{9}$$

Since the right-hand sides of Equations 8 and 9 are small, time-averaged differential equations can be used instead of the differential equations for the instantaneous values of the amplitude and phase. Hence, the changes of the amplitude and phase for a time period $t \le T$ are defined as

$$\Delta A(t) = -\int_0^{\omega_0 t} n(\tau)\sin\tau d\tau \tag{10}$$

$$\Delta\phi(t) = -\int_0^{\omega_0 t} \frac{n(\tau)}{A}\cos\tau d\tau \tag{11}$$

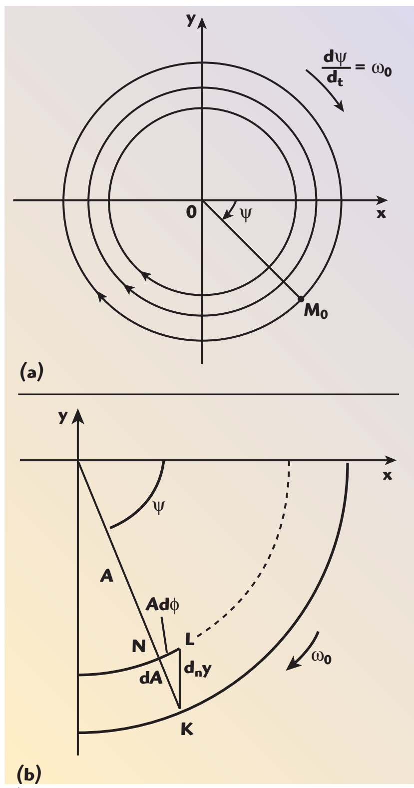

▲ *Fig. 1 Phase portrait of a second-order oscillation system (a) and the effect of an injected impulse (b).*

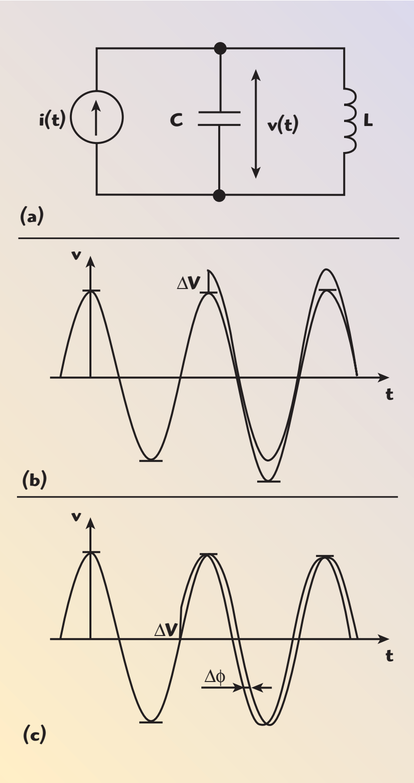

▲ *Fig. 2 Second-order LC oscillator and the effect of an injected impulse.*

Figure 2 shows the equivalent circuit of the negative resistance oscillator with an injected small perturbation current i(t). In a steady-state oscillation mode, when the losses in the resonant circuit are compensated by the energy inserted into the circuit by the active device, the second-order differential equation of the oscillator is written as

$$\frac{d^2v}{dt^2} + \omega_0^2 v = \frac{1}{C}\frac{di}{dt} \qquad (12)$$

where $\omega_0 = 1/\sqrt{LC}$ is the resonant frequency and v(t) is the voltage across the resonant circuit. If a current impulse i(t) is injected, the amplitude and phase of the oscillator will have time-dependent responses. According to Equations 10 and 11, the resultant amplitude and phase changes have a quadrature dependence with respect to each other. When an impulse is applied at the peak of the voltage across the capacitor, there will be a maximum amplitude deviation with no phase shift (b). On the other hand, if the current impulse is applied at the zero crossing, it will result in a maximum phase deviation with no amplitude response, as shown in (c).

Suppose that a perturbation current i(t), injected into the oscillation circuit, is a periodical function that can generally be expanded into a Fourier series

$$i(t) = I_0 \cos\Delta\omega t + \sum_{k=1}^{\infty}\left\{I_{kc}\cos\left[\left(k\omega_0 + \Delta\omega\right)t\right] + I_{ks}\sin\left[\left(k\omega_0 + \Delta\omega\right)t\right]\right\} \qquad (13)$$

where

I_0 = DC component of the current
I_{kc} = kth cosine current harmonic amplitude
I_{ks} = kth sinusoidal current harmonic amplitude and $\Delta\omega << \omega_0$

In this case, the small external force can be redefined as

$$n = \frac{1}{\omega_0 C}\frac{di}{d\tau} = L\frac{di}{dt} \qquad (14)$$

Consequently, substituting Equation 13 into Equations 10 and 11 and taking into account that $\omega_0 + \Delta\omega \cong \omega_0$ results in

$$\Delta V(t) = -\frac{I_{1s}}{2C}\frac{\cos(\Delta\omega t) - 1}{\Delta\omega} \qquad (15)$$

$$\Delta\phi(t) = -\frac{I_{1c}}{2CV}\frac{\sin(\Delta\omega t)}{\Delta\omega} \qquad (16)$$

where V is the voltage amplitude across the capacitor C. In this case, only the fundamental components of the injected current i(t) can contribute to the amplitude (sine amplitude) and phase (cosine amplitude) fluctuations given by Equations 15 and 16, because for the DC and kth-order current components, the arguments for all their integrals in Equations 10 and 11 are significantly attenuated by the averaging over the integration period.

The output voltage of an ideal cosine oscillator with constant amplitude V and phase fluctuations Δϕ can be written as

$$v(t) = V\cos\left[\omega_0 t + \Delta\theta(t)\right] = V\cos\left[\Delta\phi(t)\right]\cos\omega_0 t - V\sin\left[\Delta\phi(t)\right]\sin\omega_0 t \qquad (17)$$

resulting in an output spectrum of the oscillator with sidebands close to the oscillation frequency ω_0. Since, for a narrowband phase modulation with small phase fluctuations, sin $[\Delta\phi(t)] \cong \Delta\phi(t)$ and cos $[\Delta\phi(t)] \cong 1$, the phase modulation spectrum given by Equation 17 can be rewritten by using Equation 16 as

$$v(t) = V\cos\omega_0 t + \frac{1}{4C\Delta\omega}\cos\left[(\omega_0 - \Delta\omega)t\right] - \frac{I}{4C\Delta\omega}\cos\left[(\omega_0 + \Delta\omega)t\right] \quad (18)$$

which is similar to the single-tone amplitude modulation spectrum containing the spectral components corresponding to the carrier frequency ω_0 and two close sideband frequencies $\omega_0 - \Delta\omega$ and $\omega_0 + \Delta\omega$.

The injection of the current

$$i(t) = I_0\cos\Delta\omega_0 t + \sum_{k=1}^{\infty}\left\{I_{kc}\cos\left[(k\omega_0 - \Delta\omega)t\right] + I_{ks}\sin\left[(k\omega_0 - \Delta\omega)t\right]\right\} \quad (19)$$

has similar effect, resulting in twice the noise power at the sidebands. Therefore, an injected total current i(t) results in a pair of equal sidebands at $\omega_0 \pm \Delta\omega$ with a sideband power P_{sb} relative to the carrier power P_c given by

$$\frac{P_{sb}(\omega_0 \pm \Delta\omega)}{P_c(\omega_0)} = 2\left(\frac{I_{1c}}{4CV\Delta\omega}\right)^2 \quad (20)$$

Now let us assume that a stationary thermal noise current with a white power spectral density $\overline{i_n^2}$ is injected into the oscillator circuit close to carrier. Then, by making a replacement between the amplitude and root-mean-square current values when $I_{1c}^2/2 = \overline{i_n^2}$, the single sideband power spectral density for the phase fluctuations at $\Delta\omega$ offset from the carrier ω_0 in the 1/f region can be written using Equation 20 as

$$L(f_m) = \frac{\overline{i_n^2}}{4C^2V^2\Delta\omega^2} \quad (21)$$

Taking into account that $\overline{i_n^2} = 4FkT/R_L$ for $\Delta f = 1$ Hz, $Q_L = \omega_0 CR_L$ and $P_L = V^2/2R_L$, where R_L is the tank parallel or load resistance, Equation 21 can be rewritten as

$$L(f_m) = \frac{2FkT}{P_L}\left(\frac{\omega_0}{2Q_L\Delta\omega}\right) \quad (22)$$

which is similar to the one for the negative resistance oscillator (see Equation 26 in Part II[2]).

Effect of Higher Order Harmonics

Generally, the transition from soft start-up oscillation conditions to steady-state self-sustained oscillations is provided as a result of the degradation of the device transconductance in a large-signal mode, when the active device operates in both pinch-off and active regions. As a result, for the cosine voltage across the resonant circuit, the output collector (or drain) current i(t) represents a Fourier series expansion

$$i(t) = I_0 + \sum_{n=1}^{\infty} I_n\cos(n\omega_0 t) \quad (23)$$

where

I_0 = DC current
I_n = amplitude of the nth harmonic component

If the oscillation frequency is equal to the resonant circuit frequency, which means that the active device has no effect on the oscillation frequency, then the fundamental component of the collector voltage will be in phase with the fundamental component of the collector current. However, for all higher order voltage harmonics the impedance of the resonant circuit will be capacitive since the collector current harmonics are mostly flowing through the shunt capacitance. Therefore, for the Meissner oscillator circuit shown in ***Figure 3***, the voltage at the input of the active device can be approximately represented as

$$V_{in}(t) = V_{in1}\cos\omega_0 t + \sum_{k=2}^{\infty} V_{ink}\cos\left(k\omega_0 t - \frac{\pi}{2}\right) \quad (24)$$

where $V_{ink} << V_{in1}$ for a high value of the oscillator loaded quality factor.

In this case, when the active device's transfer characteristic is approximated by a second-order polynomial $i(t) = a_0 + a_1 v_{in} + a_2 v_{in}^2$ and the input voltage $v_{in}(t)$ in Equation 24 is limited to the first two factors when k = 2, the output fundamental current corresponding to the two-harmonic input voltage can be written as

$$i_1'(t) = I_1\cos\omega_0 t + a_2 V_{in1}V_{in2}\cos\left(k\omega_0 t - \frac{\pi}{2}\right) \quad (25)$$

where $I_1 = g_m V_{in1}$, $g_m = a_1$ is the average transconductance for cosine input voltage. Equation 25 can be rewritten in the form of

$$i_1'(t) = I_1'\cos(\omega_0 t + \phi_1) \quad (26)$$

where

$$I_1' = I_1\sqrt{1 + \left(\frac{a_2}{a_1}\right)^2 V_{in2}^2}$$

$$\phi_1 = -\tan\left(\frac{a_2}{a_1}V_{in2}\right)$$

From Equation 26, it follows that the presence of the second-order voltage harmonic contributes, first to the changes in the fundamental amplitude ($I_1 \neq I_1'$) and average transconductance

$$g_m' = \frac{I_1'}{V_{in1}} = gm\sqrt{1 + \left(\frac{a_2}{a_1}\right)^2 V_{in2}^2} \quad (27)$$

and second, to the appearance of the phase shift ϕ_1 between the fundamental current and fundamental voltage. The latter means that the device transconductance becomes complex due to the effect of the higher order harmonics and its magnitude and phase depend on the harmonic level. For example, an increase of the harmonic level results in a decrease in the oscillation frequency.

Physically, the influence of the harmonic content on the frequency variation can be explained as follows: if the oscillations are purely sinusoidal, the energy distribution in both arms of the resonant LC-circuit is equal; when the

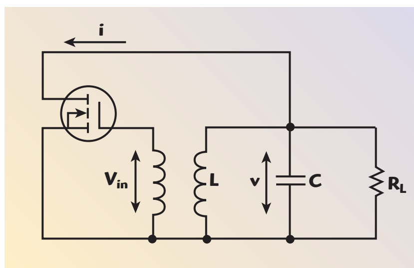

Fig. 3 Schematic of a parallel feedback oscillator.

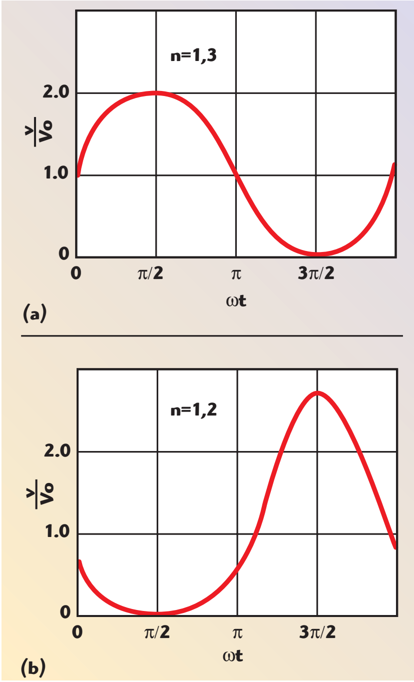

▲ *Fig. 4 Voltage waveform for n harmonic peaking.*

harmonics appear, the currents corresponding to them flow mainly through the capacitive arm, and therefore they increase the electrostatic energy of this arm in comparison with the inductive arm; in order to keep the energy equal in both arms, the fundamental frequency must slightly decrease with respect to the frequency given by the tank circuit only.[7]

In a general form, the frequency deviation $\Delta\omega$, caused by the presence of harmonics of the voltage v on the resonant circuit, can be obtained from

$$\frac{\Delta\omega}{\omega_0} = -\frac{1}{2}\sum_{k=2}^{\infty}\left(k^2-1\right)m_k^2 \qquad (28)$$

where k is the order of harmonic and $m_k = V_k/V_1$ is the ratio of the harmonic voltage component to the fundamental voltage.[7]

In view of the multiharmonic representation of the oscillator output spectrum due to the device and resonant circuit nonlinearities, the total phase fluctuations can be represented by a superposition integral as a result of each harmonic contribution. This is similar to the Fourier harmonic expansion in the frequency domain of the voltage waveform, when the phase trajectory on the phase plane is a result of the phase trajectories with different radii and velocities corresponding to the DC shift and harmonic amplitudes. In this case, Equation 11 can take the general form

$$\Delta\phi(t) = -\frac{1}{A}\int_0^{\omega_0 t} n(\tau)\Gamma(\tau)d\tau \qquad (29)$$

where

$$\Gamma(t) = \frac{c_0}{2} + \sum_{n=1}^{\infty} c_n \cos\left(n\omega_0 t + \phi_n\right) \qquad (30)$$

in a dimensionless periodic function characterizing the shape of the limit cycle or phase trajectory corresponding to the oscillation waveform and depending on the oscillator topology. It is called the impulse sensitivity function (ISF) for an approximate model for the oscillator phase behavior[3] and serves a similar role at the perturbation projection vector (PPV) for the exact model.[8] The initial phase ϕ_n in Equation 30 is not important for random noise sources and can be neglected. For an ideal case of a purely sinusoidal oscillator, c1 = 1 and $\Gamma(t) = \cos\omega_0 t$. Now if any stationary noise current with a white power spectral density $\overline{i_n^2}/\Delta f$ is injected into the oscillator circuit close to any harmonic $n\omega_0 + \Delta\omega$ or $n\omega_0 - \Delta\omega$, it will result in a pair of equal sidebands at $\omega_0 \pm \Delta\omega$. Then, the total single sideband power spectral density for the phase fluctuations in a bandwidth $\Delta f = 1$ Hz can be written, based on Equation 21, as

$$L\left(f_m\right) = \frac{\overline{i_n^2}\sum_{n=0}^{\infty} c_n^2}{4C^2V^2\Delta\omega^2} = \frac{\overline{i_n^2}\,\Gamma_{rms}^2}{2C^2V^2\Delta\omega^2} \qquad (31)$$

where Γ_{rms} is the root-mean-square value of $\Gamma(t)$.[4] Thus, the total noise power near the carrier frequency of the oscillator is a result of the up-converted 1/f noise near DC, weighted by coefficient c_0, the noise near the carrier weighted by coefficient c_1 and the down-converted white noise near the second- and higher order harmonics weighted by coefficients c_n, n = 2,3,…. The converted phase noise due to the conversion from one sideband to another can be of the order of 6 dB higher than the additive noise in the oscillator.[9]

From Equation 31, it follows that the effect of the converted phase noise can be reduced by minimizing

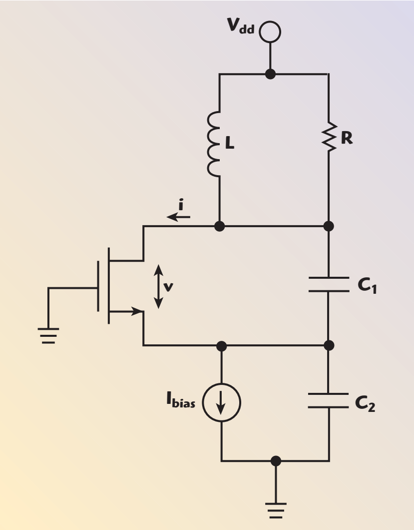

▲ *Fig. 5 Simplified Colpitts oscillator schematic.*

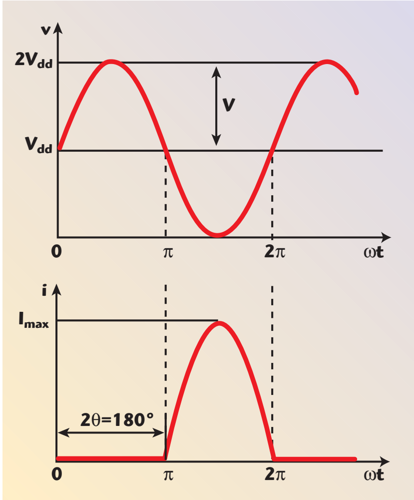

▲ *Fig. 6 Ideal class B drain voltage and current waveforms.*

the DC coefficient c_0 and the higher order harmonic coefficients c_n, n =2, 3,..., of the (τ), approximating the cosine waveform of the injected node voltage. ***Figure 4*** shows the voltage waveforms corresponding to (a) class F with flattened waveform consisting of the fundamental and third harmonics only and (b) inverse class F consisting of the fundamental and second harmonics only.[10] To realize the symmetrical flattened voltage waveform, the ratio between the fundamental and third harmonic should be equal to $V_1/V_3 = 9$, while the ratio between the fundamental and second harmonic is equal to $V_1/V_2 = 4$ for the symmetrical waveform close to the half-cosine shown. Hence, the level of higher order harmonics is significantly smaller for the symmetrical flattened voltage waveforms. It should be noted that, in class E operation with a non-symmetrical voltage waveform, the effect of the second- and higher order harmonics is significant, resulting in a high value of the voltage peak factor. The importance of the symmetry is necessary also to minimize the coefficient c_0 responsible for the low noise up-conversion and amplitude-to-phase conversion.[3] A phase noise improvement can be achieved by reducing the effect of the device and circuit nonlinear capacitances (see Part II,[2] Equation 42). Due to the amplitude-to-phase conversion, the phase for each higher order harmonic changes with amplitude resulting in a generally asymmetrical voltage waveform.

Equation 29 describes an approximate phase noise behavior, compared with the accurate equation given by Demir, et al.,[8] where the phase of φ(t) also appears in its right-hand side. Such a simplified phase noise model is valid for the case of stationary noise sources like white noise. However, when the noise sources are no longer stationary, it can be accurate only in the limits of an assumption of the small phase shifts for which cos Δφ is close to unity. This implies that the approximate model is not accurate enough to analyze neither injection-locking phenomenon nor related issues like the behavior of phase differences of coupled oscillators.[11]

The response of the oscillation system to an impulsive noise can be provided by its direct measurement with a SPICE simulator, when an impulse is injected into the node of interest of the oscillator circuit and the oscillator simulated for a few cycles afterwards.[3] By substituting the equivalent current noise source of each individual node in Equation 29, the phase contribution of each node can be calculated.[12] However, any further analytical simplification based on the orthogonal decomposition of noise into amplitude and phase components may not yield the correct result.[13]

CYCLOSTATIONARY NOISE

The noise sources in an oscillator generally cannot be modeled only as stationary since the statistical properties of some of them may change with time in a periodic manner. Such types of noise sources are referred to as cyclostationary. If the thermal noise of the resistor has a stationary nature, then the collector (or drain) shot noise of the transistor is an example of cyclostationary noise due to the time-varying nature of the collector current. The most important issue is that the collector shot noise is dominant, compared to the noise from the base resistance or tank losses, and can contribute approximately 70 percent of the total phase noise of the oscillator.[12]

Figure 5 shows a simplified, single-ended, common gate CMOS Colpitts oscillator configuration where the required regeneration factor for the start-up oscillation conditions is chosen using a proper ratio of the feedback capacitances C_1 and C_2. The idealized voltage and current waveforms corresponding to the large-signal operation in idealized class B with zero saturation voltage are shown in ***Figure 6***.

Equation 23, or the drain time-varying current, can be rewritten in the form of

$$i(t) = I_{max}\left[\alpha_0 + \sum_{n=1}^{\infty}\alpha_n \cos(n\omega_0 t)\right] \tag{32}$$

where α_n is the ratio of the nth harmonic current amplitude to the peak output current I_{max}, expressed through half the conduction angle θ as

$$\alpha_n = \frac{I_n}{I_{max}} = \frac{\gamma_n(\theta)}{1-\cos\theta} \tag{33}$$

where

$\gamma_n(\theta)$ = current coefficients

To account for the cyclostationary drain noise source as a result of total noise sources injected at frequencies $n\omega_0 \pm \Delta\omega$, Equation 31, in a general form, can be rewritten as

$$L(f_m) = \frac{\overline{i_{nd}^2}\sum_{n=0}^{\infty}(\alpha_n c_n)^2}{4C^2V^2\Delta\omega^2} \tag{34}$$

where $\overline{i_{nd}^2} = 2qI_{max}$ is the drain current noise power density in a frequency bandwidth Δf = 1 Hz. The Fourier components for the current waveform close to half-cosinusoidal show that the drain shot noise is mixed mostly with the fundamental and second harmonics to contribute to the total phase noise of the oscillator.

To minimize the oscillator phase noise, it is very important to choose the optimum value of the feedback ratio k $= C_2/C_1$ for the same total capacitance $C = C_1C_2/(C_1 + C_2)$. This is because different values of the conduction angle correspond to different harmonic contribution to the output spectrum. In the case of class B with $\theta = 90°$, the third-, fifth- and higher order harmonics can be eliminated since their current coefficients γ_n (for n = 3,5,…) become equal to zero. As a rule-of-thumb, the optimum feedback ratio for a Colpitts oscillator can be chosen to be approximately k = 3.5 to 4.[3,12]

CONCLUSION

The impulse response model for the oscillator phase noise, which has become popular recently, is explained based on a well-known phase plane approach. This model specifies the contribution of the noise components located near integer multiples of the oscillation frequency in terms of waveform properties and circuit parameters. By using this nonlinear approach, it is impossible to derive an explicit relationship between the oscillator stability conditions, amplitude-to-phase conversion and phase noise power density, unlike with the Kurokawa approach. Such an approach, however, based on the inherent time-varying nature of the oscillator, provides an important design insight by identifying and quantifying the major sources of phase noise degradation. ■

References

1. A. Grebennikov, "Transistor LC Oscillators for Wireless Applications: Theory and Design Aspects, Part I," *Microwave Journal*, Vol. 48, No. 10, October 2005, pp. 62–78.
2. A. Grebennikov, "Transistor LC Oscillators for Wireless Applications: Theory and Design Aspects, Part II," *Microwave Journal*, Vol. 48, No. 11, November 2005, pp. 62–82.
3. A. Hajimiri and T.H. Lee, "A General Theory of Phase Noise in Electrical Oscillators," *IEEE Journal of Solid-State Circuits*, Vol. 33, February 1998, pp. 179–194.
4. T.H. Lee and A. Hajimiri, "Oscillator Phase Noise: A Tutorial," *IEEE Journal of Solid-State Circuits*, Vol. 35, March 2000, pp. 326–336.
5. A.A. Andronov, A.A. Vitt and S.E. Khaikin, *Theory of Oscillations*, Dover Publications, New York, NY, 1987.
6. K.A. Samoylo, *Method of Analysis of Second-order Oscillation Systems*, Moskva: Sov. Radio, 1976.
7. J. Groszkowski, "The Interdependence of Frequency Variation and Harmonic Content, and the Problem of Constant-frequency Oscillators," *Proceeding of the IRE*, Vol. 21, July 1933, pp. 958–9813.
8. A. Demir, A. Mehrotra and J. Roychowdhury, "Phase Noise in Oscillators: A Unifying Theory and Numerical Methods for Characterization," *IEEE Transactions on Circuits and Systems I: Fundamental Theory and Applications*, Vol. I-47, April 2000, pp. 655–673.
9. J.C. Nallatamby, M. Prigent and J. Obregon, "On the Role of the Additive and Converted Noise in the Generation of Phase Noise in Nonlinear Oscillators," *IEEE Transactions on Microwave Theory and Techniques*, Vol. 53, No. 3, March 2005, pp. 901–906.
10. A. Grebennikov, *RF and Microwave Power Amplifier Design*, McGraw-Hill, New York, NY, 2004.
11. P. Vanassche, G. Gielen and W. Sansen, "On the Difference between Two Widely Publicized Methods for Analyzing Oscillator Phase Behavior," *Proceedings of the IEEE/ACM International Conference on Computer Aided Design*, 2002, pp. 229–233.
12. M.A. Margarit, J.L. Tham, R.G. Meyer and M.J. Deen, "A Low Noise, Low Power VCO with Automatic Amplitude Control for Wireless Applications," *IEEE Journal of Solid-State Circuits*, Vol. 34, June 1999, pp. 761–771.
13. G.J. Coram, "A Simple 2-D Oscillator to Determine the Correct Decomposition of Perturbations into Amplitude and Phase Noise," *IEEE Transactions on Circuits and Systems I: Fundamental Theory and Applications*, Vol. I-48, July 2001, pp. 896–898.

Andrei Grebennikov *received his MSc degree in electronics from the Moscow Institute of Physics and his PhD degree in radio engineering from the Moscow Technical University of Communications and Informatics in 1980 and 1991, respectively. He joined the scientific and research department of the Moscow Technical University of Communications and Informatics as a research assistant in 1983. From 1998 to 2001, he was a member of the technical staff at the Institute of Microelectronics, Singapore, responsible for the design and development of LDMOS FET high power amplifier modules. Since January 2001, he has been with M/A-COM Eurotec as a principal engineer, where he is involved in the design and development of the handset advanced transmitter architectures in general and in GaP/GaAs HBT power amplifier modules for new generations of wireless communications systems. His scientific and research interests include the design and development of power RF and microwave radio transmitters for base station and handset applications, hybrid integrated circuits and MMIC of high efficiency, and linear microwave and RF power amplifiers, single-frequency and voltage-controlled oscillators using any type of bipolar and field-effect transistors, and active device modeling.*

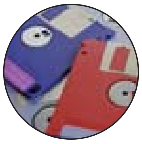

EDITORIAL INDEX

2005 • Volume 48

■ ANTENNAS

■ CAD/CAM

■ COMMERCIAL APPLICATIONS

■ COMPONENTS/SUBSYSTEMS

■ COVER FEATURES

■ DESIGN

EDITORIAL INDEX

2005 • Volume 48

Microwave Journal

CALL FOR PAPERS

To see one's work in print is the rightful reward of every creative engineer and scientist. The editors of *Microwave Journal* invite you to submit your technical manuscripts for consideration to be published in one of our upcoming issues. Technical articles, application notes and tutorial articles based on the monthly editorial themes are encouraged. Editorial themes include wireless, radar and antennas; RF components and systems; test and measurement; amplifiers and oscillators; semiconductors and MMICs; commercial applications; IVHS and ITS; dual technologies; communications and PCN; passive components; and control devices, modulation and DSP.

Design features should contain new and innovative technical ideas of practical use and interest to our predominantly engineering readers. Papers should be 14 to 16 double-spaced pages and contain 8 to 12 visual aids in the form of sketches, graphs, photographs or tables.

Papers should be submitted to the attention of the Technical Editor and will be reviewed promptly by our Editorial Review Board prior to acceptance. Articles outside of the monthy themes also will be considered.

SEND ALL MATERIAL TO:

Microwave Journal
685 Canton Street
Norwood, MA 02062
(781) 769-9750
Fax (781) 769-5037
e-mail:
fbashore@mwjournal.com

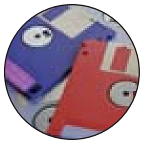

EDITORIAL INDEX

2005 • Volume 48

■ TUTORIAL SERIES

■ 2005 EuMC CONFERENCE

■ 2005 MTT-S CONFERENCE

■ 2006 RWS CONFERENCE

■ SUPPLEMENT FEATURES

Looking for an article?
Looking for an author?
Visit www.mwjournal.com to search our comprehensive on-line database for archived ***Microwave Journal*** articles dating as far back as 1997.

—*Simply click*—
"The Magazine,"
"Editorial Archives"
and then plug in
your search criteria

CALIBRATION TECHNOLOGY ENABLING 67 GHZ MULTIPORT S-PARAMETER MEASUREMENT WITH CONFIDENCE

Cascade Microtech has developed WinCal 2006™ with new software tools to address the many testing challenges brought on by the increase in the volume of complex, high speed semiconductors that are designed for use in mobile communications products such as cell phones, PDAs and laptop computers. Compounding the multi-gigabit high speed requirement is the fact that lower operating voltage ICs are becoming increasingly susceptible to random bit errors forcing engineers to differential circuit designs to increase noise immunity. With this complexity comes an increased need to make accurate and repeatable multiport RF measurements on-wafer for design validation and to ensure they do not fail in production. Since the responsibility for testing often falls to the research and development team, many engineers must perform — for the first time — high frequency device characterization using a wafer probing station coupled with a multiport vector network analyzer (VNA).

Leveraging off of 20 years of on-wafer VNA calibration and measurement experience, WinCal 2006 software offers advanced tools that exceed the needs of today's multiport VNA users. Multimedia tutorials, self-guided Wizards and pre-optimized quick set ups provide fast starts for both novices and experts. The highly interactive graphical user interface provides access and control to every element of the system — VNA, probes, calibration standards and all measurements. Fully automatic VNA calibrations using industry standard routines, or Cascade Microtech's advanced, patented routines on par with the best NIST methods are provided at the click of a button. Enhanced reporting features allow operators to manipulate multiple sets of raw and calibrated data, standard measurements and VNA error correction terms, or transform them into H-, X-, Y- or differential S-parameters.

CASCADE MICROTECH INC.
Beaverton, OR

67 GHz MULTIPORT ON-WAFER MEASUREMENT CHALLENGES

The rise in the need for reliable differential millimeter-wave S-parameter measurements for circuit modeling gave advent to the multiport VNA. Today's multiport VNA relies on four-port, single-ended S-parameters transformed mathematically to produce the needed differential S-parameters. This technique works well assuming the measurement ports are uncoupled error-corrected coaxial measurement ports. To produce the same single-mode coaxial TEM quality VNA measurement environment, metal-fingered multi-contact coplanar waveguide (CPW) probes have been replaced by Cascade Microtech's patented thin film MIC tips, which reduces crosstalk from typically > 10 percent at 20 GHz for metal-finger probes to less than 1 percent at 67 GHz for thin film tips. Additionally, for the physically larger multiport calibration standards to maintain single-mode, uncoupled operation, it is necessary to use mode-suppressing elements on the substrate — developed and patent pending by Cascade Microtech — and prober auxiliary chucks proven to be mode-free beyond 110 GHz.

CALIBRATION, VERIFICATION AND MONITORING ARE THE KEYS TO ACCURATE MEASUREMENTS

When performing on-wafer measurements above 50 GHz, there are many issues that can affect the accuracy and reliability of the data, including vector repeatability, probe contact planarity and contact cleanliness. At the heart of WinCal 2006 resides software tools designed to minimize and control all systematic errors and thus produce and maintain the environment for highest quality measurements yielding more accurate model extractions.

Under the System Qualification Tools, shown in ***Figure 1***, operators now have access to tools that assure the mechanical integrity of all of the VNA test ports, cables and multi-contact RF probes testing each of these critical parameters. Probe contact planarity is critical to high frequency S-parameter measurements because the most frequent operational error prior to calibration is due to a lack of planarity. Ensuring contact cleanliness is important because contamination can and will accumulate with multiple device contacts during the measurement routine, which can cause intermittent test errors and inaccurate results.

WinCal 2006 Repeatability Tools allow users to test the vector repeatability of all measurements necessary for calibration. At any time during calibration, a test can be performed to test the repeatability of all measurement ports, simultaneously, to ensure their stability, which is necessary for calibration. This test is done prior to calibration to ensure system integrity; the calibration will abort when repeatability is inadequate on any port.

Under the WinCal 2006 Calibration menu, users first define the number of VNA ports to calibrate,

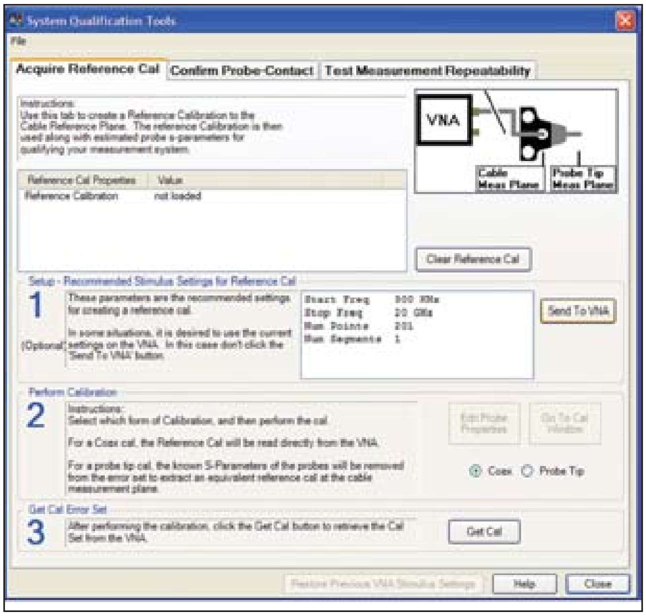

▲ *Fig. 1 System qualification and reliability tools.*

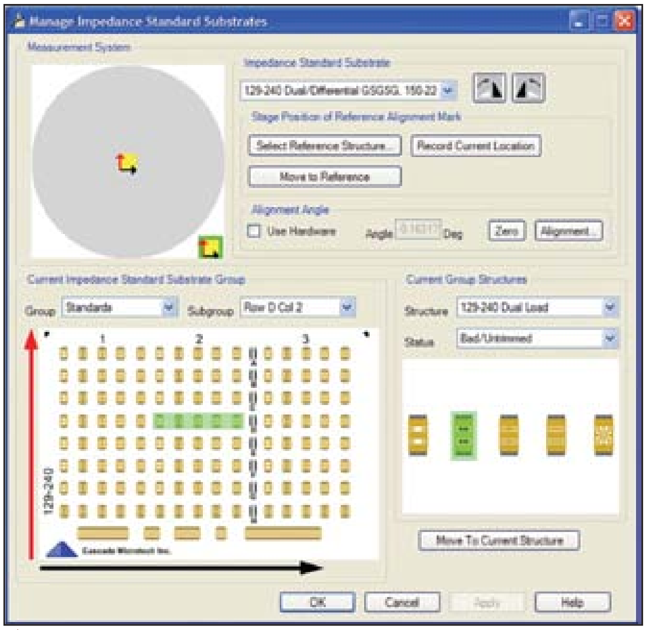

▲ *Fig. 2 Impedance standard substrate management tools for calibration.*

then select from a list of industry standard calibration methods such as SOLT, LRM or advanced algorithms such as SOLR or Cascade Microtech's proprietary LRRM algorithm. In the case of the multiport VNA, WinCal 2006's SOLT algorithm is optimized by the new reduced thru method allowing full correction from measurement of only four thrus instead of the previously required six. The reduced thru method minimizes the number of elements, definitions and moves, which speeds up the routine while reducing errors resulting from over-determination of standards. Once the calibration preferences are se-

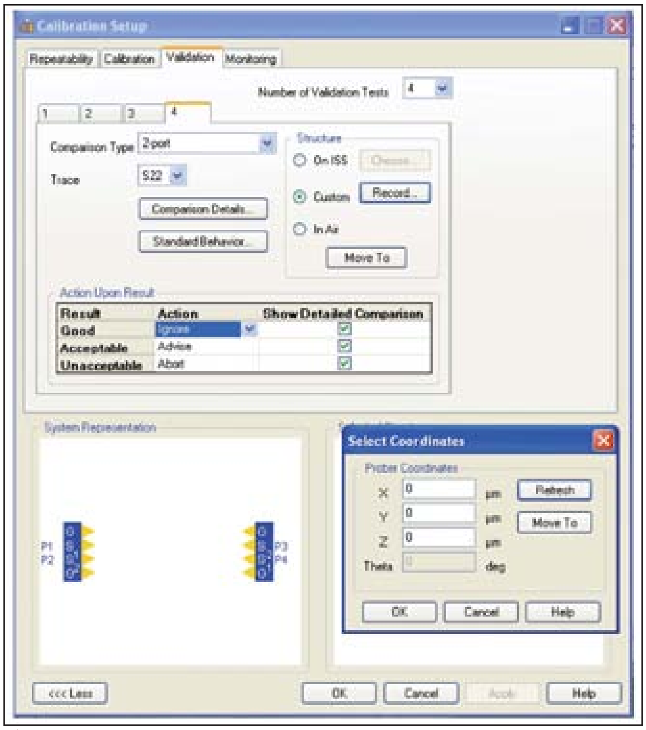

Fig. 3 Port validation tools.

lected, WinCal 2006 will direct the probe station to move to the required standards, take raw S-parameter measurements, compute the VNA error terms and set the VNA corrections — all automatically. WinCal 2006 allows users to mark when structures have reached this limit, and retain the status of these bad structures. Once a structure is marked bad, the prober will never visit it again. WinCal 2006 will keep track of the good standards and the bad standards and manage the Impedance Standard Substrates (ISS) commonly used today (see ***Figure 2***).

WinCal 2006 Validation Tools, shown in ***Figure 3***, allow the operator after calibration to check the corrected S-parameter of all the measurement ports against previously determined good measurements depending on their standard of choice. As with previous versions of WinCal, users can select from verification elements resident on Cascade Microtech's Impedance Standard Substrates as the reference standard. However, with WinCal 2006, it is also possible for a user to compare current measurements to previously filed reference measurements, or better yet, can provide their own "golden device" as the reference standard for validation. This capability allows the utmost level of flexibility while maintaining the reliability and repeatability of high frequency S-parameter measurements.

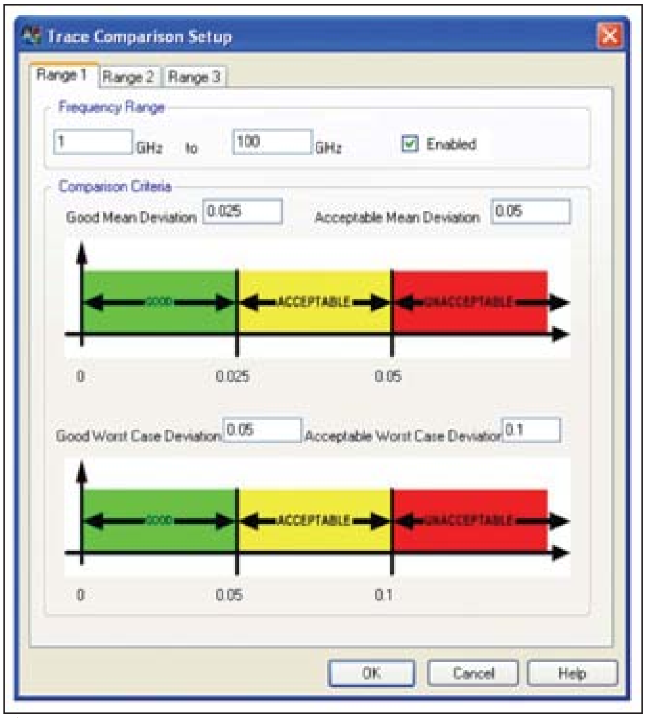

▲ *Fig. 4 User-defined drift limits for monitoring.*

WinCal 2006 Monitoring Tools allow the user to measure the drift of any or all of the VNA ports simultaneously. User defined drift limits can be set for any or all S-parameters to monitor the stability of the VNA test system and assure the integrity of the resultant S-parameter measurements (see ***Figure 4***). Any change to the VNA test system after calibration could cause the calibration to be invalid. With WinCal 2006's monitoring tools, a user is notified in real-time when any port drifts past the defined drift limits.

CONCLUSION

WinCal 2006 offers the most trustworthy and efficient vector network analyzer calibration available for metrology grade S-parameter measurement. Through on-line wizards and tutorials, it provides a fast start for new and experienced users. The enhanced validation capabilities as well as flexible reporting functions offer a higher level of confidence in RF measurements. WinCal 2006 was developed as the calibration platform for the future by allowing for customization and future functionality. Its ease-of-use will eliminate errors in the VNA calibration process in RF device characterization, and allow more users to make meaningful and valuable measurements.

Cascade Microtech Inc.,
Beaverton, OR (503) 601-1000,
www.cascademicrotech.com.

RS No. 302

COMPLETE TRANSMIT SOLUTIONS USING A QUAD-BAND TX/RX FRONT-END MODULE WITH INTEGRATED POWER CONTROL

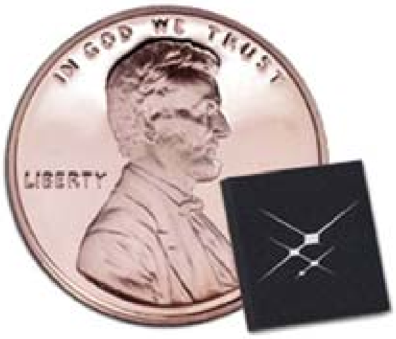

Leaping ahead in the race to deliver more and more functionality and value to the handset maker, Skyworks Solutions has introduced the industry's best transmit front-end solution (SKY77506) for GSM/GPRS segment. Two InGaP HBT power amplifiers (PA), a BiCMOS power controller and two PHEMT-based RF switches have been integrated into a compact 8 × 8 × 1.2 mm module. All RF output and input ports are DC blocked, ESD protected and matched to 50 Ω. ***Figure 1*** shows the block diagram of the device.

KEY FEATURES

The SKY77506 module features direct antenna connection without additional harmonic filtering or ESD protection components. It represents the lowest power consumption transmit solution and offers 48 percent GSM power-added efficiency (1200 mA @ 33 dBm) and 42 percent DCS/PCS power-added efficiency (680 mA @ 30 dBm), resulting in the longest talk-time transmit solution. Its power flatness allows calibration at only one frequency per band. It also features a wide input power range (0 to 6 dBm) and there are no oscillations greater than –36 dBm at 12:1 VSWR.

Receive port selectivity is 25 dB and only four external passive components are required. The new SKY77506 module is extremely rugged with no risk of damage transmitting into any load impedance.

COMPARATIVE ADVANTAGE

SKY77506 provides a significant advantage over the PA + ASM approach to design front-end solutions. In summary, the front-end module (FEM):

- Eliminates the need for a PA-to-switch design effort while providing optimal matching and all harmonic filtering.
- Offers significantly lower current than a PA + ASM combination, which directly translates to longer talk-time (see ***Figure 2***).
- Post-PA losses are minimized, enabling higher efficiency and longer talk-time.

SKYWORKS SOLUTIONS INC.
Woburn, MA

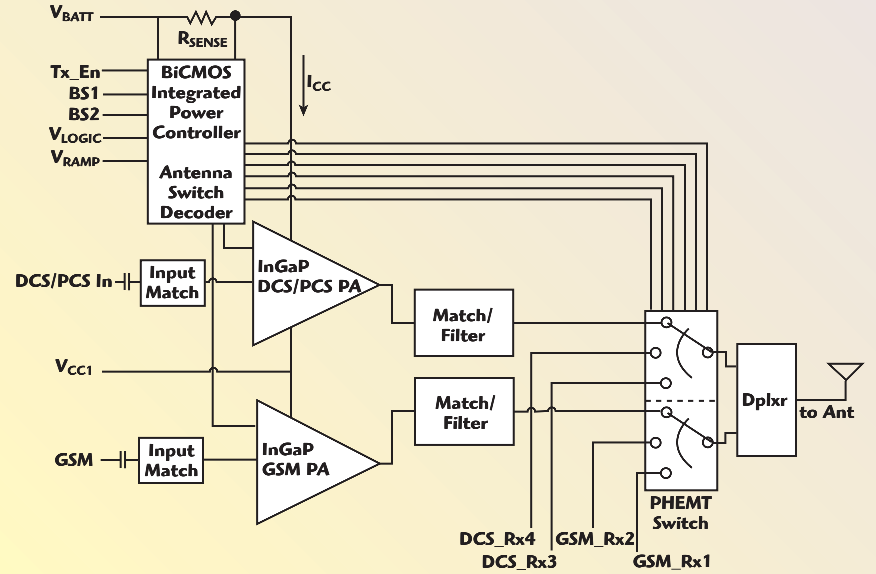

▲ *Fig. 1 Block diagram of the SKY77506 front-end module.*

- Reduces BOM part count, easing supply chain, purchasing and inventory management.
- Provides tested, guaranteed performance at the highest assembly level; no yield loss due to tolerances stack-up or mismatch between PA and an ASM on the phone board.
- Is compatible with 1.2, 1.5, 1.8, 2.5, or 3.3 V control logic.

SWITCH DIPLEXER FRONT END

The SKY77506 is configured with separate 1P3T T/R switches for high and low bands. A diplexer, positioned between the switches and the antenna, combines the two bands but also provides additional value to the designer. It provides a DC path between the antenna pin and ground, which provides a high degree of ESD protection and eliminates the need for an external shunt inductor or spark gap. It also provides DC blocking between the antenna pin and active internal circuits. The antenna pin can be directly connected to the antenna or a coax connector. The diplexer provides a significant amount of frequency selectivity between the PHEMT switches and the antenna (see **Figure 3**). This greatly reduces the handsets' vulnerability to strong out-of-band interferers or "blockers," such as from broadcast television or radio transmitters that can intermodulate with unprotected switches and generate unwanted interference.

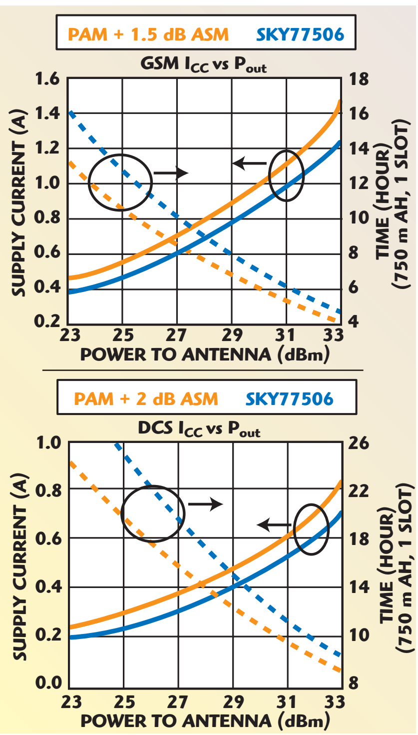

▲ *Fig. 2 Battery current and talk time.*

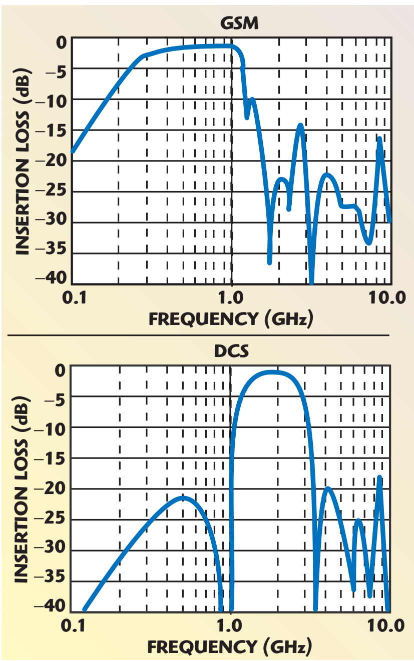

▲ *Fig. 3 GSM/DCS switch insertion loss.*

CURRENT-REGULATION POWER CONTROL ADVANTAGES

The SKY77506 is based on the innovative Skyworks integrated power control (iPAC) current-regulation power control approach, which has proven to result in the lowest current and longest handset talk-times. Current regulation is accomplished by measuring the differential voltage across an internal precision low loss sense resistor. An internal control loop automatically adjusts the PA bias to maintain a constant ratio between I_{CC} and V_{RAMP}. Unique design approaches were used to provide immunity to temperature and supply voltage variations. The iPAC function also eliminates the need for directional couplers, detector diodes, power control ASICs and other power control circuitry. The power-added efficiency (PAE) versus P_{OUT} characteristic of a current controlled PA is distinctly different than that of a voltage-controlled PA. Most importantly, the peak efficiency occurs at a power level that is approximately 0.5 dB lower than the maximum output power. This results in a PAE that is 5 to 8 percent higher over the critical output power range (see **Figure 4**). This translates to a current that is more than 15 percent lower at the highest power levels. The current-regulation method of power control also maintains a predictable supply current that is independent of antenna impedance changes commonly caused by hand/body proximity. This alleviates

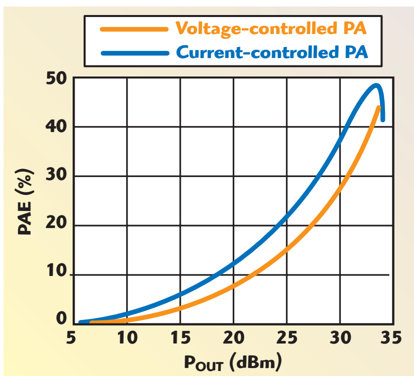

▲ *Fig. 4 Power-added efficiency of a current-controlled PA versus a voltage-controlled PA.*

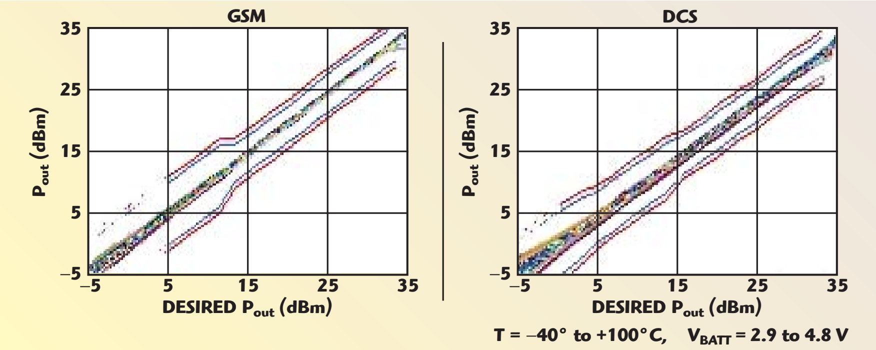

Fig. 5 Power-controlled accuracy in GSM and DCS/PCS bands.

any need for concern about call-drops due to drooping battery voltage during high current surges, and allows more of the battery discharge cycle to be used.

POWER CONTROL ACCURACY

Integrating the power amplifiers, matching networks and harmonic filters into a single module enables predictable impedances to be optimally tuned by design. This results in a very flat output power versus frequency. This allows accurate power control to be achieved by calibrating at only one frequency per band (see ***Figure 5***). Additionally, Skyworks has developed a quick calibration algorithm based on an algebraic curve fitting that has enabled customers to achieve complete power calibration of a quad-band handset in less than six seconds. This greatly enhances the production test capacity and throughput by reducing the amount of test stations required. Contact Skyworks application engineering for calibration details and S/W tools.

EASY DESIGN-IN FOR RAPID DEVELOPMENT

The result is a compact, high performance module that greatly simplifies transmitter design. The repetitive layout turns, previously required to match a discrete PA to a discrete antenna switch module, are no longer necessary. With these functions integrated into a single module, optimal matching and harmonic filtering can be easily achieved in a single design pass.

CONCLUSION

Skyworks' industry-leading RF integration expertise has been combined with its best-in-class power amplifier performance to yield a high performance, highly integrated, low cost, easy to use transmit solution for GSM/GPRS handsets. The SKY77506 is a third generation transmit plus front-end module (Tx-FEM) that is a significantly evolved successor to the SKY77500 and SKY77501, Tx-FEMs that are presently shipping at a millions-per-week rate.

Skyworks Solutions Inc.
(781) 376-3000,
www.skyworksinc.com.

RS No. 300

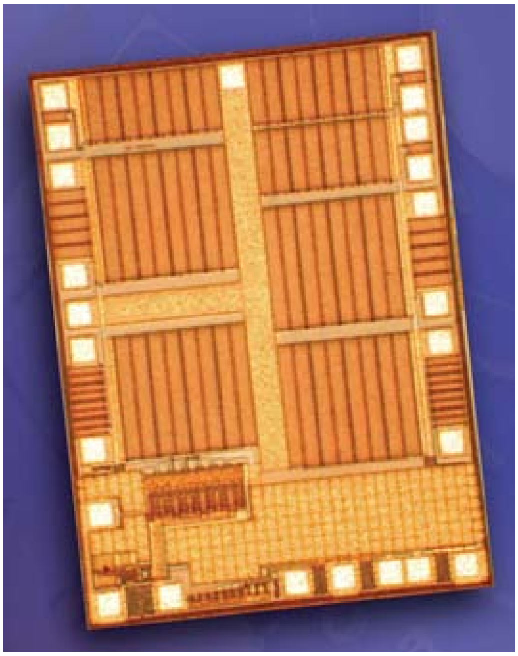

AN ULTRA-LINEAR SP7T HANDSET ANTENNA SWITCH FOR GSM/PCS/EDGE/WCDMA APPLICATIONS

Industry standards bodies — such as the 3GPP Standards organization governing global cellular networks such as GSM, PCS, EDGE and WCDMA — are traditionally chartered to create a stable business environment for advancing technology in a competitive market. These industry standards — as simple as the pitch of a PCB or as influential as the premise of Moore's Law — offer suppliers an equal opportunity to compete, and provides an industry the best chance to grow and prosper. Additionally, industry standards enable well-defined product roadmaps, which in turn set clear objectives for rapid technology advancement using focused resources. Without achievable directives, an industry stagnates as misaligned resources and product roadmaps reach a dead-end.

The cellular phone industry enjoyed well-defined guidelines for performance and mechanical footprint during the transition from analog to Second Generation (2G and 2.5G) standards. Today's 3G environment, however, is more complicated. The market continues to grow, however through consolidation now fewer companies compete for a larger share of the integrated design.

At the "RF front end" of the cellular handset, the antenna switch module (ASM) and power amplifier (PA) module have advanced on a steep learning curve due to the well defined expectations of handset manufacturers. The initial ASMs supported a single frequency band and were 5.5 × 10 mm. Today's ASMs — 81 percent smaller than their predecessors — are tasked to support four bands with significantly better RF performance, and to fit in 3.2 mm^2. Complexity is at an all time high, and the learning curve has hit an inflection point. The number of variations and the lack of GSM/WCDMA architectural, functional and mechanical standards has stalled advancement. As well, the number of frequency bands and the aggressive technical requirements of the multi-mode, multi-band GSM/WCDMA

PEREGRINE SEMICONDUCTOR CORP.
San Diego, CA

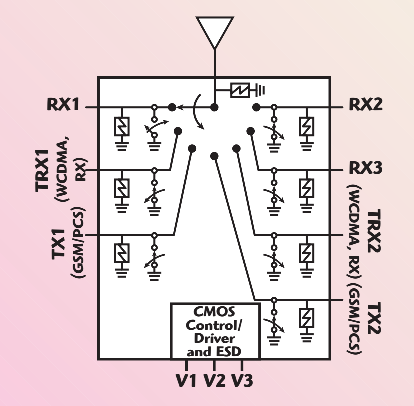

▲ *Fig. 1 The PE42671 SP7T switch.*

handset have overcome the limits of traditional RFIC technologies such as GaAs. Most critically affected by these ultra-high performance specs are the antenna and the RF switch. The antenna must effectively radiate from 800 to 2200 MHz, a daunting task given the miniscule area allowed for the antenna. The RF switch must be capable of switching up to eight paths of high power RF signals with low insertion loss, high isolation and exceptional linearity.

To create a WCDMA/GSM handset that is spec compliant, handset manufacturers have been incorporating separate WCDMA and GSM radio sections in one case — not a strategy any handset manufacturer would want on its roadmap for long. So while the industry has set its sights high, it has struggled to find a solution, until now. At the European Microwave Conference (EuMC) in Paris, France, Nokia presented a paper addressing its quest to integrate into a single radio architecture.[1] The Peregrine PE42660 SP6T switch, designed in Peregrine's UltraCMOS™ process with HaRP™ technology, was identified as a high throw count switch that meets the linearity requirements defined by the 3GPP standard: an IP3 of +65 dBm. Typical SP6T/SP7T GaAs pHEMT switches have IP3 of only +57 dBm. And now, Peregrine's newest HaRP-enhanced PE42671 SP7T switch provides for dual WCDMA bands and a quad-band GSM radio to be connected to a single antenna, delivering an unprecedented +68 dBm IP3.

PE42671 – TRUE MULTI-BAND PERFORMANCE

The PE42671 SP7T switch integrates one or two WCDMA and three or four GSM frequency bands (see ***Figure 1***). Its four transmit ports with unprecedented linearity (IP3 = +68 dBm) allow for spec-compliant handsets and efficient front-end architectures. Beyond linearity, the PE42671 switch also provides significant design value over other technologies such as PIN diode and pHEMT configurations. Small size and versatile layout, as shown in ***Figure 2***, enable the application designer to use the PE42671 switch in extremely small RF modules. The SP7T switch is comprised of two transmit ports that can be used for GSM/PCS/EDGE, two transmit/receive ports that can be used for either WCDMA or as receive ports and three symmetric receive ports. On-chip CMOS decode logic facilitates three-pin low voltage CMOS control, while high ESD tolerance of 1500 V at all ports, no blocking capacitor requirements and on-chip SAW filter overvoltage protection devices make this

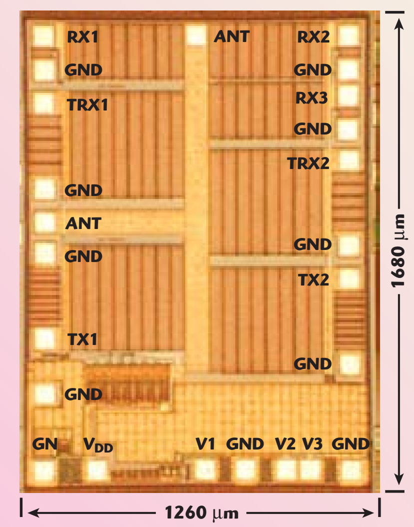

▲ *Fig. 2 PE42671 die top view.*

device the ultimate in integration and ruggedness. The switch operates at 2.75 V over a frequency range of 100 to 3000 MHz and offers low transmit insertion loss of 0.60 dB at 900 MHz and 0.80 dB at 1900 MHz. Tx-Rx isolation is 47 dB at 900 MHz and 40 dB at 1900 MHz. Its input third-order intercept is +68 dBm at 50 Ω and its IMD3 is –111 dBm (with +20 dBm Tx and –15 dBm blocker signals).

STATE-OF-THE ART HARMONICS

Harmonic performance of the RF switch is a critical element of the antenna switch module. Typical switch technologies such as PIN diode and GaAs pHEMT provide only 6 dB of margin, requiring up to three or four design iterations to match the LTCC to the switch before hitting the specification. At the maximum operating power of +35 dBm, the HaRP-enhanced UltraCMOS switch delivers –50 dBm P3fo, which is 20 dB of margin to the GSM specification of –30 dBm. The second harmonic is fundamentally low in UltraCMOS technology because distortion is symmetric on positive and negative voltage swings. In the GSM system, this very low even-order distortion for the second harmonic is desirable because the second harmonic of the GSM transmit band falls in the DCS receive band. The less than –50 dBm second-harmonic performance allows for less noise transmitted in the DCS band and increased system capacity for the carrier.

ULTRACMOS PERFORMANCE ADVANTAGE

UltraCMOS is a standard CMOS processing technology, however as opposed to building devices on silicon, a conducting substrate, it places devices directly on top of a sapphire substrate. The perfectly insulating sapphire allows UltraCMOS to maintain all the positive attributes of bulk CMOS including low power operation, manufacturability, repeatability, scaling properties and IP block re-use, and to deliver the RF performance required for 3G applications and beyond.

Reference

1. T. Ranta, J. Ellä and H. Pohjonen, "Antenna Switch Linearity Requirements for GSM/WCDMA Mobile Phone Front-ends," 8th *European Conference on Wireless Technology Proceedings*, Paris, France, Oct. 2005, pp. 23–26.

Peregrine Semiconductor Corp., San Diego, CA (858) 731-9400, www.psemi.com.

RS No. 301

Broadband Power Amplifier

The model SSPA 0.5-2.0-20 is a high power, broadband, silicon carbide (SiC) RF amplifier that operates from 0.5 to 2 GHz and delivers approximately 20 W of RF power to the load. This power amplifier (PA) can be used from 400 to 2200 MHz with minor degradation in gain and power. This PA is ideal for broadband military platforms as well as commercial applications because it is robust and offers high power over a multi-octave bandwidth. This model operates with a base plate temperature of 85°C with no degradation in the MTBF for the SiC devices inside.

Aethercomm Inc.,
San Marcos, CA (760) 598-4340,
www.aethercomm.com.
Booth 718 **RS 216**

Bandwidth Digitizer

This 40 MHz bandwidth (BW) digitizer offers 14-bit resolution and 78 dB dynamic range for use with its 6.7, 13.2 and 26.5 GHz PSA series high performance spectrum analyzers. The new wide bandwidth digitizer provides high precision signal capture for designers of radar, satellite, military, emerging digital communications and 3G wireless systems employing high data rate modulation. Additionally, the company's 80 MHz bandwidth digitizer is now available for the lower frequency 6.7 and 13.2 GHz PSA models.

Agilent Technologies Inc.,
Palo Alto, CA (800) 829-4444,
www.agilent.com.
Booth 425 **RS 217**

Microwave Synthetic Instruments

This family of six high performance microwave synthetic instruments supports the US Department of Defense NxTest vision of flexible, modular and morphable instrumentation, and will be LXI compliant. The six modules include: N8201A, a 26.5 GHz performance downconverter that provides three IF output frequencies of 7.5, 21.4 and 321.4 MHz to offer three different signal bandwidth capabilities; the N8221A, a 30 MS/s IF digitizer with a 21.4 MHz IF input that provides 80 dB dynamic range, 14 bits of resolution and 8 MHz modulation bandwidth; the N8241A, an arbitrary waveform generator featuring a 1.25 GS/s sampling rate and 15 bits of resolution simultaneously; the N8212A, a 20 GHz performance vector upconverter that functions as a microwave source with greater than 2 GHz I/Q modulation bandwidth; and the final two are the 20 GHz and 40 GHz versions of the N8211A, a performance analog upconverter that generates a stimulus signal with good AM, FM and pulse modulation capabilities.

Agilent Technologies Netherlands B.V.,
Amstelveen, The Netherlands
+31 20 547 2000, www.agilent.com.
Booth 425 **RS 218**

Circuit-design Software Tool

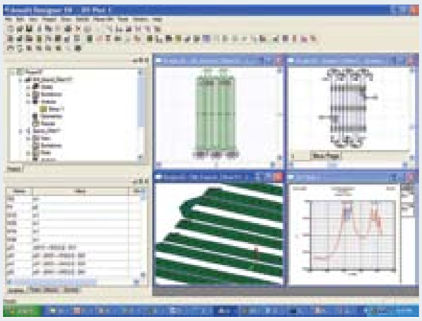

Ansoft Designer SV is a free microwave and radio frequency circuit-design software tool based on the latest commercial version of Ansoft Designer. The software provides students and professionals with an easy-to-use tool for applying basic circuit theories and techniques while developing high frequency engineering skills. This version introduces a new planar electromagnetic solver and a complete high frequency linear circuit simulator. Features include a problem-size-restricted planar EM solver, a complete set of linear component electrical models, company proprietary physics-based distributed and discontinuity models, and a fully integrated schematic/layout editor.

Ansoft Corp.,
Pittsburgh, PA (412) 261-3200,
www.ansoft.com.
Booth 713 **RS 219**

High Frequency Software

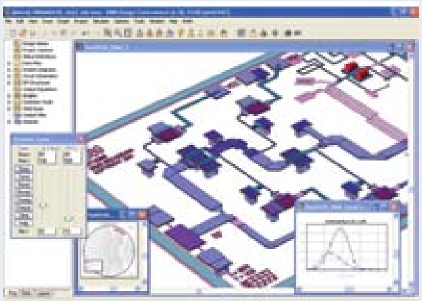

This feature-packed 2006 version of Microwave Office® design suite continues to deliver key productivity improvements to microwave designers that shortens design cycle time and speeding time-to-market for RF and microwave products. The latest version of this software offers a new integrated filter synthesis solution using Nuhertz Technologies' filter synthesis technology. High frequency circuit designers can now perform accurate filter synthesis quickly and easily from within the unified AWR design platform. The feature offers complete synthesis capability for passive, transmission line, active, switched capacitor and digital filters, as well as two graphical user interfaces.

Applied Wave Research Inc.,
El Segundo, CA (310) 726-3000,
www.appwave.com.
Booth 839 **RS 220**

Solid-state Amplifiers

The model 200S1G4 is a 200 W, 0.8 to 4.2 GHz solid-state amplifier. All "S" series amplifiers (1 to 800 W) are well suited for wireless applications because of the linearity, low noise power output and frequency coverage from 0.8 to 10.6 GHz.

AR Worldwide RF/Microwave Instrumentation,
Souderton, PA
(215) 723-8181, www.ar-worldwide. com.
Booth 702 **RS 221**

Obsolete Connector Replacements

These functional equivalents are available for most RF coaxial connectors and adapters that are obsolete or discontinued. Available interfaces include SMA, SMB, SMC, MCX, NC, TNC, N, C, SC, HN, LT and C. Body materials include brass, stainless steel and aluminum, plated with gold, silver, nickel, anodize and olive drab. Contact materials are brass, beryllium copper or phosphor bronze, with gold or silver plating. Dielectric options include virgin PTFE and other dielectric materials. Various body configurations are available.

Aviel Electronics,
Las Vegas, NV (702) 739-8155,
www.rfindustries.com.
Booth 700 **RS 222**

VSA Transmitter Tester

NEW WAVES

Agilent's E4406A is a flexible R&D or production test set for cellular base stations, amplifiers and components. Electro Rent, a national test equipment provider, offers for rent, lease, trade and purchase wireless communications test sets, spectrum analyzers, vector signal generators/analyzers, network analyzers, RF power meters, noise figure analyzers, phase noise measurement systems, RFI/EMI analyzers, cable/antenna analyzers, cell site testers, and RF/microwave amplifiers from Agilent/HP, Rohde & Schwarz, Anritsu/Wiltron, Tektronix and Boonton.
Electro Rent Corp.,
Van Nuys, CA (800) 688-1111,
www.electrorent.com.
Booth 535 **RS 254**

Calibration and Measurement Software

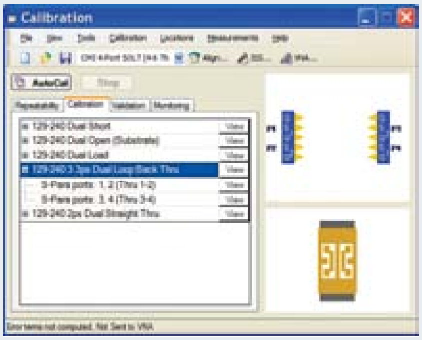

WinCal 2006 is a next generation vector network analyzer calibration software platform that provides users a precision 2-port and 4-port RF calibration/measurement tool as well as many powerful features that remove the complexity of using a vector network analyzer. WinCal's guided and intelligent system configuration, Wizards and Tutorials allow both new and experienced users to get started quickly, producing accurate and reliable RF measurements. Price: $5000.
Cascade Microtech,
Beaverton, OR (503) 601-1180,
www.cascademicrotech.com.
Booth 537 **RS 223**

High Frequency Connectors

This extended frequency line of SMA connectors offers a maximum VSWR of 1.25 to 26.5 GHz and has Teflon TFE insulators. Receptacles in this series have conductive-polymer gaskets available for EMI/RFI sensitive applications. These connectors feature a maximum VSWR of 1.10 in the range of DC through 18 GHz and 1.15 from 18 to 27 GHz. These connectors use an Ultem 1000 contact-support bead, allowing them to withstand temperatures as high as 160°C. Panel receptacles in this series incorporate a metal pressure ring to provide 360° of good RF grounding capability.

Delta Electronics Manufacturing Corp.,
Beverly, MA (978) 927-1060,
www.deltarf.com.
Booth 621 **RS 225**

WiMAX Amplifier

The model 7059 is an amplifier module designed for the emerging WiMAX market. This module is capable of handling single and multi-FA WiMAX signals for small base stations and repeaters. This 3.4 to 3.6 GHz/20 W (2 W WiMAX) amplifier utilizes linear advanced GaAs FET power devices that provide high gain, wide dynamic range, low distortions and good group delay and phase linearity. Good performance, long-term reliability and high efficiency are achieved by employing direct injection Pre-D™, advanced matching networks and combining techniques.

Empower RF Systems Inc.,
Technology Distribution Division,
Inglewood, CA (310) 412-8100,
www.rf-components.net.
Booth 635 **RS 226**

Wideband Voltage-controlled Oscillators

The model HMC586LC4B, model HMC587LC4B and model HMC588LC4B are wideband voltage-controlled oscillators (VCO). These fully integrated MMIC VCOs cover frequencies from 4 to 8 GHz, 5 to 10 GHz and 8 to 12.5 GHz, and feature ultra small QFN 4×4 mm RoHS compliant packaging, SSB phase noise as low as –105 dBc/Hz at 100 kHz offset, and minimal DC power consumption of 55 mA at +5 V.

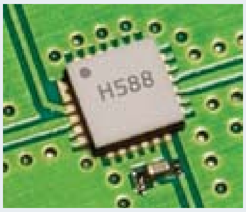

Hittite Microwave Corp.,
Chelmsford, MA (978) 250-3343,
www.hittite.com.
Booth 329 **RS 227**

Electromagnetic Software

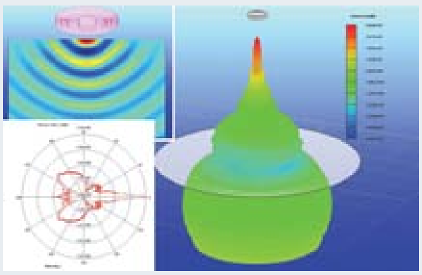

The version 6.2 of SINGULA is a 3D full-wave, electromagnetic simulator that helps researchers and scientists reduce design time while improving product performance. Based on the combined-field integral equation (CFIE), SINGULA uses the method of moments (MoM) coupled with physical optics. Accurate and easy to use, SINGULA is ideal for high frequency problems with large open regions and where the modeling boundaries must be precise. SINGULA solves high frequency applications such as antennas, EMC/EMI problems, microstrip power dividers and filters, and waveguide filters and transitions. Promotional price: $10,900.
Integrated Engineering Software,
Winnipeg, MB, Canada (204) 632-5636,
www.integratedsoft.com.
Booth 815 **RS 228**

Band Reject Filter

The model CMN485 is a band reject filter that has been developed for service providers that are experiencing co-location issues arising from the current Sprint-Nextel re-banding. The CMN-485 offers a passband of 869 to 894 MHz with insertion loss of less than 1 dB maximum. Rejection is 65 dB minimum from 896 to 901 MHz.

Commercial Microwave Technology Inc.,
Rancho Cordova, CA (916) 631-4364,
www.cmtfilters.com.
Booth 812 **RS 224**

Switch Attenuators

The model 50RA-003 and model 50RA-004 are rocker switch attenuators. The 50RA-003 operates in a frequency range from DC to 500 MHz while the 50RA-004 operates in a range from DC to 1000 MHz. Both models offer an impedance of 50 Ω nominal, attenuation range of 0 to 65 dB in 1 dB steps, attenuation steps of 1, 2, 4, 8, 10 and 20 dB, and RF input power of 1 W average at 25°C, 250 W peak (1 µs). RF connector types include BNC, TNC, SMA or N female.

JFW Industries Inc.,
Indianapolis, IN (317) 887-1340,
www.jfwindustries.com.
Booth 520 **RS 229**

Combline Filters

This family of surface-mount combline filters operates in a frequency range from 5 to 15 GHz and offers a bandwidth from 3 to 20 percent, with exceptionally low insertion loss. These filters offer an impedance of 50 Ω and insertion loss between 0.5 to 1.5 dB. The filters are designed to meet military environmental standards. Size: 0.5" × 0.5" × 0.75" – 2.125".

Lark Engineering Co.,
San Juan Capistrano, CA (949) 240-1233,
www.larkengineering.com.
Booth 646 **RS 230**

SPDT Switches

The model MASWSS0192 and model MASW-007107 are RoHS compliant SPDT switches designed for applications where ultra fast settling time, high linearity, low insertion loss, high isolation, small size and low cost are required. Time and measurement applications that require this fast response time can utilize either the MASWSS0192 (0.5 to 3 GHz) or the MASW-007107 (0.5 to 6 GHz), which are designed to have a settled on state within 0.1 µs. The MASWSS0192 is packaged in a SC-70 and the MASW-007107 is packaged in a 2 mm 8-lead PQFN.

M/A-COM Tyco Electronics,
Lowell, MA (800) 366-2266,
www.macom.com.
Booth 213 **RS 232**

SMA Reverse Polarity Connectors

These SMA reverse polarity connectors are designed for RF applications. A variety of con-

nector options are available including jacks and plugs, cable and PCB termination, bulkhead and panel mounts, and straight and right angle. These connectors are suitable for ZigBee radio, WLAN, WiFi and RFID applications.

Lighthorse Technologies Inc.,
San Diego, CA (858) 292-8876,
www.rfconnector.com.
Booth 220 **RS 231**

Automated Tuner

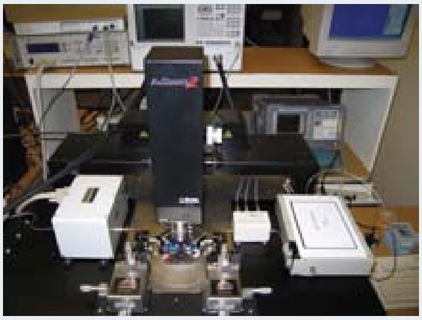

This automated tuner features over 200:1 VSWR. This super high matching tuner allows users to make measurement on large devices. The 50 GHz turnkey noise parameter system operates from 250 MHz to 110 GHz.

Maury Microwave Corp.,
Ontario, CA (909) 987-4715,
www.maurymw.com.
Booth 419 **RS 233**

Power Divider/Combiners

These compact, high performance Wilkinson power divider/combiners are ideally suited for

C-, X- and Ku-band systems applications. Two- and four-way SMA female models feature high isolation, low insertion loss, good VSWR and good phase/amplitude balance. Available in 4 to 8 GHz, 7 to 12.4 GHz and 12.4 to 18 GHz bands from stock. These divider/combiners are made in the US.

MECA Electronics Inc.,
Denville, NJ (973) 625-0661,
www.e-meca.com.
Booth 534 **RS 255**

Power Amplifier

The model LX™5511 is a power amplifier optimized for WLAN applications in the 2.3 to

2.5 GHz frequency range. The LX5511 power amplifier is implemented as a two-stage monolithic microwave integrated circuit with active bias and output pre-matching. This device is manufactured with an InGaP/GaAs heterojunction bipolar transistor IC process with a single low voltage supply of 3.3 V, 26 dB power gain between 2.3 to 2.5 GHz at a low quiescent current of 90 mA. Size: 16-pin 0.9 high × 3 mm square. Price: $0.45 (10,000).

Microsemi Corp.,
Irvine, CA (949) 221-7100,
www.microsemi.com.
Booth 216 **RS 234**

Three-chip Transceiver Solution

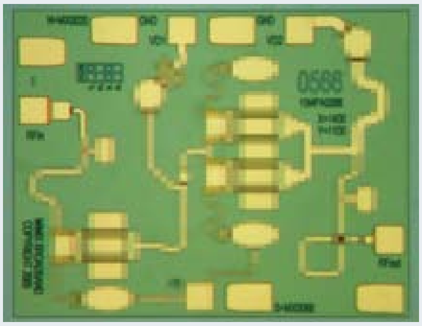

This gallium arsenide (GaAs) monolithic microwave integrated circuit (MMIC) 13/15 GHz chip set consists of a highly integrated image reject receiver and transmitter, and a compact, two-stage power amplifier. The image reject mixers eliminate the need for an image bandpass filter after the amplifier to remove thermal noise at the image frequency. The receiver, model 14REC0607, the transmitter, model 14TX0614, and the amplifier, model 15MPA0566, feature an Rx conversion gain of 13 dB, Rx noise figure of 3 dB, Rx IIP3 of +3 dBm, Tx conversion gain of 8 dB, Tx OIP3 of +17 dBm, PA gain of 20 dB and PA P_{sat} of 27 dBm.

Mimix Broadband Inc.,
Houston, TX (281) 988-4600,
www.mimixbroadband.com.
Booth 834 **RS 235**

RF Switches

The model PE42672 SP7T and model PE42660 SP6T are RF switches that have been released

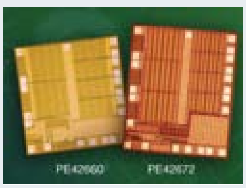

on the HaRP-enhanced UltraCMOS process and are designed for quad-band GSM and GSM/WCDMA handset applications. The former is said to be the world's first monolithic SP7T switch with an on-board CMOS decoder. This highly integrated solution simplifies and lowers the cost of RF designs by reducing overall part count by as many as six devices and 13 wire bonds. The PE42660 switch is drop-in compatible with the PE4263 GSM handset switch that was released at the end of 2004. Both devices have good RF performance levels offering exceptional linearity (PE42672: $2f_o$ –85 dBc and $3f_o$ –79 dBc; PE42660: $2f_o$ –88 dBc and $3f_o$ –85 dBc); IP3 better than +70 dBm; 1.5 kV ESD tolerance; 2.75 V operating voltage and ultra-low power consumption.

Peregrine Semiconductor Corp.,
San Diego, CA (858) 731-9400,
www.psemi.com.
Booth 723 **RS 237**

Substrate Material

The N4350-13 RF and N4380-13 RF are enhanced epoxy resin system materials with tightly controlled dielectric constants, low signal loss properties and good thermal properties designed to be used in many cost and performance-sensitive applications that would otherwise require a PTFE material. These products are suitable for many applications including amplifiers, components, multi-layer boards and short-range antennas.

Neltec,
Tempe, AZ (480) 967-5600,
www.parknelco.com.
Booth 418 **RS 236**

RF Coaxial Relay

The TTL series is a single-pole, double-throw relay with a single-line TTL driver. This SMA

connectorized relay allows for cost reduction while promoting efficiency by requiring only one TTL line to be used, which results in no timing issues when switched from line to line. Product is available with a latching configuration. Size: 1.34" × 1.50".

RelComm Technologies Inc.,
Salisbury, MD (410) 749-4488,
www.relcommtech.com.
Booth 729 **RS 253**

Radio Module

The POLARIS™ 2 TOTAL RADIO™ module is a highly integrated complete radio consisting

of transceiver and transmitter modules designed to support up to four frequency bands while operating under the GSM, GPRS and EDGE interface standards. This solution provides handset manufacturers the benefits of minimal size, reduced component count and flexible baseband interfaces, reducing time to market while still achieving good RF performance. Reduced power consumption through unique digital polar and GMSK modulators provides extended talk time, minimal heat dissipation and long battery life.

RF Micro Devices Inc.,
Greensboro, NC (336) 664-1233,
www.rfmd.com.
Booth 313 **RS 238**

NEW WAVES

Circuit Materials

The R/flex® 3000 family of liquid crystalline polymer (LCP)-based circuit materials includes the R/flex 3600 LCP single-clad laminate and the R/flex 3850 double-clad laminate. R/flex 3850 laminate is produced in a range of copper and film thicknesses, just as the single-clad laminate, and is available in standard panel formats. These materials offer a unique combination of mechanical, electrical, thermal and environmental properties for tightly controlled impedance flex interconnections, next generation wireless handsets, high density flip chip packages and moisture resistance sensors.

Rogers Corp.,
Rogers, CT (860) 774-9605,
www.rogerscorporation.com.
Booth 328 ***RS 239***

8 and 24 GHz Vector Network Analyzers

The ZVA series of vector network analyzers includes the ZVA8 (300 kHz to 8 GHz) and ZVA24 (10 MHz to 24 GHz). Dynamic range is greater than 135 dB, output power is more than 15 dBm and power sweep range is greater than 50 dB. Measurement speed is less than 3.5 µs per test point, and less than 6 ms for 201 test points. Switching time between channels is less than 1 ms and less than 10 ms when switching between measurement routines. The instruments provide broad measurement functionality and are easy to use.

Rohde & Schwarz Inc.,
Columbia, MD (410) 910-7800,
www.rohde-schwarz.com/usa.
Booth 613 ***RS 240***

Gain Block Amplifiers

The model SKY65013, model SKY65014, model SKY65015, model SKY65016 and model SKY65017 are 50 Ω, InGaP HBT, gain block amplifiers that deliver good broadband performance. The models feature gain from 13 to 21 dB and output power (P1dB) from 14 to 19 dBm. These gain blocks have high output third-order intercept (IP3) and gain compression points (P1dB).

Skyworks Solutions Inc.,
Woburn, MA (781) 376-3000,
www.skyworksinc.com.
Booth 523 ***RS 241***

Cluster Computing

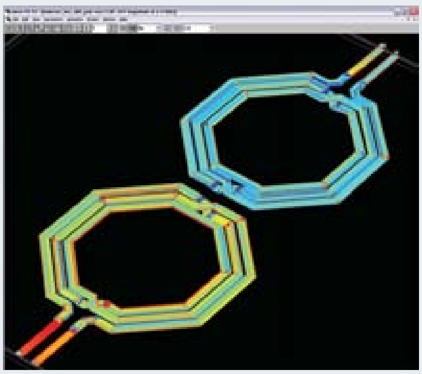

The emCluster™ computing solution reduces EM analysis time and shortens design cycles. This newly added emCluster module can split a project and assign individual analysis frequencies to available resources across an IT cluster environment. This parallel process approach significantly reduces the completion time of the EM analysis to just a fraction of what it would have taken with a single computing resource.

Sonnet Software Inc.,
North Syracuse, NY (315) 453-3096,
www.sonnetsoftware.com.
Booth 728 ***RS 242***

60 GHz Microwave Contacts

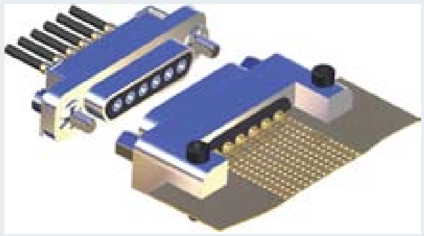

These SSBP microwave contacts provide broad bandwidth while drastically reducing packaging space. Using standard plastic insertion/extraction tools, versions of SSBP contacts fit in size 20 contact cavities for D-Sub, Micro-D and D38999 connectors. These "next generation" microwave contacts provide high density packaging, increased signal integrity, improved system reliability and assembly cost reduction.

Southwest Microwave Inc.,
Tempe, AZ (480) 783-0201,
www.southwestmicrowave.com.
Booth 843 ***RS 243***

Switch Filter Bank

This isolated switch filter bank offers a compact, two-channel selectable filter suitable for IF filtering. This filter bank uses integral input and output isolators for the required return loss (VSWR) without compromising its narrowband performance. This isolated switched filter bank assembly enables RF engineers and system designers to dynamically configure a system's capabilities. The assembly features input and output isolators to provide a consistent 50 Ω load, dual selectable bandwidths (85 and 50 MHz), lightweight aluminum housing, 40 dB reverse isolation and internal voltage regulation. Size: 6.5" × 1.75" × 1". Weight: 8 ounces.

Spectrum Microwave Inc.,
Palm Bay, FL (321) 727-1838,
www.specwave.com.
Booth 828 ***RS 244***

Prepregs and Laminates

This line of low loss, bromine-free prepregs and laminates are designed for antennas. TLG prepregs and laminates are ideal for antenna designs with dielectric constants, which are consistent throughout the material and are available from 2.90 to 3.50.

Taconic, Advanced Dielectric Division,
Petersburgh, NY (800) 833-1805,
www.taconic-add.com.
Booth 629 ***RS 246***

NEW WAVES

Voltage-controlled Oscillators

The DCSR series of voltage-controlled oscillators (VCO) are based on the company's proprietary and patented technology that matches ceramic resonator oscillators in phase noise performance, but additionally improves immunity to phase hits.

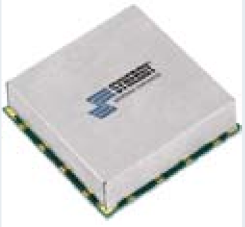

These high performance VCOs are designed for single frequency applications, with enough bandwidth to cover thermal drift, pulling and pushing. These VCOs are ideal for carrier generators in high data capacity radios.

Synergy Microwave Corp., Paterson, NJ (973) 881-8800, www.synergymwave.com.
Booth 715 **RS 245**

EMC Guide

This fully revised, updated and expanded edition of the book, *Introduction to Electromagnetic Compatibility*, is now available. This guide is an invaluable reference for industrial professionals interested in EMC design. This second edition has been substantially rewritten and revised to reflect the developments in the field of EMC.

John Wiley & Sons, Hoboken, NJ (877) 762-2974, www.wiley.com.
Booth 435 **RS 250**

Reverse-polarity RF Coax Connectors

The term "reverse-polarity connector" refers to a standard sized cable plug that contains a female center contact instead of the standard male contact. Conversely, the mating receptacle must also contain a non-standard male center contact instead of a female center contact. These connectors are commonly used as the interfaces on antennas, access points and WLAN circuit cards making it necessary for the mating connectors to be compatible. The company offers a wide range of reverse-polarity TNC and SMA connectors for WLAN applications.

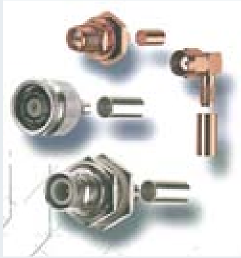

Telegartner Inc., Franklin Park, IL (630) 616-7600, www.telegartner.com.
Booth 807 **RS 247**

Foundry Services

These foundry services are designed for design and system-based clientele. The company's advanced 6" HBT and HEMT MMIC technologies support RF applications from 100 MHz up to 100 GHz. Current customers cover various applications including mobile communications, satellite and auto radar.

WIN Semiconductors Corp., Kuei Shan Hsiang, Tao Yuan Shien, Taiwan 886-3-397-5999, www.winfoundry.com.
Booth 814 **RS 251**

Eight-way Power Divider

The model WPD-50/8 SMA is a 50 Ω, eight-way broadband Wilkinson power divider that covers an 800 to 2500 MHz frequency range and offers a minimum of 20 dB (25 dB typical) of port-to-port isolation with an insertion loss of 1.4 dB nominal above the theoretical split. This model features an aluminum enclosure with SMA female connectors on all ports and is well suited for applications including integrated test modules, and test and verification labs. Delivery: available from stock.

Trilithic Inc., Indianapolis, IN (800) 344-2412, www.trilithic.com.
Booth 619 **RS 248**

Quad-band Filter

The model 890054 is a quad-band filter module compatible with Freescale's "Transamm" EDGE transceiver. This filter bank offers its best receive path noise figure when paired with Transamm. The company utilizes its smallest chip-scale SAW filters in this module, which enables a low cost, small size solution for EDGE phone manufacturers.

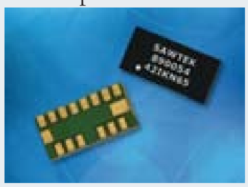

TriQuint Semiconductor Inc., Hillsboro, OR (503) 615-9000, www.triquint.com.
Booth 701 **RS 249**

Electromagnetic Software

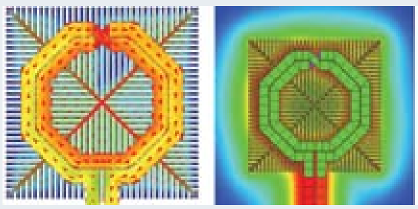

IE3D EM Package 11.2 is seamlessly integrated into Cadence Virtuoso for RFIC design. IE3D can also create models ready for simulations directly from Cadence Allegro. IE3D's Automatic GDSII to IE3D Flow is integrated into the design flow of some major semiconductor companies for device modeling. IE3D is seamlessly integrated into Microwave Office 2004 from AWR. The company's most recent release of FIDELITY FDTD EM Simulator 5.0 offers formula-based geometry modeling and fully automated meshing.

Zeland Software Inc., Fremont, CA (510) 623-7162, www.zeland.com.
Booth 413 **RS 252**

ERRATUM

In "Transistor LC Oscillators for Wireless Applications: Theory and Design Aspects, Part I," a tutorial by Andrei Grebennikov that appeared in the October issue of *Microwave Journal*, Equation 11 should read

$$V = \frac{\gamma_1(\theta)}{\gamma_0(\theta)} \frac{Q_L}{\omega_0 C} I_0 \qquad (11)$$

In addition, in Equations 25, 26 and 28 the effect of feedback capacitances C_2 and C_3 are not taken into account for simplicity.

MICROWAVE METRICS

NEXT GENERATION MOBILE HANDSETS

Juniper Research estimates that the total mobile subscriber market will reach \$2.7 B by 2010 and that shipments of handsets will break the \$1 B mark by 2009 on the back of emerging Asia Pacific markets and increasing replacement rates in mature markets.

3G subscribers are predicted to grow from 30 million in 2004 to over 300 million by 2010. However, while representing a step-jump in technology for delivering current services with better quality, 3G's benefits derive more from its ability to accommodate greater numbers of users and network traffic, especially voice, than its support of advanced services delivery.

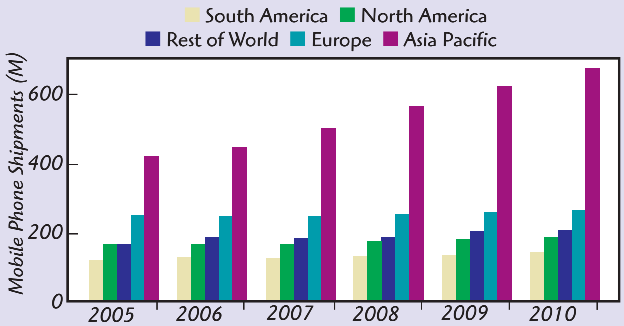

All Mobile Phone Shipments (M) Regional Forecast 2005–2010

Source: Juniper Research Ltd., Century House, Vickers Business Centre, Priestly Road, Basingstoke, Hampshire RG24 9RA England (www.juniperresearch.com)

EMBEDDED MILITARY COTS MARKET TO REACH \$3.25 B BY 2008

A recent report by Venture Development Corp. forecasts the market for embedded merchant COTS boards, integrated systems, operating systems and software development tools to grow at a compound annual growth rate of 6.27%, reaching an estimated \$3.25 B by 2008.

The merchant COTS market comprised 0.4% of combined North American and Western European defense expenditures in 2003. Although this represents only a small fraction of total expenditures, COTS is still a very attractive market.

United States military expenditures account for 47% of global military spending and are more than double those of Western Europe, so it's not surprising that North America comprised 76.4% of the total market for the examined embedded COTS products in 2003.

Combined North American and European COTS Merchant Shipments and Projections, 2003–2008 (US\$ in Millions)

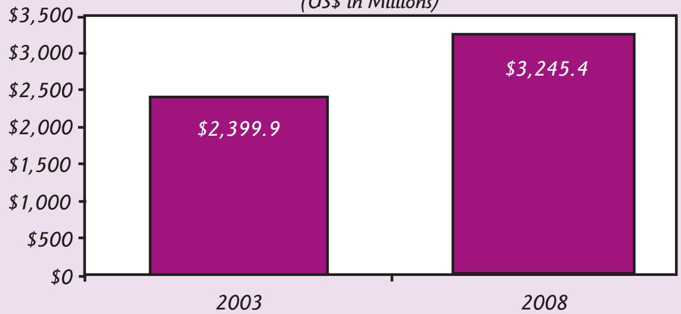

Source: Venture Development Corp., One Apple Hill Drive, Suite 206, Box 8190, Natick, MA 01760 (www.vdc-corp.com)

The Design of Modern Microwave Oscillators for Wireless Applications: Theory and Optimization

U.L. Rohde, A.K. Poddar and G. Böck
Wiley-Interscience

558 pages; $120
ISBN: 0-471-72342-8

Many technical and scientific works have been published with respect to oscillator development, without comprehensive work covering all the important aspects of oscillator development ranging from fundamentals, device technology, supply noise, analysis methods, design and optimization methodologies for practical design of various types of oscillators. Most articles concentrate on classic design strategies based on measurements, simulation and optimization of output power and phase noise, and not on a systematic composition of the whole design procedure, leading to optimum performance of all relevant oscillator features. The purpose of this book, which is based on practical and theoretical research and decades of work, is to fill this gap. Chapter 1 summarizes the historical evolution of harmonic oscillators and analysis methods. Chapters 2 to 5 deal with the most important building blocks. Following a discussion of the basic theory on semiconductor devices and large-signal parameters, the most modern devices are chosen as examples. A whole chapter is devoted to the various types of resonators, an important subject for microwave applications. Chapter 6 concentrates on the fundamentals of oscillator design, starting with the derivation of the oscillating condition under the assumption of a simplified linear network. Next, the nonlinear case is analyzed. Chapter 7 addresses the fundamentals of oscillator noise. Derivation and application of the extended Leeson formula is shown extensively. A tutorial treatise on phase noise measurements closes the chapter. Chapter 8 concentrates on analysis and optimization of phase noise in oscillators. Chapter 9 gives five design examples for practical oscillators and for extensive validation of the circuit synthesis described. Chapter 10 addresses the topic of coupled oscillators. It is shown that the design of ultra-low phase noise voltage-controlled oscillators (VCO) with a wide tuning range is possible using this concept. In Chapter 11, a variety of validation circuits for wide band coupled resonator VCOs are given.

"...a systematic composition of the whole design procedure, leading to optimum performance of all relevant oscillator features."

To order this book, contact: John Wiley & Sons Inc., One Wiley Drive, Somerset, NJ 08875 (800) 225-5945.

Intelligent Vehicle Technology Trends

Richard Bishop
Artech House

362 pages; $89, £55
ISBN: 1-58053-911-4

This book is intended to provide an overview of developments in the Intelligent Vehicle (IV) domain for engineers, researchers, government officials and others interested in this technology. The book opens with "big picture" considerations, introduces the major players in the IV domain and then addresses key functional areas in-depth. The latter portion of the book is devoted to addressing some non-technical issues and a view toward the future is offered in conclusion. Chapter 2 reviews government safety goals and takes a look at long-term visions that have been developed worldwide. Chapter 3 reviews the key IV application areas of convenience, safety, productivity and traffic assistance. Chapter 4 examines major government IV R&D programs and strategies. Chapter 5 examines the stance of the vehicle industry with respect to IV systems. Chapter 6 focuses on lateral/side sensing and control systems. Chapter 7 focuses on longitudinal sensing and control systems. Chapter 8 addresses integrated systems, the next logical step beyond stand-alone lateral or longitudinal systems. Chapter 9 extends the system concept to cooperative vehicle-highway systems. Fully automated road vehicles, a dream long-held by futurists, are the focus of Chapter 10. Chapter 11 speaks to floating car data systems, a relatively near-term IV application that can extend the "information horizon" for both drivers and automatic crash avoidance systems. A review of IV systems would be incomplete without examining the interaction of drivers with IV technology. Chapter 12 addresses IVs as human-centered systems. Chapter 13 moves beyond the technology to examine challenges in product introduction. IV system design must be responsive to customer and societal issues to be successful in a market-driven arena. Chapter 14 looks forward to identify enabling technologies important to future progress. Finally, Chapter 15 offers a brief synthesis of the overall IV domain and some observations on the part of the author.

"IV system design must be responsive to customer and societal issues to be successful in a market-driven arena."

To order this book, contact: Artech House, 685 Canton St., Norwood, MA 02062 (781) 769-9750 ext. 4030; or 46 Gillingham St., London SW1V 1HH UK +44 (0) 207-8750.

Dan Massé

Dan Massé is a member of the Microwave Journal *staff.*

ADVERTISING INDEX

CIRCLE NO.	ADVERTISER	PAGE NO.	PHONE	FAX	WEB ADDRESS
1	AA MCS	169	+33(0)8 11 09 76 76	+33(0)1 76 91 50 31	http://mwj.ims.ca/5547-1
2	Advanced Control Components Inc.	133	732-460-0212	732-460-0214	http://mwj.ims.ca/5547-2
3	Advanced Power Technology RF	164	408-986-8031	408-986-8120	http://mwj.ims.ca/5547-3
4	Advanced Switch Technology	181	613-384-3939	613-384-5026	http://mwj.ims.ca/5547-4
5	Aeroflex/Weinschel, Inc.	81	800-638-2048	301-846-9116	http://mwj.ims.ca/5547-5
6	Aethercomm	38	760-598-4340	760-598-4342	http://mwj.ims.ca/5547-6
	Agilent Technologies, Inc.	27	800-829-4444	415-857-5518	www.agilent.com/ find/eesof-innovations
7	Ametek Specialty Metal Products	92	203-949-8837		http://mwj.ims.ca/5547-7
8,9	AML Communications Inc.	41,84	805-388-1345	805-484-2191	http://mwj.ims.ca/5547-8
11	AMTA	166			http://mwj.ims.ca/5547-11
12	Anaren Microwave	167	800-411-6596	315-432-9121	http://mwj.ims.ca/5547-12
13,14,15	Ansoft Corporation	7,85,143	412-261-3200	412-471-9427	http://mwj.ims.ca/5547-13
16	Applied Computational Sciences	96			http://mwj.ims.ca/5547-16
17	Applied Thin Film Products	139	510-661-4287	510-661-4250	http://mwj.ims.ca/5547-17
18	AR Worldwide	45	215-723-8181	215-723-5688	http://mwj.ims.ca/5547-18
19	Artech House	148	800-225-9977	781-769-6334	http://mwj.ims.ca/5547-19
20	Auriga Measurement Systems, LLC	64	978-441-1117	978-441-2666	http://mwj.ims.ca/5547-20
21	Bird Technologies Group	153	866-695-4569		http://mwj.ims.ca/5547-21
22	Cernex, Inc.	18	408-541-9226	408-541-9229	http://mwj.ims.ca/5547-22
23	Chelton Microwave	6	603-775-5200	603-775-5201	http://mwj.ims.ca/5547-23
24	Ciao Wireless, Inc.	62	805-389-3224	805-389-3629	http://mwj.ims.ca/5547-24
25	Colby Instruments	128	425-452-8889	425-452-8802	http://mwj.ims.ca/5547-25
26	COM DEV Saw Products	44	647-887-SAWS	519-622-1691	http://mwj.ims.ca/5547-26
27	Commercial Microwave Technology, Inc.	88	916-631-4363	530-642-9798	http://mwj.ims.ca/5547-27
28	CPI Beverly Microwave Division	17	978-922-6000	978-922-2736	http://mwj.ims.ca/5547-28
29	Crane Aerospace & Electronics	66	480-961-6269		http://mwj.ims.ca/5547-29
30	CST of America, Inc.	25	781-416-2782	781-576-5702	http://mwj.ims.ca/5547-30
31	Cuming Microwave Corporation	129	800-432-6464	508-584-2309	http://mwj.ims.ca/5547-31
32	Daico Industries, Inc.	83	310-507-3242	310-507-5701	http://mwj.ims.ca/5547-32
33	Deutsch Bus & Microwave	56	+33 (0)2 32 23 58 83	+33 (0)2 32 23 58 61	http://mwj.ims.ca/5547-33
34	Eastern Wireless TeleComm, Inc.	48	410-749-3800	410-749-4852	http://mwj.ims.ca/5547-34
35	Elisra Electronic Systems Ltd. (Microwave Division)	39	972(3)617-5655	972(3)617-5299	http://mwj.ims.ca/5547-35
36	EM Research, Inc.	127	775-345-2411	775-345-1030	http://mwj.ims.ca/5547-36
37	EMC Technology Inc.	15	772-286-9300	772-283-5286	http://mwj.ims.ca/5547-37
38	Emhiser Micro-Tech	53	775-345-0461	775-345-1152	http://mwj.ims.ca/5547-38
39	Empower RF Systems, Inc.	43	310-412-8100	310-412-9232	http://mwj.ims.ca/5547-39
40	Endwave Defense Systems	23	408-522-3180	408-522-3181	http://mwj.ims.ca/5547-40
41	Eudyna Devices USA Inc.	35	408-232-9500	408-428-9111	http://mwj.ims.ca/5547-41
42,43	EuMW 2006	159,185	+ 44 20 7596 8742	+ 44 20 7596 8749	http://mwj.ims.ca/5547-42
44	Feko	112	+27 21 880 1880		http://mwj.ims.ca/5547-44
45	Filtronic Compound Semiconductors, Inc.	50	408-850-5790	408-850-5766	http://mwj.ims.ca/5547-45
46	Focus Microwaves Inc.	33	514-684-4554	514-684-8581	http://mwj.ims.ca/5547-46
47	Freescale Semiconductor, Inc.	37			http://mwj.ims.ca/5547-47
48	G.T. Microwave Inc.	160	973-361-5700	973-361-5722	http://mwj.ims.ca/5547-48
49	GGB Industries, Inc.	3	239-643-4400	239-643-4403	http://mwj.ims.ca/5547-49
50	Herley Industries, Inc.	137	717-397-2777	717-393-0416	http://mwj.ims.ca/5547-50
51	Herotek, Inc.	86	408-941-8399	408-941-8388	http://mwj.ims.ca/5547-51
52	Hittite Microwave Corporation	77	978-250-3343	978-250-3373	http://mwj.ims.ca/5547-52
53	Huber + Suhner AG	131	+41 (0)71 353 41 11	+41 (0)71 353 45 90	http://mwj.ims.ca/5547-53
	IEEE MTT-S International Microwave Symposium	187	781-769-9750	781-769-5037	www.ims2006.org
	IEEE Radio and Wireless Symposium	154	781-769-9750	781-769-5037	www.mttwireless.org
54	Integra Technologies, Inc.	142	310-606-0855	310-606-0865	http://mwj.ims.ca/5547-54
55	Integrated Engineering Software	78	204-632-5636		http://mwj.ims.ca/5547-55
56	Isola Corp.	30–31	800-845-2904		http://mwj.ims.ca/5547-56
57,58,59	J microTechnology	181	503-614-9509	503-531-9325	http://mwj.ims.ca/5547-57
60	Jersey Microwave	34	908-684-2390 ext. 23	908-684-2391	http://mwj.ims.ca/5547-60
61	Locus Microwave, Inc.	182	814-861-3200	814-861-5195	http://mwj.ims.ca/5547-61
62	Lorch Microwave	65	800-780-2169	410-860-1949	http://mwj.ims.ca/5547-62
63	M/A-COM, Inc.	119	800-366-2266	978-442-5350	http://mwj.ims.ca/5547-63

ADVERTISING INDEX

Circle No.	Advertiser	Page No.	Phone	Fax	Web Address
64	M2 Global Technology, Ltd.	98	210-561-4800	210-561-4852	http://mwj.ims.ca/5547-64
65	Marki Microwave, Inc.	123	408-778-4200	408-778-4300	http://mwj.ims.ca/5547-65
66	Maury Microwave Corporation	9	909-987-4715	909-987-1112	http://mwj.ims.ca/5547-66
67	MECA Electronics Inc.	60	973-625-0661	973-625-9277	http://mwj.ims.ca/5547-67
68	MiCIAN	54	+49(421)16899351	+49(421)16899352	http://mwj.ims.ca/5547-68
69	Micro Lambda Wireless, Inc.	97	510-770-9221		http://mwj.ims.ca/5547-69
70	Microlab/FXR, (a Wireless Telecom Group Company)	19	973-992-7700	973-992-0513	http://mwj.ims.ca/5547-70
71	MicroMetrics Inc.	95	603-641-3800	603-641-3500	http://mwj.ims.ca/5547-71
72	Micronetics Test Solutions	113	603-883-2900	603-882-8987	http://mwj.ims.ca/5547-72
73	Microsemi Corporation	108	949-221-7112	949-756-0308	http://mwj.ims.ca/5547-73
74	Microwave Development Laboratories	117	781-292-6680/6684	781-453-8629	http://mwj.ims.ca/5547-74
75	Microwave Device Technology	91	978-692-7800		http://mwj.ims.ca/5547-75
	Microwave Journal	*105,138,181,189	800-225-9977	781-769-5037	www.mwjournal.com
76	Midwest Microwave	80	+44(0) 1245 359515	+44(0) 1245 358938	http://mwj.ims.ca/5547-76
77	Mimix Broadband, Inc.	COV 3	281-988-4600	281-988-4615	http://mwj.ims.ca/5547-77
78,79,80, 81,82,83, 84,85,86, 87,88,89	Mini-Circuits	4–5,16,29, 57,69,70, 89,124–125,135, 145,165,173	718-934-4500	718-332-4661	http://mwj.ims.ca/5547-78
90,91	MITEQ Inc.	46–47,115	631-436-7400	631-436-7430	http://mwj.ims.ca/5547-90
92	Modelithics, Inc.	148	888-359-6359	813-558-1102	http://mwj.ims.ca/5547-92
93,94	Narda Microwave-East, an L3 Communications Co.	101,149	631-231-1700	631-231-1711	http://mwj.ims.ca/5547-93
95	Narda Microwave-West, an L3 Communications Co.	49	916-351-4500	916-351-4550	http://mwj.ims.ca/5547-95
96	Neltec	55	480-967-5600		http://mwj.ims.ca/5547-96
97	Noble Publishing Corporation	181	800-247-6553	770-448-2839	http://mwj.ims.ca/5547-97
10	NoiseWave Corp.	8	973-386-1119	973-386-1131	http://mwj.ims.ca/5547-10
98	OML Inc.	141	408-779-2698	408-778-0491	http://mwj.ims.ca/5547-98
99	Peak Devices, Inc.	51	978-422-7641	978-422-0011	http://mwj.ims.ca/5547-99
100,101	Peregrine Semiconductor Corp.	59,163	800-737-6937	858-731-9499	http://mwj.ims.ca/5547-100
102	Picosecond Pulse Labs Inc.	99	303-209-8100	303-447-2236	http://mwj.ims.ca/5547-102
103	Prewell Corporation	120	82-31-420-8362	82-31-420-8301	http://mwj.ims.ca/5547-103
104	Quest Microwave Inc.	94	408-778-4949	408-778-4950	http://mwj.ims.ca/5547-104
105	Reactel, Incorporated	14	301-519-3660	301-519-2447	http://mwj.ims.ca/5547-105
106	RelComm Technologies, Inc.	151	410-749-4488	410-860-2327	http://mwj.ims.ca/5547-106
107	Renaissance Electronics Corporation	68	978-772-7774	978-772-7775	http://mwj.ims.ca/5547-107
108	RF & Hyper Europe 2005	183	33 (0)1 49 68 51 00	33 (0)1 44 78 99 49	http://mwj.ims.ca/5547-108
109	RF Micro Devices	20–21	336-678-5570	336-931-7454	http://mwj.ims.ca/5547-109
110	RFHIC	132	82-31-250-5011	82-31-250-5089	http://mwj.ims.ca/5547-110
100	Richardson Electronics, Ltd.	59	800-737-6937	630-208-2550	http://mwj.ims.ca/5547-100
111	Rogers Corporation	93	480-961-1382	480-961-4533	http://mwj.ims.ca/5547-111
112	Rohde & Schwarz GmbH	79	+49-1805-124242	+49-89-412913777	http://mwj.ims.ca/5547-112
113	Rohde & Schwarz, Inc.	*105	888-837-8772	410-910-7801	http://mwj.ims.ca/5547-113
114	San-Tron Inc.	COV 2	978-356-1585	978-356-1573	http://mwj.ims.ca/5547-114
115	Satellink, Inc.	181	972-487-1434	972-487-1204	http://mwj.ims.ca/5547-115
116	Satellite 2006	179	301-354-1797		http://mwj.ims.ca/5547-116
117	Sawtek, a TriQuint Company	13	407-886-8860	407-886-7061	http://mwj.ims.ca/5547-117
118	Sector Microwave Industries, Inc.	181	631-242-2300	631-242-8158	http://mwj.ims.ca/5547-118
119	Sirenza Microdevices	90	303-327-3030		http://mwj.ims.ca/5547-119
120	Skyworks Solutions, Inc.	73	781-376-3000		http://mwj.ims.ca/5547-120
121	SM Electronics	111	800-715-4396	972-984-1218	http://mwj.ims.ca/5547-121
122	Sonnet Software, Inc.	11	315-453-3096	315-451-1694	http://mwj.ims.ca/5547-122
123	Spacek Labs	52	805-564-4404	805-966-3249	http://mwj.ims.ca/5547-123
124	Special Hermetic Products, Inc.	72	603-654-2002	603-654-2533	http://mwj.ims.ca/5547-124
125	Spectrum Elektrotechnik GmbH	109	+49-89-3548-040	+49-89-3548-0490	http://mwj.ims.ca/5547-125
126	SSI Cable Corporation	180	360-426-5719	360-426-5912	http://mwj.ims.ca/5547-126
127	Statek	61	714-639-7810		http://mwj.ims.ca/5547-127
128	Stealth Microwave, Inc.	40	888-772-7791	609-538-8587	http://mwj.ims.ca/5547-128
129,130,131	Suss MicroTec AG	106,110,114	(+49) 35240/73-0		http://mwj.ims.ca/5547-129
132	Swift & Associates	175	818-989-1133	818-989-4784	http://mwj.ims.ca/5547-132
133,134,135	Synergy Microwave Corporation	75,147,171	973-881-8800	973-881-8361	http://mwj.ims.ca/5547-133

ADVERTISING INDEX

*REGIONAL DISTRIBUTION ONLY

Visit Microwave Journal *on the Web at* **www.mwjournal.com**

Visit mwjournal.com/info and enter RS# to request information from our advertisers

Microwave Journal

JANUARY 2006 ISSUE

Phased Arrays and Radars – Past, Present and Future

UWB Triangular Monopole Antenna

2005 European Microwave Week Wrap-up

SALES REPRESENTATIVES

microwave journal

CARL SHEFFRES, PUBLISHER **ED JOHNSON, ASSOCIATE PUBLISHER** **KEN HERNANDEZ, TRAFFIC ADMINISTRATOR**

Eastern and Central Time Zones
Chuck Curley
Eastern Reg. Sales Mgr.
685 Canton Street
Norwood, MA 02062
Tel: (781) 769-9750
FAX: (781) 769-5037
ccurley@mwjournal.com

Michael Hallman
Eastern Reg. Sales Mgr.
4 Valley View Court
Middletown, MD 21769
Tel: (301) 371-8830
FAX: (301) 371-8832
mhallman@mwjournal.com

Eastern and Central Time Zones
Ed Johnson
Associate Publisher
PO Box 5962
Ocala, FL 34478-5962
Tel: (352) 620-2442
FAX: (352) 620-2443
ejohnson@mwjournal.com

Pacific and Mountain Time Zones
Wynn Cook
Western Reg. Sales Mgr.
PO Box 23200
San Jose, CA 95153
Tel: (408) 224-9060
FAX: (408) 224-6106
wcook@mwjournal.com

International Sales
Richard Vaughan
International Sales Manager
Tel: +44 207 596 8742
rvaughan@horizonhouse.co.uk

Michel Zoghob
Deputy Publisher
Tel: +44 207 596 8741
mzoghob@horizonhouse.co.uk

46 Gillingham Street
London SW1V 1HH, England
Tel: +44 207 596 8740
FAX: +44 207 596 8749

Germany, Austria, and Switzerland (German-speaking)
Juergen Wissling
Wissling Marketing Services
Riedstrasse 5
72813 St. Johann-Wuertingen
Germany
Tel: +49 7122 828140
FAX: +49 7122 828145
jwissling@horizonhouse.com

Israel
Oreet Ben Yaacov
Oreet International Media
15 Kineret Street
51201 Bene-Berak, Israel
Tel: +972 3 570 6527
FAX: +972 3 570 65126
obenyaacov@horizonhouse.com

Korea
Young-Seoh Chinn
JES Media International
2nd Floor, ANA Bldg.
257-1, Myungil-Dong
Kangdong-Gu
Seoul, 134-070 Korea
Tel: +82 2 481-3411
FAX: +82 2 481-3414
yschinn@horizonhouse.com

Singapore
Hoong-Mun Koo
Publicitas
02-01 Wellington Bldg.
20 Bideford Road
Singapore 229921
Tel: +65 6836 2272
FAX: +65 6735 9653